

2016

Functionalized Electrospun Nanofibers for Food Science Applications

Minhui Dai

Follow this and additional works at: https://scholarworks.umass.edu/dissertations_2



Part of the [Food Science Commons](#)

Recommended Citation

Dai, Minhui, "Functionalized Electrospun Nanofibers for Food Science Applications" (2016). *Doctoral Dissertations*. 714.
https://scholarworks.umass.edu/dissertations_2/714

This Open Access Dissertation is brought to you for free and open access by the Dissertations and Theses at ScholarWorks@UMass Amherst. It has been accepted for inclusion in Doctoral Dissertations by an authorized administrator of ScholarWorks@UMass Amherst. For more information, please contact scholarworks@library.umass.edu.

FUNCTIONALIZED ELECTROSPUN NANOFIBERS FOR FOOD SCIENCE APPLICATIONS

A Dissertation Presented

by

MINHUI DAI

Submitted to the Graduate School of the
University of Massachusetts Amherst in partial fulfillment
of the requirements for the degree of

DOCTOR OF PHILOSOPHY

May 2016

Department of Food Science

© Copyright by Minhui Dai 2016
All Rights Reserved

Functionalized Electrospun Nanofibers for Food Science Applications

A Dissertation Presented

by

MINHUI DAI

Approved as to style and content by:

Sam R. Nugen, Chair

Julie M. Goddard, Member

Sarah Perry, Member

Eric A. Decker, Department Head
Department of Food Science

DEDICATION

A project is a golden opportunity for learning about yourself. I think I am very lucky and honored to have so many brilliant professors, faculties, lab-mates and friends lead me in completion of this project.

ACKNOWLEDGMENTS

I would like to express my sincere gratitude to my supervisor Dr. Nugen for his professional guidance and support to my research. Especially for his patience and understanding. All my researches would not be finished without his help. I would also like to extend my gratitude to the members of my committee, Dr. Julie M. Goddard and Dr. Sarah Perry, who provided encouraging and constructive feedback. I am grateful for their helpful comments and suggestions on all stages of this project.

My special thanks to all bioeng lab mates, Juhong Chen, Danhui Wang, Ziyuan Wang, Chairman Co, Fei He, Fang Tian, Dana Wong, Maxine Roman, Anna Denis-Rohr, Stephanie Andler, Kang Huang, Jason Lin, Chanelle Adams for their support and help throughout these years.

ABSTRACT

FUNCTIONALIZED ELECTROSPUN NANOFIBERS FOR FOOD SCIENCE

APPLICATIONS

MAY 2016

MINHUI DAI

B.S., CHINA AGRICULTURAL UNIVERSITY

Ph.D., UNIVERSITY OF MASSACHUSETTS AMHERST

Directed by: Professor Sam R. Nogen

This work is separated into two individual parts. The first part demonstrates the ability to electrospin reagents into water-soluble nanofibers resulting in a stable on-chip enzyme and a microphage storage format.

1a) Polyvinylpyrrolidone (PVP) nanofibers were spun incorporating the enzyme horseradish peroxidase (HRP). Scanning electron microscopy of the spun nanofibers was used to confirm the non-woven structure with an average diameter of 155 ± 34 nm. The HRP containing fibers were tested for a change in activity following electrospinning and during storage. A colorimetric assay was used to characterize the activity of HRP reacting with the nanofiber mats in a microtiter plate and monitoring the change in absorption over time. Immediately following electrospinning, the activity peak for the HRP decreased by approximately 20%. During a 280 day storage study, the loss in activity began to stabilize at approximately 40%.

1b) We then investigated PVP fibers for T7 bacteriophage storage. The bacteriophage was added to mixtures of polyvinylpyrrolidone and water and electrospun the mixture onto a grounded plate. Trehalose and magnesium salts were added to the mixtures to determine their effect on the infectivity of the bacteriophage following electrospinning, and during storage. The

fibers were stored at 20 °C in dry conditions for predetermined amounts of time. The loss of T7 infectivity was determined immediately following electrospinning and during storage using agar overlay plating and plaque counting. It was found that the addition of the magnesium salts resulted in less than a 1 log drop of infective *T7* as compared to a drop of approximately 4 logs without the salts. The trehalose did not protect the T7 during the electrospinning process, but had a more significant storage effect. None of the electrospinning methods were as effective as lyophilization. The results indicate that the addition of magnesium salts protects the bacteriophage during the relatively violent and high voltage electrospinning process, but is not as effective as a protectant during storage of the dried *T7*. Conversely, the addition of trehalose into the electrospinning mix has little effect on the electrospinning, but a more significant role as a protectant during storage. Previous studies have attempted to encapsulate bacteriophage in water-soluble nanofibers for delivery and storage, but the treatment has typically resulted almost complete deactivation of the phage. Here we investigated the effect reagents on the activity of *T7* during the electrospinning process as well as storage following the electrospinning.

Electrospinning can therefore be seen as a low-cost method for rapid dehydration of viruses.

2) The second part of this work is to produce a conductive polymer electrode. The conducting polymer PEDOT(Poly (3,4-ethylenedioxythiophene) modified with a functional group, gold nanoparticles or nano-structured fibers were investigated for use as electrochemical sensing electrodes. synthesized through a vapor polymerization route. 1) Carboxylic functionalized EDOT monomers was synthesized through electrochemical polymerization. 2) Gold nanoparticles were deposited by monomer reduction. 3) PEDOT nanofibers were synthesized by electrospinning followed by vapor phase polymerization. 4) One-step PEDOT fibers were made from wet vapor-phase polymerization. These materials and structures were characterized using TEM, FE-SEM XPS and FTIR. The advantages of these films are the

potential to provide bio-probes binding sites and nano-structures for increased sensitivity. The PEDOT matrix is known to improve catalytic oxidation of the ascorbic acid and functional carboxylic groups provide bonding sites. Additionally, the nanometer-sized gold particles or fiber structures have been demonstrated to allow nanomolar sensing of analyte. Thus, these methods should provide a bio-functionalizable surface with the possibility to detect nanomolar levels of a bio-analyte.

TABLE OF CONTENTS

	Page
ACKNOWLEDGMENTS.....	v
ABSTRACT.....	vi
LIST OF TABLES	xi
LIST OF FIGURES.....	xii

CHAPTER

1. INTRODUCTION

1.1.1 History of electrospinning.....	1
1.1.2 Applications of electrospinning in food science.....	5
1.2 Conductive polymers.....	10
1.2.1 History of conductive polymers.....	10
1.2.2 PEDOT: Poly(3,4-ethylenedioxythiophene)	12
1.2.3 Applications of PEDOT.....	14
1.3 Electrochemistry theory and biosensors	17
1.3.1 Cyclic voltammetry	17
1.3.2 Amperometry.....	20
1.4 Biosensors	23
1.4.1 Concept of biosensors and bioelectrodes	23
1.4.2 Conducting polymers in biosensors	25
1.5 Biosensors in food science	28

2. WATER-SOLUBLE ELECTROSPUN NANOFIBERS AS A METHOD FOR ON-CHIP REAGENT STORAGE

2.1 Abstract.....	34
2.2 Introduction	35
2.2.1 Lab-on -a chip.....	35
2.2.2 Nanofibers applications	35
2.2.3 PVP [Poly(vinylpyrrolidone)] nanofiber applications	35

2.3 Experimental.....	37
2.3.1 Electrospun Nanofiber Preparation	37
2.3.2 Materials	39
2.3.3 Scanning Electronic Microscope (SEM)	39
2.3.4 HRP Activity Measurement	39
2.3.5 On-chip Microfluidic Devices with Nanofibers	40
2.4. Results and Discussions	41
2.4.1 Morphology of Nanofibers.....	41
2.4.2 HRP Enzyme Activity	41
2.4.3 On-Chip Microfluidic System.....	44
2.5 Conclusions	46

3. BACTERIOPHAGE *T7* DEHYDRATION AND STORAGE IN ELECTROSPUN POLYVINYLPYRROLIDONE NANOFIBERS

3.1 Abstract.....	47
3.2 Introduction	49
3.2.1 Introduction of bacteriophages	49
3.2.2 Bacteriophage application in food safety.....	49
3.2.3 Dehydration and storage methods of bacteriophages	50
3.2.4 Review of electrospinning of bacteriophages.....	50
3.3 Materials and Methods.....	52
3.3.1 Materials	52
3.3.2 Bacteriophage harvest	52
3.3.3 Electrospinning and freeze-drying	52
3.3.4 Quantification of infectious bacteriophage	53
3.3.5 Electronic-microscopy analysis	54
3.4 Results and discussions	55
3.4.1 Morphology from electron microscopy	55
3.4.2 Bacteriophage infectivity change after desiccation(electrospinning vs freeze-drying)	56
3.4.3 Bacteriophage activity change during storage.....	57
3.5 Conclusions	61

4. VAPOR-PHASE POLYMERIZATION WITH GOLD PARTICLE SYNTHESIS FOR ELECTROCHEMICAL ELECTRODES

4.1 Abstract.....	67
4.2 Introduction	68
4.3 Materials and Methods.....	71
4.3.1 Materials and equipment.....	71
4.3.2 Preparation of FeTos film	71
4.3.3 Electrospinning of FeTos and PVP nano-fibers	72
4.3.4 Vapor-phase polymerization with Fetos films and electrospun(EVP) nanofibers.....	72
4.3.5 One step vapor-phase polymerization (OSVP) of PEDOT nanofibers	72
4.3.6 Au-nanoparticle composite synthesis and SAM layer formed on Au-nanoparticle	73
4.3.7 TBO assay	74
4.3.8 Raman Spectroscopy	74
4.3.9 X-ray photoelectron spectroscopy (XPS)	74
4.3.10 Electrostatic immobilization of streptavidin and quantification with Biotin-HRP	75
4.3.11 Electrochemical Characterizations	75
4.4 Results and discussions.....	77
4.4.1 Electrospinning with vapor phase polymerization(EVP) technique polymerization fiber morphology.....	77
4.4.2 SEM results of gold nanoparticle synthesis composites	79
4.4.3 X-ray photoelectron spectroscopy (XPS) results	80
4.4.4 Raman results	83
4.4.4 TBO results	84
4.4.5 Streptavidin (SA) immobilization and biotin-HRP measurement	85
4.4.6 Amperometry detection of ascorbic acid(AA)	87
4.5 Conclusions	90
REFERENCE.....	91

LIST OF TABLES

	Page
1. Polymer mixture formulation and bacteriophage initial titer.....	53
2. The elemental ration of electrospun vapor phase polymerized PEDOT (EVP) and one step vapor phase polymerized PEDOT(OSVP) fibers with/without Au synthesis	82

LIST OF FIGURES

	Page
1.1 Illustration of an electrospinning set-up. Electrospinning uses an electrical charge to draw fibers from a conductive liquid. When a sufficiently high voltage is applied on the surface of liquid jet, the surface is charged. The force of electrostatic repulsion counteracts the force of the surface tension. Because of these two interactions the droplet is stretched. When this interaction reaches a critical point, the repulsion exceeds the surface tension force and a stream of liquid erupts from the surface resulting in a cone shape round the jet tip. As the solvents evaporate, the dry fiber is deposited on the grounded collector.....	2
1.2 Popular conducting polymers chemical structures listed in order: polyacetylene, polypyrrole, polythiophene and poly(3,4-ethylenedioxythiophene).....	11
1.3 a) Non doped polyacetylene structure and resonance of electronic states. The mobility of electrons on double conjugated carbon backbones limited by saturated double bonds. b) Doped polyacetylene structure with one empty hole position for valent electron transfer. Compared to the structure a), electron showed more mobility and feasibility to travel along carbon backbones.....	12
1.4 The three electrodes system, a) WE refers to working electrode, electrochemical reaction takes place on its surface ; b) RE, reference electrode, which tracks the potential solution ; c) CE represents the counter electrode, where supplies the current for the reaction on WE. WE and CE always appear as a pair.....	17
1.5 The CV curve gained by using 2mm gold electrode in 0.1M H ₂ SO ₄ solution. And the scan rate is 50mV/s.....	19
1.6 Single strand DNA(capture DNA) is immobilized on gold electrode with thiolated functional end. Target DNA and DNA with HRP(probe DNA) are loaded on capture DNA through complementary base pairing. Hydroperoxide in solution is oxidized by HRP to generate oxygen, then oxygen oxidize hydroquinone(HQ). Chronoamperometry experiments are performed, HQ gives electrons to electrode when been reduced on electrode surface. HQ in the electrochemistry system could be used as a electron transfer chemical, which is called mediator. The requirement for a mediator chemical is oxidation-reduction reversible and stable. Capture DNA on this electrode plays a biocomponent part while HRP, hydroperoxide, mediator HQ and electrodes are electrical transducer part. They can transfer the DNA hybridization information to electrical signal.	24
2.1 Lab-made electrospinning set-up. Electrospinning uses an electrical charge to draw fibers from a liquid. When a sufficiently high voltage is applied to a liquid droplet, the body of the liquid becomes charged, and electrostatic repulsion counteracts the surface tension and the droplet is stretched, at a critical point a stream of liquid erupts from the	

surface. Then the jet dries in flight and finally deposited on the grounded collector.....	38
2.2 (A) Horseradish peroxidase (HRP) activities before and after electrospinning was detected by 1-step slow TMB kit. 1501 1-step slow TMB kit mixed with 100 L water was used by measuring change in absorption at 652 nm every 15 s for 1 h. The equivalent quantity of HRP was 0.04g. The reaction initially oxidized the TMB substrate yielding a blue color and 652 nm peak in absorbance. As the reaction progresses, the color shifts to yellow and has a 450 nm maximal absorbance. (B) The activity of the enzyme initially dropped and stabilized over time.	43
2.3 Images of electrospun nanofiber in microfluidic chip. The image demonstrates how a nanofiber mat can be incorporated into a microfluidic chip. The images are before (A) and after (B) 100 L 1-step TMB reaction solution was added. The color change was observed after approximately 60 s.....	45
3.1 SEM images of electrospun PVP (15% w/v) fibers with T-7 phages: (a1) DI-water, (a2) DI-water after 2 months storage, (b1) 5% trehalose in DI-water, (b2) 5% trehalose in DI-water after 2 months storage, (c1) SM buffer, (c2) SM buffer after 2 months storage, (d1) 5% trehalose in SM buffer, (d2) 5% trehalose in SM buffer after 2 months storage.....	62
3.2 TEM images of electrospun PVP nanofibers from SM buffer solution before 200kV electron beam damaging (a) and after (b).....	62
3.3 SEM images of PVP nanofibers electrospun from SM buffer with trehalose 0% (a), 5% (b), 10% (c).....	64
3.4 The bacteriophage activity after electrospinning and freeze-drying four PVP mixture solutions. The data represent the averages of a minimum of three replicates and error bars represent the standard deviations of the replicates.....	65
3.5 Bacteriophage activity changing during storage at 20 °C. Phage activity changing in electrospun fiber format (a), freeze-dried powder format (b). The data represent the averages of a minimum of three replicates and error bars represent the standard deviations of the replicates.....	66
4.1 SEM TEM micrographs of Electrospun FeTos and EVP PEDOT nanofibers and at 5000× magnification 5 kV accelerating voltage and 20000 × magnification 200.0 kV. The diameter distribution was analyzed by Image J. Each distribution was composed of 50 counts fibers. A) SEM image of FeTos Fibers, B) TEM image of FeTos Fibers C) Fetos Nanofiber diameters range from 500 nm to 1100 nm, D) SEM image of PEDOT Fibers, E) TEM image of PEDOT Fibers, F) PEDOT Nanofiber diameters range from 100 nm to 500 nm.....	77

4.2 SEM of 27 min one step vapor phase polymerized PEDOT(OSVP) nanofibers. The image was taken at 10KV in JEOL and 5 kV accelerating voltage by Magellan. The diameter distribution was analyzed by Image J. Each distribution was composed of 50 fibers count. A)300× magnification of OSVP fibers image was taken by JEOL, B) 5K magnification of OSVP fibers in Magellan, C) OSVP PEDOT Nanofiber diameters range from 100 nm to 350 nm.....	78
4.3 SEM of vapor phased polymerized PEDOT nanofibers with 60s gold synthesis. The image was taken at 5K and 20K magnification 5 kV accelerating voltage. The diameter distribution was analyzed by Image J. Each distribution was composed of 50 particles count. A) 5K magnification of EVP/Au particles, B) 20K magnification of EVP/Au particles, C) Gold diameters range from 100 nm to 700 nm, D) 5K magnification of OSVP/Au particles, E) 20K magnification of OSVP/Au particles, F) Gold diameters range from 200 nm to 700 nm on OSVP fibers.....	79
4.4 XPS results of electrospun with vapor phase polymerization (EVP) PEDOT fibers (dash black), one step vapor polymerization (OSVP) PEDOT fibers (dash maroon), EVP/Au (solid blue) and OSVP/Au (solid red).....	81
4.5 Overlapped Raman spectra results of electrospun vapor phase (EVP) (black) PEDOT and one step vapor phase polymerization (OSVP) (green) PEDOT fibers with or without gold.....	83
4.6 TBO absorbance on the surface of electrospun vapor phase polymerization and one step vapor phase polymerization PEDOT nanofibers with or without gold, or gold with or without self-assembly(SAM) alkanethiol monolayer (n=5).....	85
4.7 The absorbance of one-step TMB oxidation at 652nm of different samples, gold electrodes as blank and electrospun vapor phased PEDOT fibers and one-step vapor phase polymerization with or without gold.....	86
4.8 Amperometry test of different ascorbic acid detection with standard gold electrode, PEDOT film, PEDOT film with gold nanoparticles, PEDOT electrospun- nanofiber, PEDOT electrospun nanofibers with Au-particle synthesis, one-step vapor phase polymerization PEDOT.....	88

CHAPTER 1

INTRODUCTION

1.1 Electrospinning

1.1.1 History of electrospinning

Electro spinning is a simple technology known since 1930s' for the production of continuous fibers (as thin as 5 nm) from a variety of materials such as polymers and inorganic ceramics. Electrospun fibers' diameters vary from nano to micrometers. Due to such small sizes, they showed some interesting characteristics such as large surface area, higher surface bonding efficiency, and some better mechanical performance like super strong strength compared to bulk materials. The process of electro spinning was first patented by Farmhals in 1934. He then published a series of patents [1-3] in fallowing years and established an experimental setup using electrostatic force to form polymer filament **Fig 1.1**. Although the process of spinning artificial threads was experimented even before Farmhals, it did not get much attention because of technical difficulties on solvent evaporation and fibers collection. His process consisted of a rolling thread device to collect the threads. The first rolling collector was invented. However drying the fiber was still a problem. In order to overcome this disadvantage, Farmhals repatented his work in 1940. A polymer solution was placed on to one electrode, a collector was on the other electrode. The polymer fibers were formed between two electrodes and collected on collector. The two electrodes provided the electric field. The polymer solution was ejected out and evaporated to become dry fibers. In the 1960's, Taylor initiated studies on the jet forming. He proposed a theory, and his studied was known as "Taylor cone". He found out that the applied electric field will result a cone form during the ejection [4]. This cone shape is known as "Taylor cone" in the literature.

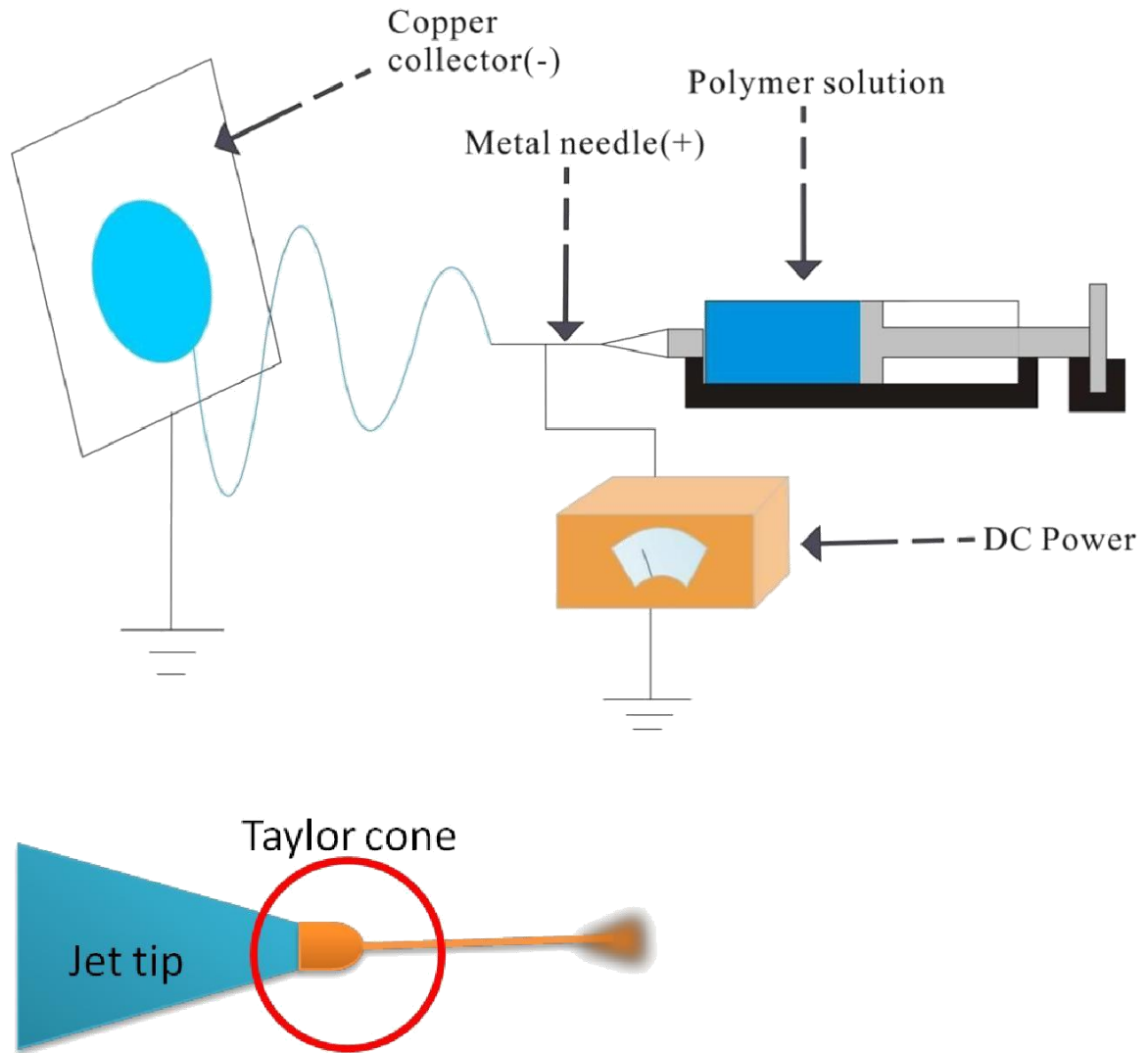


Fig 1.1 Illustration of an electrospinning set-up. Electrospinning uses an electrical charge to draw fibers from a conductive liquid. When a sufficiently high voltage is applied on the surface of liquid jet, the surface is charged. The force of electrostatic repulsion counteracts the force of the surface tension. Because of these two interaction the droplet is stretched. When this interaction reaches a critical point, repulsion exceeds surface tension force, a stream of liquid erupts from the surface and a cone shape begins to form round the jet tip. Then the jet dries during flight and will be finally deposited on the grounded collector.

In subsequent years, much attention was given to the structural morphology of the fibers. And a great amount of effort was invested by researchers in the structural characterization of the

fibers and understanding the relationship between the structures and electrical field parameters. The common characterization methods were electronic microscopy including SEM, TEM and AFM. Baumgarten proved that the fibers' diameter changed with different powers[5]. Melting electrospinning was discovered in the study of producing polyethylene nanofibers from Larrondo [6]. After that more and more studies were focused on revealing the factors that affects fibers diameters. Shin showed streams were unstable by increasing potentials[7]. And jet ejected to directions. All fibers were made of water insoluble polymer materials until Doshi used poly(ethylene oxide)[8]. The fiber's diameters vary from 50nm to 5 μ m. Through this study, he described the processing conditions, fiber morphology and potential applications of electrospun fibers. His paper has been cited over 2000 times, and people began to be interested in water soluble electrospun nanofibers. Jaeger group observed chain packing in electrospun polyethylene oxide (PEO) via the atomic force microscopy (AFM). He discovered that at the molecular level the electrospun PEO nanofibers had a highly ordered surface layer[9]. From this study, a ultra-thin PEO fibers mat could be made. Gibson studied the transport properties of electrospun fiber films. He showed that there was minimal impedance to moisture vapor diffusion required for cooling during evaporation. From this study, porous nanofiber structures were discovered [10]. Nanofibers of aromatic heterocyclic polybenzimidazole (PBI) were electrospun by Kim[11]. Fibers' diameter were around 300 nm. Sulfuric acid and heat treatment could increase the mechanical strength of PBI fibers. Fiber's morphology was influenced by applied voltage on jet, viscosity and concentration of polymer solutions. This hypothesis was systematically studied by Deitzel[12] in 2001. Demir successfully produced elastic fibers by electro spinning of polyurethane urea (PUU) solutions[13]. He studied fibers with diameters ranging from 7 nm to 1500 nm by using different concentrations of polymer. It was shown that fiber diameters increase as the third power of solution concentration. Besides all these efforts to understand the process of electro spinning and make fiber growth adaptable in various technologies, new materials were discovered and their

properties were studied at micro/nano scale. The electronic properties of various types of nano fibers were studied by Wang[14].

Electrospun fibers can be prepared from a wide variety of polymers, but materials of electrospun fibers are, however, not limited to neat or blended polymers. Electrospinning can be conducted in the presence of additives. The use of additives can be roughly divided into two groups according to purpose. One group of them is used to influence processing. The other is to modify the properties of the electrospun fibers. Sometimes, however, the boundary between the two groups is unclear since many additives affect the process and the properties of fibers alike. Electrospun fibers can be functionalized using additives, and encapsulate fillers to form composite fibres. Metal-containing nanofibers, for example, can be pyrolysed on ceramic nanofibers, and organic nanofibers graphitized to carbon nanofibers. Typically, electrospun nanofiber web have high porosity with a tortuous pore structure and good interconnectivity of pores, which is of benefit in many applications.

Due to the countless possibilities of materials and the many potential structures, electrospun nanofibers can be utilized in a wide variety of technical applications fields. biotechnology and environmental engineering utilizes electrospun materials in filters and membranes. Electrospun nanofibers can be used as reinforcement materials. Electrospun fibers can also be used in defense and security applications such as chemical and biological protection as well as sensors for security or other purposes. In the healthcare sector electrospun fibers have many potential applications. They can be used for example, in tissue engineering and wound dressing. Electrospun fibers containing photoactive fullerene derivatives have potential applications in photodynamic cancer therapy and in the treatment of multi-drug resistant bacteria. Drug delivery materials can be prepared by encapsulating medicines into electrospun structure. Live organism can partly survive during electrospinning process. Modified electrospun fibers can also be used in energy storage applications, including photovoltaic such as solar cells, fuel cells,

and batteries, and catalyte-containing electrospun nanofibers are suitable for variety of catalyst applications. Electrospun fibers of intrinsically conducting polymers as well as conducting composite fibers, photoluminescence fiber and light emitting fibers may be utilized in nanoelectronics and optoelectronics. The flexibility of conducting electrospun fibers opens possibility in wearable electronics. The sound absorption and heat transfer properties of electrospun fiber mats proved usefulness in sound and thermal insulation. Electrospun fibers from removable polymer can be used as fiber templates in the preparation of nanotubes with TUFT(tubes by fiber template) process. The surface morphology of the electrospun coating might enhance hydrophobicity, and electrospun coatings can be used to form super hydrophobic surfaces that can also have self-cleaning properties.

The book titled *An introduction to Electrospinning and Nanofibers* published in 2005 covers a wide spectrum of this technology including the basic materials, processing techniques, various characterizations methods, different formats of fibers, surface modifications and functionalization, theories, modeling methods and lots of applications[15]. In this book, it listed the most commonly used polymers with the corresponding solvent. Polymers used for electrospinning can be categorized to two groups, one is non-biodegradable synthetic polymers such as nylon[16], polyacrylnitrile[17], polyamide and poly(ethylene oxide)[18]. Those polymers could be used as filter media[18], protective clothing[19], sensor material[14] and composite reinforcement[20]. The other group is biocompatible polymers or biodegradable polymers such as poly(ϵ -caprolactone)[21], polydioxanone[22], polyglycolide[23] and poly(L-lactic acid)[24] or natural polymers including casein [25], cellulose acetate[26], chitosan[27] and collagen[28]. This group of polymers can be used in the field of tissue engineering, medical delivery, wound dressing and also packaging and encapsulation material in food science.

1.1.2 Applications of electrospinning in food science

Electrospinning is known since 1930s', but the applications in food science field is new. The food industry use electrospun nanofibers for packaging, encapsulation material and nanostructured scaffolding for bacterial cultures. The limitations of electrospinning technique are polymers and solvents toxic. Only a few chemical synthesized polymers are proved by FDA as packaging materials. Then people were trying to use food grade natural materials such as chitosan from crab shell, zein protein from corn and albumen from egg white. During the electrospinning, the most solvent evaporated but as a encapsulation material, toxic organic solvent can destroy the structure of encapsulated ingredients or contaminate food systems.

Food packaging

Food packaging can protect food from processing, distribution handling and storage. It not only can provide protection but also can be named active. Active packaging could act as an oxygen scavenger or antimicrobial agent. Nanofibers were produced to be biocompatible and with functional active compounds. Those compounds could be immobilized on the surface of fibers or encapsulated inside of fibers. The advantages of this nano-fiber structured package are large surface and high encapsulation ability. An active packaging used electrospun nanofiber made of soy protein or PLA fibers with allyl isothiocyanate, a natural antimicrobial compound. The electrospun fibers can release the active compound through humidity triggering[29]. Similarly, zein/chitosan nanofibers with biocide was studied by Torres group[30]. Recently, more natural active compounds encapsulated fibers were studied. Su produced a PVA fibers containing tea powder. Green tea has natural antibiotic properties. As the results, it showed antibacterial function against E.coli[31]. Wang added red raspberry extract, a great source of natural phenolic compounds, and gallic acid in zein nanofibers and found they showed high antioxidant property [32].

Apart from active packaging, electrospun nanofibers can also be used as a smart packaging. Smart packaging refers to the material used for packages that could monitor the quality changing during storage. It shows great significance in the food industry. A fiber mat using pH-sensitive dye was produced to monitor real-time pH change in food system[33]. A similar study was done by Teng group[34], they added multiple pH dyes inside of fibers. The pH sensitive fibers were able to detect pH from a large range.

In addition to these active and smart packaging, electrospun fibers can be used as multilayered structures. Nanofibers can provide mechanical reinforcement as a better protection for fragile textured foods and add other functional properties. Fabra group produces fibers with oxygen barrier to reduce food oxidation during storage[34]. Zein nanofibers incorporated with PLA and PEO to develop a transparent composite packaging materials, which could reduce oxygen permeability and provide a better gas barrier[35].

Filtration process

Due to the fibrous structure of fibers by electrospinning, nanofibers are good candidates for filtering material, gas and liquid filtration. The electrospun nanofibers can be applied in air filtration on commercial systems due to their small pore size and large surface area. In food industry, nanofibrous membranes are able to filter liquids through pressure-driven liquid separation systems. Polyvinylidene fluoride (PVF) nanofibers were used in liquid separation due to polymer functionality. Owing to their small porosity, 90% of the microparticles with size varying from 1 to 10 μm would be filtered out from the flow[36]. This filter could be used to clarify drinking water. Similarly, Rajesh group electrospun a neutrally charged antifouling nanofiltration membrane by coating a layer of sulfonated poly (ether ether ketone) on a water filtration[37]. Veleirinho electrospun nanofibrous membrane in apple juice clarification[38]. The filter membrane made from poly (ethylene terephthalate) (PET) with an average diameter of 420 nm

and a thickness of 0.20 mm was found to be a faster and higher filtration efficient material than using traditional filters.

Enzyme immobilization

Immobilization of functional composite on the surface of nanofibers is another way to produce customized nanofiber for food. Enzyme is one of the most common used functional compound for packaging. Enzyme, a natural catalysts, has been widely used in food industry. For example, cellulase is used to clarify fruit juices and β -galactosidase is used in industry to produce lactose free milk. However, enzyme is high cost, sensitive to temperature, pH and chemicals, difficult to recover after reaction. In order to overcome these difficulties, food industry prefers to immobilize enzyme on reaction surface with food ingredients. Immobilized enzyme shows increased stability, higher activity and is able to use in continuous enzymatic reactions. Due to large surface area provided by electrospun fiber, it considered a potential material substitution for food industry. Despite from encapsulation, enzymes can be bond on nanofibers through physically adsorbed or covalently attached. Here are some examples of electrospun nanofibers with enzyme immobilization. Wu proved that because of higher loading enzymes on the surface of fibers, the use of electrospun nanofibers could increase cellulase catalyzing ability[39]. El- Assa produced poly(acrylonitrile-co-methyl methacrylate) fibers with β -galactosidase. Enzyme immobilized on the surface of fibers by crosslinking using glutaraldehyde. The immobilized form showed greater temperature, pH and storage stabilities than free enzyme. Song group encapsulated lipase in PVA/PEO and casein nanofibers. Though activity of free enzyme is higher than immobilized one[40]. However the stability immobilized form is better. Compared to cast membrane, activity of lipase in nanofibers showed 6 folds greater. Sakai made PVA nanofibers which was encapsulated of lipase and used these fibers in continuous food processing flow[41]. Lipase could be chemical co-valent bonded on fibers, physically encapsulated inside fibers or physically adsorbed on surface. Wang made PEO fibers for immobilizing lipase by physical adsorption. No matter which polymers had been used, lipase

immobilized on nanofibers showed enhanced storage stability.

Oxidase enzyme can be used as a sensor component in sensor field. This part will be discussed with more details later. GOD ,short for glucose oxidase, is used in glucose biosensors and is important in analytical detection and food fermentation industries . The nanofibers with GOD was coupled with oxygen electrode. GOD was successfully immobilized on electrospun PVA or silk fibers. Amperometric biosensors electrode were designed to response vs current[42]. Furthermore, PVA with chitosan nanofibres were proved increase the stability of GOD used in glucose biosensor. In additional, GOD can be used in packaging and preservation by using electrospun PVA and chitosan fibers[43]. The electrospun fiber membrane was shown to exert 73% deoxidization from food samples.

Monitoring food quality or detection of food safety will be discused with more dilates in next chapter. As the conclusion, electrospun microfibers could be used as a barrier or reinforcement protection layer, a encapsulation composite of active or smart for food packagin, as a nanostructured mat for enzyme loading and immobilization, and a filtration system for beverage processing.

1.2 Conductive polymers

1.2.1 History of conductive polymers

In 2000, the Chemistry Nobel Prize was awarded to Alan J. Heeger, Alan G. MacDiarmid, and Hideki Shirakawa for their contribution of discovery and development of conducting polymers. Conductive polymers are organic polymers that are able to conduct electricity. Based on different conductivities, they can be categorized to conductors like metals or semiconductors like metal oxides. The biggest advantage of utilization of conducting polymers is processibility. The most conductive polymers are semi-conductive or insulating in their undoped state, such as polythiophenes, polyacetylenes, their conductivities are around 10^{-10} to 10^{-8} S/cm. However conductivity could be increased dramatically by several orders of magnitude with oxidation and reduction. This modification is named doping. Even with less than 1% doping, polymers' conductivities can be increased to around 10^{-1} S/cm. Therefore, conductive polymers are also called doped polymers. Different polymers' conductivity ranges from 100-10000 S/cm with different saturation contents doping.

The first electrically conductive polymer, polypyrrole (PPy), has been discovered in early 1960s [44, 45]. Even though PPy is the first studied conductive polymer, until today, it remains the most interesting group of conducting polymers and have wide applications in various fields. One of the most significant conductive polymer polyaniline (PAi) was discovered in 1977 by MacDiarmid [46]. PAi's (10^{-9} S/cm) electrical conductivity could be increased to 10^5 S/cm by doping two kinds of doping. One is oxidizing doping, such as I_2 , AsF_5 , $NOPF_6$. Another is n-doping with reducing agents such as sodium naphthalide [47]. A big breakthrough of conductive polymers studies was the discovery of polyacetylene (PAC). Even though polyacetylene was discovered as early as 1874, as a potentially conductive polymer, polyacetylene was first observed in 1961 in Tokyo Japan. In the next 15 years scientist struggled to find methods to increase conductivity of PAC, until 1976 a 7 order of magnitude conductivity of the doped PAC

was obtained **Fig 1.2** [48]. It is the first highly conducting hydrocarbon polymer. An number of significant research has been inspired by this discovery. At the end of 1980s, the highest iodine-doped PAc could reach to 10^5 S/cm[49] and vast scientific progress has been achieved, several applications were suggested.

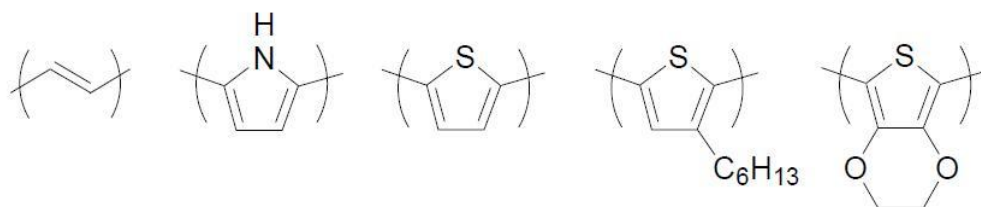


Fig 1.2 Popular conducting polymers chemical structures listed in order: polyacetylene, polypyrrole, polythiophene and poly(3,4-ethylenedioxythiophene).

With similar conjugated double bond structure, conducting polymers showed several similar chemical characteristics. None conjugated polymer, such as polyethylenes (PE), its valence electrons are in orbital sp^3 . Those electrons only have limited mobility which could not transfer along carbon backbones and could not contribute to the conductivity. On the other hand, valence electrons on conjugated carbon backbone are in sp^2 which offer contiguous hybridized carbon centers. On each carbon center there is a movable valence electron in a p_z orbital. Free valence electrons link with neighboring p_z orbitals to form a molecule wide delocalized set of orbitals. However as mentioned before, just conjugation alone, is not sufficient for conductivity. The electrons in those delocalized orbitals have high mobility when the material is "doped". That means doped element removes some of these delocalized electrons by alternating double bond structure and a one-dimensional electronic band of conjugated p-orbitals within this band become mobile when it is removed. Therefore doping is required to change the band structure of the conductive polymer backbone. **Fig1.3**

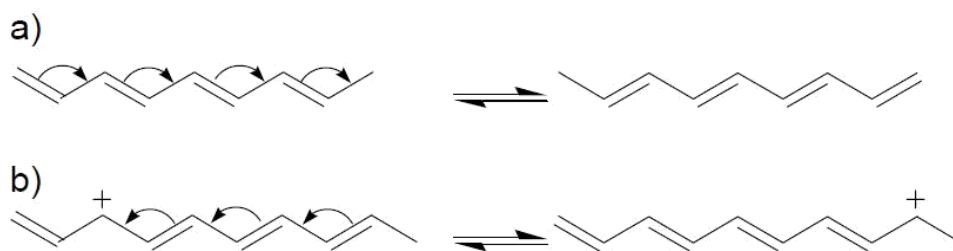


Fig 1.3 a) Non doped polyacetylene structure and resonance of electronic states. The mobility of electrons on double conjugated carbon backbones limited by saturated double bonds. b) Doped polyacetylene structure with one empty hole position for valent electron transfer. Compared to the structure a), electron showed more mobility and feasibility to travel along carbon backbones.

Starting with doped polyacetylene, the simplest conducting polymer structure, as the prototype, people started to discover their π -conjugated polymers. The first discovery of polythiophenes as potential conducting polymers was made in 1967[50]. However the true electronic conductivity in poly-thiophenes was observed in 1982[51], which is 15 years later. Conductivity of poly thiophene was 10-100 S/cm. The discovery of polythiophene showed an enormous potential for technical applications. Oxygen substituents on the 3- and 4-position have electron donating properties, which can stabilize the doped, bipolaronic state on the thiophene moiety. Among all substitutions, the EDOT, short for 3,4-ethylenedioxythiophene, emerged as the most attractive monomer.

1.2.2 PEDOT: Poly(3,4-ethylenedioxythiophene)

PEDOT, the polymer of EDOT, can be synthesized by polymerization of its monomer through electrochemical or chemical methods. One of the inherent difficulties of polymerizing EDOT is its low solubility in water. Therefore the polymerizations are normally carried out either in non-aqueous solutions or in solutions with monomers or surfactants. However, such surfactants or polyelectrolytes are difficult to be removed completely from the reaction mixtures and their

residues may affect the electronic properties of PEDOT. The most successful commercial product is made by Baytron P, which is a stable PEDOT/ PSS(poly(styrene sulfonic acid) suspension solution. With this product, people can easily produce films with conductivities around 10 S/cm. However, 10 S/cm is not sufficient for applications in electronic devices. In situ polymerization, the polymerization reaction is deposited onto the substrate directly. The first one is liquid oxidation polymerization, which involves mixing oxidant and monomer together on substrate. Second one is vapor-phase polymerization (VPP), which represents a vapor of monomer polymerized on oxidant covered substrate. This method could produce a film with high conductivity. Its conductivity could reach up to 550 S/cm. Another method is electrochemical polymerization. This method presents several advantages such as fast, absence of catalyst, controlled thickness by deposition charge and direct deposition of the polymer film in conductive oxidized form. Aleshin et al produced PEDOT-PF6 by electrochemical polymerization from acetonitrile at -30 °C and obtained conductivity up to 300 S/cm.

Among all strong oxidant, Iron (III) salts are the most common oxidation agents for PEDOT in solvent and vapor polymerization. Due to the low solubility of EDOT in aqueous reaction system, ferric tosylate (FeTos) is an idea oxidant. FeTos is well soluble in various organic solvents such as alcohols. In addition, tosylate ions provide a soluble co-polymer chain, which can increase the PEDOT/PSS solubility in water suspension. PEDOT is at the present time the most successful conducting polymer in commercial applications and is used for various applications. Depending on the extent of doping, oxidation and film thickness, PEDOT films can range in appearance from almost transparent with a sky-blue tint, to an intense blue-black. As a result, much of the research on PEDOT has centered on its use in low color anti-static coatings and electrochromic devices.

1.2.3 Applications of PEDOT

Applications: solid electrolytic capacitors, ITO substitution, antistatic coatings, hole - injection layer, organic solar cells and FET(field effect transistors)

Sensing applications take advantage of simple amperometric techniques to quantitatively analyze solutions. As mentioned before, biosensors are prospective sensors, but other potential options include electronic tongues, and other anodic stripping sensors.

PEDOT-based glucose biosensors have been studied by Kros, Hovell, Sommerdijk, and Nolte [7]. The basic biological interactions between glucose and the enzyme glucose oxidase (GOx) in the body shed some light onto potential sensor applications. Essentially, in the body, the enzyme GOx oxidizes glucose, gaining two electrons, and becoming reduced. They coated a track-etch membrane with PEDOT. This coating was physically attached with enzyme GOx onto the surface of the polymer coating. After the enzyme becomes reduced, it in turn reduces PEDOT, producing a current signal that can be used to measure concentrations of glucose. Their research concluded that glucose could be detected using potentials as low as 150 mV, with an average sensitivity for glucose of approximately 25 nA/mM, and a response time of less than 3 minutes.

They also tested polypyrrole, and as highlighted before, PEDOT's stability as an electrode makes it more appealing than other polymers studied for the same purpose. It is therefore a likely candidate for long-term glucose measurement in medical devices.

Another promising application involves the development of PEDOT-based electronic tongues. According to Martina, an electronic tongue is defined as *“an analytical instrument that comprises a number of chemical sensors with partial selectivity for one class of analytes and only “occasional” specificity for precisely one analyte; such an instrument is capable of discriminating between complex samples without requiring knowledge of the compositions of the samples”*[8]. Their study tested and compared a PEDOT electrode with more commonly used Pt and Au electrodes by

analyzing the responses after applying a DPV potential waveform. They conclude that all three electrodes are capable of differentiating between different kinds of fruit juices, as well as different brand of the same kinds of juice. However, the PEDOT electrode offered the advantage of taking roughly half the time to conduct analysis compared to the other two electrodes. Furthermore, this electrode resulted in a higher degree of cross-selectivity, as it was best able to differentiate between the different brands of same juice. Another study tests

PEDOT's potential as an electrode to operate as a quality control device in the wine industry [9]. It confirms that it has a sensitivity range reaching threshold limits for certain chemicals applicable to the trade, and highlights the fact that while it may be used as an electrode in a simple sensing arrangement, it could also be used as a single component in a larger sensing system comprised of other individual sensors, and enhance the system as a whole.

The last kind of amperometric sensor to be discussed involves the measurement of mercury in solution. Mercury and heavy metals in general are of great concern due to their possible toxicity, even at low concentrations. Research by Giannetto, Mori, Terzi, Zanardi and Seeber explores PEDOT-modified electrodes for use in the measurement of mercury [10]. Traditionally, Au electrodes are utilized, but they have the drawback that sometimes mercury can irreversibly diffuse into the electrode. Hence, the electrodes were modified to include the polymer. Some of the advantages for this specific application include anti-fouling properties, reproducibility of PEDOT films, and once again, high electrochemical stability after charge and discharge cycles. The group concludes that the modified electrodes are less expensive than the conventionally used gold electrodes, and have higher rapidity of analysis.

These are a few examples of potential sensor applications for PEDOT films. It is evident throughout this compilation that conductivity, selectivity, processability, and stability are the most appealing properties provided by PEDOT, and they serve as a driving force for further development in the area of electrochemical sensors.

Therefore, this study serves as a preliminary assessment of PEDOT electrodeposition, with the goal of understanding the process and properties of generated films. As a long-term goal, these properties can be improved so that a material for the discussed potential applications may be developed.

1.3 Electrochemistry theory and biosensors

Electrochemistry as the name interpreted, is a technique combining with the interaction between electricity and chemistry. Briefly saying is that the chemical reactions can generate electrical parameters. In other words is that the electrical informations, such as current, potential, or charge represent analytical chemical reaction on electrical devices. Analytical electrical measurements can be applied in wide fields, such as environmental monitoring, quality control and medical analysis. There are broad classes of electrochemistry measurement methods. The most common and feasible electrochemical analyses and we used in these following projects are cyclic voltammetry and amperometry. Cyclic voltammetry measures the current that oxidized or reduced during cyclic voltage changing in an electrochemical cell, while amperometry shows current changing flows from two electrodes under a constant voltage.

1.3.1 Cyclic voltammetry

Cyclic voltammetry (CV) is measuring current performed by cycling the potential on the working electrode. This measurement requires three electrodes system, working electrode, counter electrode and reference electrodes. **Fig 1. 4** is a basic three electrodes system.

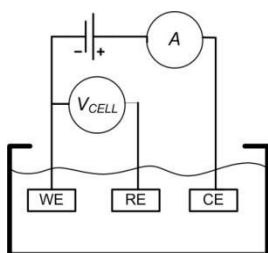


Fig 1.4 The three electrodes system, a) WE refers to working electrode, electrochemical reaction takes place on its surface ; b) RE, reference electrode, which tracks the potential solution ; c) CE represents the counter electrode, where supplies the current for the reaction on WE. WE and CE always appear as a pair.

Reaction solution occurs in electrolyte solution, electrons transfer through circuit from WE to CE, positive and negative ions moves from one electrode to another in solutions. This movement can generate the electrode solution surface reaction, ions get electrons from electrode or the other direction. Therefore oxidation and reduction reactions occur on the interface of electrode and solution. During the reduction, a positive ion is capable to receive an electron from the electrode. This ion is reduced and diffuses away from the surface. Current on the surface is generated through electrons transferring from the electrode to the redox ions in electrolyte solution. The interface of electrode and solution behave as a capacitor. When the potential is different, ions migrate from low to high potential and generate a current. The interface is formed a double-layer electrons which behaves like a parallel-plate capacitor. Using of a parallel-plate capacitor model, we can understand the behavior of electrodes. In that case the charge, Q , on the capacitor meets the same equation as in parallel-plate model.

$$Q = C * I * t$$

Q is the charge on electrode. E is potential between two electrodes. C is the capacitor number for the interface electron double layers and determined by semiconductor material on surface and electrolyte in solutions. During the electrochemistry reaction, C is changing along with oxidation and reduction cycle. According to E/Q , capacity of the double interface could be calculated. I is the current measured by electrochemistry system and t is the time.

CV is a type of potentiodynamic measurement. That means, during the experiment, the potential E applied between WE and FE electrodes is changed linearly versus time. The rate of voltage change over time is known as the scan rate (V/s). The current between WE and CE is measured and plotted versus the E . However in a semiconductor double layer interface, C changed during the oxidation and reduction reaction. During the first half of E scan cycle, an increasingly reducing potential is applied. Meanwhile thus the current i , will increase over the time period,

if there are reducible analytes in the system. When the potential reaches the chemical potential of analyte reduction gap, the concentration of analytes decreased. As the result of the current decreases. During the other half cycle, the reduced analyte begins to recover from oxidation. it will bring a rise to a current to before. One reversible redox regant can provide one oxidation peak and one reduction peak. Fig 5 is a standard H_2SO_4 CV curve on 2mm gold electrode.

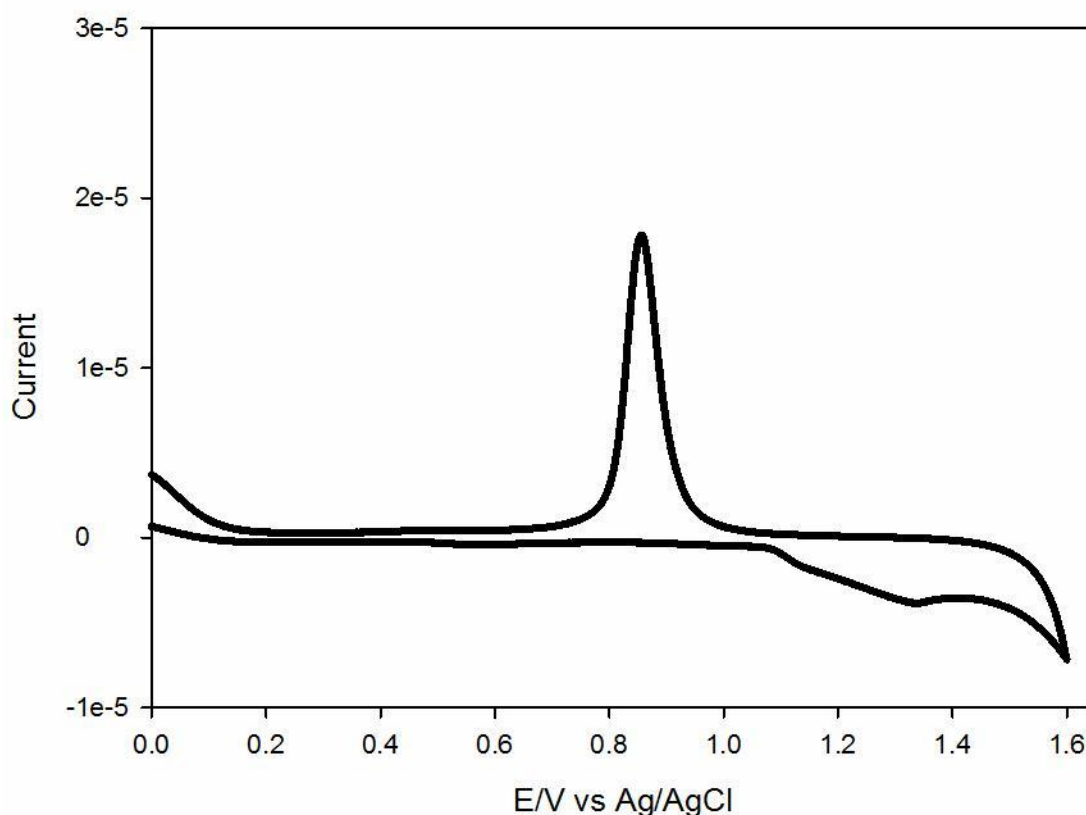


Fig 1.5 The CV curve gained by using 2mm gold electrode in 01M H_2SO_4 solution. And the scan rate is 50mV/s.

CV can tell qualitative information of reversible redox reagent's oxidation-reduction reactions. It also be used to determine the diffusion coefficient of an analyte to electrode surface. For example, if the electron transfer to the working electrode surface is fast then the current is limited by the diffusion of ions to the electrode surface. In that case, increasing the scan rate will increase the height of peak proportionally. Meanwhile the concentration of ions in solution also is proportional to the current. That means it can be used to determine concentration of an unknown solution which by generating a calibration a concentration vs current standard curve. Therefore, CV curve can give the information of the reversible redox potentials(where the peak is), the quantity of redox reagents(height of the peak) and also the electrochemical reaction rates(slope of curve).

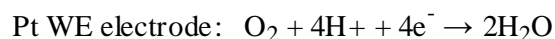
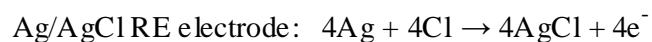
In addition, CV curve also can be used to calculate the real reaction area on electrode, which will be used in this thesis project. Electrochemical active surface area(EASA) can indicate the capacitance of surface material on electrodes and efficiency of electrons transfer. The procedure is using CV to gain adsorption and desorption curve. When the surface reach the adsorption-limited on active site, the number refers to active surface area. As the example of **Fig 1.4**, the EASA of 2mm gold electrode can be represented by the sum of two peaks area. This number can be obtained by recording the total charge required for monolayer adsorption/desorption. In the other word the area of oxidation and reduction peak from CV curve is direct ration to EASA.

1.3.2 Amperometry

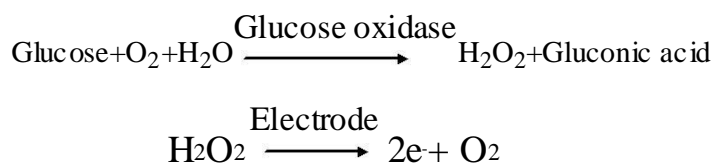
Amperometry is the simplest measurement on the electrochemical station. It does not like CV using linear changing potential, it only uses a constant potential to the electrochemical cell, and the current is measured. Amperometry is usually used in electrolyte titrations, simple gas or chemical sensors and it can combine with chromatography for detection. Ions concentration is determined by change of current or charges in certain time. Therefore, when a potential is applied between WE

and RE electrode, based on $i/[c]$, concentration, standard curve, it could determine unknown concentrations. Amperometry can be used in biosensors, which the electrode is functionalized with reagent which can produce a current when a constant potential is applied. The data could represent response times, dynamic ranges and sensitivities. The simplest amperometry system is an oxygen electrode. Oxygen electrode is a kind of electronic device can reduce oxygen to water, which is the opposite to electrolysis. A platinum electrode works as a WE and Ag/AgCl works as the RE electrode. When a potential is -0.6 V, the reduction potential for Ag/AgCl to platinum electrode, oxygen is reduced on platinum electrodes. As the result, a current proportional to the oxygen concentration is produced. Usually this system is bathed in a solution of saturated KCl solution to protect RE and separated by an oxygen-permeable plastic membrane such as teflon.

The reaction equation is:



Assuming that the original concentration of the oxygen on Pt surface is zero, the rate of this electrochemical reduction only determine by diffusion of the oxygen from the bulk solution to the double layer near electrode. On the other hand, on an ion selective electrode, diffusion equilibrium between electrode and solution is higher than gas diffusion on oxygen electrode. The diffusion rate is depended on the concentration of oxygen in the bulk solution. Temperature changed the rate of oxygen diffusion significantly. Increasing temperature can burst oxygen movement, which can cause electrode reaction. As the result, the oxygen electrodes is observed to be much more sensitive of the temperature changing. Similar to oxygen detection, a typical oxygen electrode application is glucose detection. Glucose oxidase enzyme is immobilized on electrode. The reaction is as following:



Glucose concentrations is determined by oxygen concentration on the cathode. WE electrode detects a reduction current between two electrodes. Glucose oxidase can be replaced by multiple oxidase enzyme which can oxidize different substrate for different uses. Horseradish peroxidase(HRP is the most common used enzyme for bio-electrochemistry in biosensor electrodes. H_2O_2 is oxidase by HRP, and oxygen could be detected by oxygen electrode. Through this reaction, HRP concentration could be determined, which makes HRP a good bio-marker to represent bio-analyte concentration.

1.4 Biosensors

1.4.1 Concept of biosensors and bioelectrodes

A biosensor, short for biological sensor, is an analytical device which consists of a transducer and a biological composite such as enzyme, peptides, nucleic acids or antibodies. The bio-component reacts with analyte which is interested. Meanwhile this biological response can be converted into an measurable electrical signal by the transducer. Based on different measurements, transducers are classified as optical, electrochemical, thermal or mass signal transducers. Electrochemical transducer among them is the most popular for bio-components sensing device because it can transfer bio-information to electrical signal directly and be miniaturized by hi-technology electronics manufactures.

The definition of bioelectrodes is narrowed the biosensor to an functional electrode with as a bio-components. Usually bioelectrode uses current to quantify analyte. First of all, biocomponents react with analytes such as antibody and antigen reaction or nucleic acid hybridization. Then, a biomarker combines with the hybridized product proportionally. This biomarker could generate substrates, which could be oxidized or reduced on electrode interface. The oxidation-reduction reaction between electrode and substrates finally generate currents. Therefore, currents give the information of quantity of analyte. **Fig 1.6** shows a simple and typical bioelectrode to detect DNA concentration.

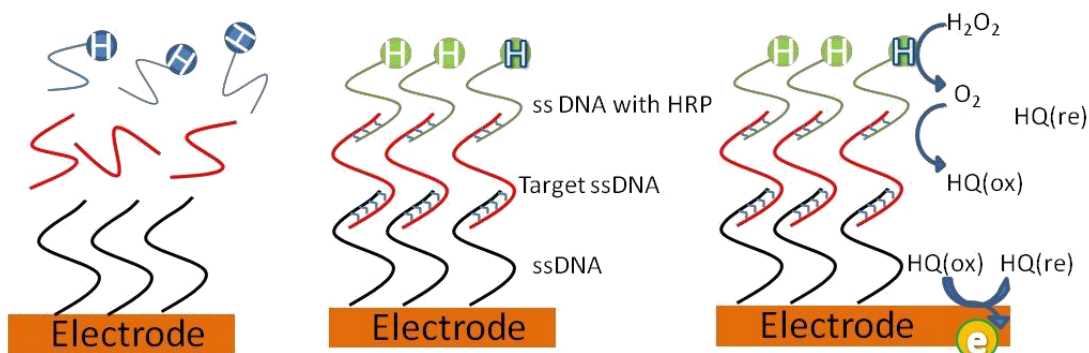


Fig 1.6 Single strand DNA(capture DNA) is immobilized on gold electrode with thiolated functional end. Target DNA and DNA with HRP(probe DNA) are loaded on capture DNA through complementary base pairing. Hydroperoxide in solution is oxidized by HRP to generate oxygen, then oxygen oxidize hydroquinone(HQ). Chronoamperometry experiments are performed, HQ gives electrons to electrode when been reduced on electrode surface. HQ in the electrochemistry system could be used as a electron transfer chemical, which is called mediator. The requirement for a mediator chemical is oxidation-reduction reversible and stable. Capture DNA on this electrode plays a biocomponent part while HRP, hydroperoxide, mediator HQ and electrodes are electrical transducer part. They can transfer the DNA hybridization information to electrical signal.

A successful biosensor consist of some of these critical characteristics, including high specificity for analytes, stability during measurement and storage, accurate and precise response. As an electrochemistry detection cell, solutions effect could be eliminated by reference electrodes uses. If the biosensor is to be used in medical, environmental or food field monitoring, small device size, non-toxic material uses and easy operations are critical for its applications. For example if an biosensor will be used in fermentation in food industry, this device at lease should be sterilisable. Then a heat resistant material and enzymes should be immobilized on this electrodes.

In order to meet the specificity requirements, specific bio-components should be used. Antibody-antigen reaction, nucleic acid hybridizations and enzyme inhibitor reactions are considered to have high specificity in bio-reactions. Those can be produced as immunosensors, DNA sensors and glucose sensors bioelectrodes. With the specific recognition components on electrodes, its performance limitation is the rate of external diffusion which is proportional to the concentration of analyses and parameters of environment.

On the other hand, the transducer is critical in biosensors. Since the electrical signal generated by transducers is low and noisy is relatively high. Increasing the performance of transducer to target, decreasing background noise are important for biosensor devices. In order to solve those problems, nanostructure material and new conductive materials are introduced. Nanostructures, firstly could increase the reaction surface between solution to electrode interface, have high electron transmission efficiency and offer more capture bio-components bonding sits. New materials, on the other hand, can offer more sensitive oxidation-reduction electron transmission. In this thesis project, new materials like conductive polymers has been used. And gold nanoparticles also involve in increasing performance of electrodes.

1.4.2 Conducting polymers in biosensors

Conductive polymers gain more popularity to enhance performance of biosensors. Conductivity and spectroscopic properties can be changed significantly from doped to undoped state of conductive polymers, while this properties can be applied in biochemical reaction. Since conductive polymers with the conjugated carbon backbone are flexible in derivatives structures, it can be modified with different functional groups. With different chemical structures, it is possible to modulate the required electronic, mechanical and chemical properties. When the polymeric chain changes, of conductive polymers is highly sensitive to this changes such as DNA hybridization and antibody-antigen reaction. As the results, electron delocalized, electronic and optical properties

changed. These changes or delocalization can be measured and represent the concentration of a target analyte molecule.

Some conducting polymers are bio-compatible and bio-friendly in neutral aqueous solutions. With functionalized side chains, the polymer can be modified to bind bio-components like nucleic acid and proteins. Ionsu used PPy with functionalized NHS side group to covalently bind an amino-21-mer ssDNA probe for detection of a short ssDNA of the WEST Nile Virus. When a target ssDNA was incubated with modified PPy electrode, a complementary biotinylated probe ssDNA with a biotinylated glucose oxidase solution was added. ssDNA probe was specifically bonded with glucose oxidase through an avidin bridge. After that, the hybridization DNA complex PPy electrode was tested in glucose solution. The limit detection of ssDNA in this study was 1 fg/ml [52]. Besides PPy, other conductive polymers are used in many studies. For example, polythiophene. Water-soluble cationic polythiophene derivatives are applied in optical DNA detection. When polymers interact with ssDNA and dsDNA, polymer conformation varies and its color changes [53]. Meanwhile, thiophenes ended with functional groups such as primary amine ($-NH_2$) and carboxylic acid ($-COOH$), suitable for the immobilization of biomolecules. Lee proposed an approach for electropolymerizing terthiophene monomer with a carboxyl group on a glassy carbon electrode. This electrode showed high specificity of DNA detection with comparing with single base mismatched DNA. Mismatched DNA only had 14.3% response of target DNA [54].

Utilization of conductive polymers is not only a benefit of immobilization substrate but is also an active transduction. Polymers are capable to be synthesized directly on electrodes and deposited on the surface of electrode, while it traps bio-component simultaneously. Keith produced a virus-PEDOT film by electro-oxidation of EDOT in solutions containing the virus (M13) at a gold electrode. When an antibody (p-Ab) bound to the M13 specifically, virus-PEDOT's electrochemical impedance increased. As the results, it causes a shift in both real (Z_{RE})

and imaginary (ZIM) impedance from a broad range, 50 Hz to 10 kHz [55]. Through trapping with bio-components, conductive polymers can provide a 3-D electrically structures for many applications. Gao presented a research for DNA detection by using PANi as a hybridization indicator. 4-aminothiophenol and peptide nucleic acid was self-assembled onto a gold electrode. This peptide nucleic acid played as a capture probe in biosensor system and formed a heteroduplex when was hybridized with target DNA. When probe ssDNA with HRP labeled was added in, it hybridized with target DNA. As the results, HRP was immobilized onto the electrode surface. Monomer aniline was added in this reaction system with H_2O_2 . HRP catalyzed the polymerization of monomer and result in forming PANi on the heteroduplex structure of DNA molecules. When PANi was deposited on DNA, it indicated the electroactivity of the HRP, which could represent quantity of target DNA in solution. The limit of detection was 1.0 fm. In this study, PANi worked as both indicator and signal-amplification unit, which effectively decreased the non-hybridization background noise.

1.5 Biosensors in food science

Food can be contaminated by various sources, such as overdose veterinary drugs and pesticides, phytotoxins and marine toxins, pathogen bacteria. Reliable and fast analysis of food is not only important for consumers safety but also significant for food industries. Real-time and early detection can prevent food industries from crisis and losses. For example, though liquid chromatography–mass spectrometry (LC-MS/MS) is used to detect multiple chemicals like toxins, pesticide and veterinary drugs, it is expensive, time-consuming and sample preparation is complicated. Since biosensor devices could offer real-time monitoring in low costs, it shows more popularity to apply in food processing. For example, Liu described a flow injection amperometric biosensor for organophosphate pesticides detection. This research used a carbon nanotube (CNT)-modified glassy carbon (GC) electrode as substrate, and acetylcholinesterase (AChE) as a cationic layer. AChE was immobilized layer-by-layer on the negatively charged CNT surface by and formed polymers, poly(diallyldimethylammonium chloride) (PDDA), spontaneously. Since this layer-by-layer structure (PDDA/AChE/PDDA) on the CNT surface provided a favorable microenvironment to stabilize and activate AChE, electrochemical detection of the enzymatically generated thiocholine product increased greatly due to high activity of AChE. The advantage of this layer-by-layer modified electrode was using a low oxidation overvoltage (+150 mV), higher sensitive and stable. Compared to LC-MS/MS, this complex biosensor electrode could measure paraoxon as low as 0.4 pM within 6 mins. This study showed that biosensor system was an ideal tool potentially for real-time and online monitoring of organophosphate pesticides[56].

Enzyme-linked immunosorbent assays (ELISAs) is the most common method for bio-analyte and organic chemicals detection. The basic format of ELISAs is in 96-well-plate. It has been widely used in food security lab to monitor to monitor mycotoxin like aflatoxin[57] and bacteria toxin such as botulinum toxin[58]. Even though some level of automation and miniature

devices have been produced in the recent years, it still considered as a complex and time consuming method. Biosensors on the other hand, represent a potential alternative to ELISAs. It is one of the most promising ways to provide a fast, simple, cheap, reproducible and multi-analyte detection methods. Most of biosensor devices are based on ELISAs basic theories, however instead of using colorimetric or fluorescent signals, biosensors provides digital information which is easy to see and report. For example, Liu's group provided a new ELISAs concept to detect aflatoxin B1 (AfB1) on a micro-comb electrode. This biosensor electrode was fabricated with HRP and AfB1 antibodies onto gold electrode where functionalized with nanoparticles (AuNP). AuNP in this study provided a microenvironment for immobilization of antibody and decreased the electron transfer impedance. Since the anti-AfB1 and AfB1 was formed in reaction solution, a barrier of electrolyte mediator was built to block the electron transferring between HRP and electrode surfaces. The conductance of electrode varied when different concentration of AfB1 was added in. The limit detection limit from this study was 0.1 ng/ml[59]. Moreover, this method could be used to the detection of other bio-analytes extendedly.

Despite of multiple toxins and pesticide, allergens are dangerous and life-threatening for people with food allergies. The most common allergen are these eight ingredients: eggs, milk, fish, peanuts, crustacean shellfish, tree nuts, soybean and wheat. These eight allergens in food are been called Big-8. Big-8 causes about 90% of food allergies in the United States and must be declared labeled on any processed food. Moreover, unlabeled contamination happens during storage, manufacturing procedures or cleaning procedures. Both labeled and unlabeled allergens contamination must be avoided and monitored. A sensitive, specific, and rapid method to identify foods containing allergens is required by the food industry. Biosensor is considered as a potential method for real-time, direct, on-line detection of allergens along the food processing chain. Research from Eissa introduced a novel label-free voltammetric immunosensor for sensitive detection of β -lactoglobulin. β -lactoglobulin is the protein which causes milk allergic reaction. They were

trying to use graphene modified screen printed electrodes with covalent immobilized β -lactoglobulin antibodies. This study was focused on the electrode functionalization, an organic film was formed through aryl diazonium salt electrografting. When the concentration of β -lactoglobulin increased, DPV reduction peak of mediator, $[\text{Fe}(\text{CN})_6]^{3-/4-}$, decreased linearly. The limit detection of this procedure was 0.85 pg mL^{-1} in PBS buffer. This device was also tested in various food systems such as cheese snacks, cake and sweet biscuits. The results of using biosensor electrode correlated with the results obtained from commercial ELISA kit[60].

The most serious crisis for food industries are micro contaminations. The annual report of food-borne disease out breaks of 2012 showed that 88% of hospitalizations are because of pathogens. Among the all foodborne pathogens, these pathogens are responsible for the most outbreaks. *Salmonella enterica* caused 113 outbreaks, *Campylobacter* 37, *Escherichia coli*, *Shiga toxin-producing (STEC)* 29, *Clostridium perfringens* 25 respectively. Since several continuous outbreaks, food-borne pathogens are considered a major public health concern and cost the food industry many millions of dollars each year. High-risk food products are inspected strictly of certain pathogens before sold for human consumption. Therefore, developing methods that can be utilized by industry directly and detect any or multiple pathogens showed attracted. Conventional methods of bacteria detection are time consuming and those methods them-self bring risk of contamination because of bacteria enrichment procedures. The commercially available test kits such as ELISAs are expensive and requires laboratory skills. Biosensors for real-time and multipathogen testing approaches are becoming attractive. Since bacteria contains unique nucleic acid, surface antibodies and special enzymes, all of them could act as bio-analytes as the detection target in biosensors.

Optical biosensor is a fiber optic device, when fluorescent-labeled pathogens bound to the fiber, it excited fluoresce which could be detected by the laser wave (635 nm). It could be used as a real-time inspection method for not only bacteria but also toxins when fluorescent detector

exists. When a fluorescent-labeled antibodies specific react with target(antigens), target was labeled with fluorescence and then be delectated. DeMarco in 1999 reported a fiber optic biosensor to detect *E.coli O157:H7* in ground beef. They used cyanine 5-labeled anti-*E. coli O157:H7* on a silica fiber and signal acquired by launching a 635-nm laser light and collected at 670 to 710 nm. This method was able to detect *E. coli O157:H7* to 3 CFU/ml in ground beef samples[61]. Similarly, An immunosensor optic fiber to detect *Listeria monocytogenes* was introduced by Tao from 2003. From this research, polyclonal antibody was immobilized on polystyrene fiber[62]. A fiber optic biosensor using fluorescence resonance energy transfer (FRET) was developed to detect in ground pork by Ko. Anti-*Salmonella* antibodies labeled with FRET donor fluorophores and G protein labeled with FRET acceptor fluorophore formed antibody–G protein via the incubation. This complex was then loaded on silica fiber. The limit detection of *Salmonella* in homogenized pork samples was 10^5 CFU/g with only 5min response time[63]. Optical biosensor cooperated with antibodies showed high specificity and quick response time.

Surface plasmon resonance(SRP) biosensor is an optical illumination on metal surface. Pathogens were captured by antibodies on surface of thin film electrode. Electron cloud of on the metal and light interacted and generated strong resonance at certain wavelengths. When metal surface loaded with pathogens, the peak of resonance shifted and amount of shift could linearly reflected the concentration of bound cells. The limit of SPR biosensors could be as low as femtomolar. SPR system was studied to detect of whole cells such as *E. coli O157:H7*, *Salmonella*, and *Listeria* in low concentrations. A study was done by Taylor, which introduced a 8-channel SRP for four species of bacteria, *E.coli O157:H7*, *Salmonella*, *Listeria monocytogenes*, and *Campylobacter jejuni*[64].

Piezoelectric sensor is another method based on resonance. This resonance is sensitive to the mass varies on the surface. When the surface of piezoelectric sensor is coated with bio-captures, bacterial specific target loads on the surface will result in increasing mass of quartz crystal. This increment could be detected by the quartz crystal microbalance (QCM). Chen provided a circulating-flow piezoelectric biosensor for real-time *E.coli O157:H7* detection. They used thiolated gold modified electrode as ssDNA capture probe (Probe 1). When *E. coli O157:H7* eaeA ssDNA fragment amplified by PCR, it hybridized with capture DNA on probe. As the results, the mass changed and a consequent frequency shifted of the piezoelectric biosensor. AuNP with complementary DNA sequences conjugated on the second thiolated probe (Probe 2).

Since AuNP here acted as a “mass enhancer” and “sequence verifier”, it amplified the frequency change on piezoelectric biosensor. The limit detection of this method was 1.2×10^2 CFU/ml. This method also could be used in complex food matrix[65].

Electrochemical detections are most common methods to be used in food biosensor devices. Compared to other biosensors methods, this methods do not require high cost equipment such as SPR spectrometer or QCM or environmental vulnerable reagent such as fluorescent reagent. Electrochemical devices are very sensitive and have been used to studied for detection of different pathogens. These biosensors are cooperated with HRP or ALP labelled target used as genosensors or immunosensors. An example used immunosensors was using magnetic beads in electrochemical assays for the detection of *Salmonella*. Since the magnetic beads was coated with anti-*Salmonella* antibodies, they coupled with another ALP-labeled antibodies. *Salmonella* was sandwiched between two antibodies and formed antibodies-antigens complexes. These complexed was localized onto the surface of a disposable graphite ink electrode by magnet. The limit detection was 8×10^3 cells/ml in a total analysis time of 80 min[66]. While this method requires to use magnetic bead for separation and concentration. Rishpon introduced a separation-free method for detection of *S. aureus*. GO and anti-Protein A antibodies were bounded on the

surface of a carbon electrode. Target, *S. aureus*, with HRP-labeled anti-Protein A antibodies was added. With the sandwich antibody-antigen-antibody complexes, H_2O_2 could be oxidized by HRP on the electrode surface. H_2O_2 was generated through glucose oxidized by GO. Iodide ions worked as electron mediator and reduced on the surface of electrode. The limit of detection of this method was 10^3 cells/ in 30 min[67].

Electrochemical impedance spectroscopy (EIS) is a method to characterize the dynamics of an electrochemical process. Compared to electrochemistry methods, EIS can be used in label free system which will simplify sample preparation. Tully described a method using EIS for the detection *Listeria monocytogenes* based on protein on cells' surface. PANi was electro-polymerization on carbon electrodes and loaded with anti-InIB (Internalin B) protein antibody using a biotin-avidin system. Various concentrations of InIB antigens were added and the impedimetric responses were recorded simultaneously. Conducting polymer redox states varied when antigen was applied. The impedance analyses were based on charge transfer on polymer layers which was influenced by redox state of polymers. Subsequently, monitoring the impedance of the conductive polymers determined the antigen loaded on the surface surface. The limit detection of InIB was 4.1 pg/ml[68].

CHAPTER 2

WATER-SOLUBLE ELECTROSPUN NANOFIBERS AS A METHOD FOR ON-CHIP REAGENT STORAGE

2.1 Abstract

This work demonstrates the ability to electrospin reagents into water-soluble nanofibers resulting in a stable on-chip enzyme storage format. Polyvinylpyrrolidone (PVP) nanofibers were spun incorporating the enzyme horseradish peroxidase (HRP). Scanning electron microscopy of the spun nanofibers was used to confirm the non-woven structure with an average diameter of 155 ± 34 nm. The HRP containing fibers were tested for change in activity following electrospinning and during storage. A colorimetric assay was used to characterize the activity of HRP reacting with the nanofiber mats in a microtiter plate and monitoring the change in absorption over time. Immediately following electrospinning, the activity peak for the HRP decreased by approximately 20%. During a 280 day storage study, the loss in activity began to stabilize at approximately 40%.

In addition to activity, the fibers were observed to solubility in the microfluidic chamber. The chromogenic 3,3',5,5'-tetramethylbenzidine solution reacted immediately with the fibers as they passed through a microfluidic channel. The ability to store enzymes and other reagents on-chip in a rapidly dispersible format could reduce the assay steps necessary by an operator.

Keywords: polyvinylpyrrolidone (PVP); nanofiber; electrospinning; microfluidic biosensor; enzyme storage

2.2 Introduction

2.2.1 Lab-on-a chip

Lab-on-a-chip (LOC) devices have been applied in many fields, such as point-of-care diagnostics, biowarfare detection and food safety. But their application as biosensors often require the use of sensitive bioreagents to enable detection [1]. Often, reagents are pumped into the device from an off-chip source using a syringe pump [2] or pneumatic pump [3]. Unfortunately, incorporation of these peripherals reduces portability and miniaturization of a finished device. Ideally, a LOC would store all necessary reagents directly on-chip thereby reducing user handling and simplifying the final device.

2.2.2 Nanofibers applications

Nanofibers containing multiple components are a promising method for on-chip storage [4]. Electrospinning is not only a simple, inexpensive and versatile process to form nano-scale fibers with large surface areas [5] but also a rapid way to evaporate solvent while maintaining the integrity of the components [6]. These unique features ensure the potential applications of electrospun bio-composite nanofibers in many aspects, such as clothing [7,8], membrane distillation [9,10], biomedical sensing [11], catalysis [12], biomedical application [13] and enzyme storage [14].

2.2.3 PVP [Poly(vinylpyrrolidone)] nanofiber applications

Polyvinylpyrrolidone (PVP), a common hydrophilic polymer [15], has good film formation properties which makes it popular for electrospun nanofibers. PVP is soluble in water and absorbs up to 40% of its weight at ambient conditions [16]. Typically, enzymes have a shortened shelf life when stored at ambient conditions and would require lyophilization. Electrospinning, which is able to dehydrate samples in a timescale of milliseconds, may offer ideal alternative preservation methods for biological samples [17]. In this study, PVP electrospun nanofibers were made to store

HRP in ambient conditions. The fibers serve as a mechanism to not only store the enzyme, but also to distribute it evenly within the sample solution. The solubility and small dimensions of the fibers make them ideal for a rapid delivery of reagents.

2.3 Experimental

2.3.1 Electrospun Nanofiber Preparation

The spinning solutions were prepared by mixing 15 wt% PVP, 5 wt% sucrose and 0.01 mg/mL HRP/water solution. The sample was stirred gently for 30 min to allow for a uniform distribution. The mixed solutions were pulled into a 1 mL plastic syringe (National Scientific Company, Rockwood, TN), equipped with a stainless steel 22 gauge blunt needle (SmallParts, Inc., Seattle, WA). The positive electrode from a high voltage (10–30 kV) DC power supply (Gamma High Voltage Research Inc., Ormond Beach, FL) was clipped to the needle. A grounded copper plate used as a collector was placed 12 cm away from the tip of the needle. The nanofibers were formed using a potential of 20 kV and pumped at 1 mL/hr using a syringe pump. The collected fibers were removed from the copper plate and placed in a desiccator at room temperature until use.

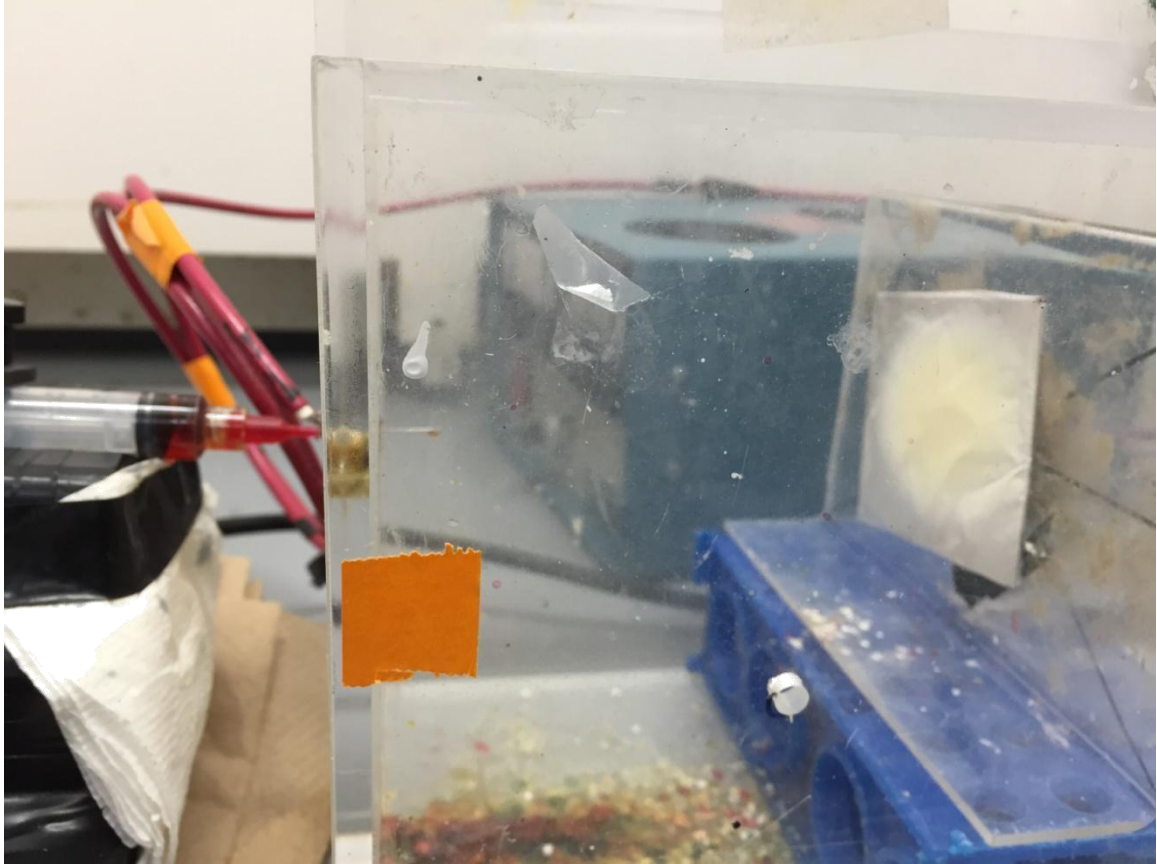


Fig 2.1 Lab-made electrospinning set-up. Electrospinning uses an electrical charge to

draw fibers from a liquid. When a sufficiently high voltage is applied to a liquid droplet, the body of the liquid becomes charged, and electrostatic repulsion counteracts the surface tension and the droplet is stretched, at a critical point a stream of liquid erupts from the surface. Then the jet dries in flight and finally deposited on the grounded collector.

An electrode that is maintained in contact with the polymer solution

A high-voltage DC generator connected to the electrode

A grounded or oppositely charged surface to collect the nanofibers.

A viscous polymer solution

2.3.2 Materials

PVP of M.W. 130,000 was purchased from Sigma-Aldrich (St. Louis, MO). D(+)-Sucrose (99+%), Horseradish peroxidase(HRP) and 1-step slow 3,3',5,5'-tetramethylbenzidine (TMB) kit (1-StepTMSlow TMB-ELISA) was obtained from Thermo Fisher Scientific Inc. (Rockford, IL).

2.3.3 Scanning Electronic Microscope (SEM)

Fiber mats were sputter-coated with gold for 90 s and observed with a scanning electronic microscope (JEOL JSM 6320F) at an accelerating voltage of 5 kV. The average fiber diameters, the standard deviations were calculated from the SEM images using the software ImageJ (National Institutes of Health) to measure 30 fibers.

2.3.4 HRP Activity Measurement

Fibers mats were removed from the copper plate and cut into round pieces using a 1cm diameter punch. The mass of the fiber pieces were extremely low and therefore five cut pieces were then cumulatively weighed and an average mass was determined. From the average mass, the quantity of HRP within each cut piece was calculated using the original mass fraction of the dry constituents. Each piece was placed into a single well of a 96-microtiter plate for reaction analysis. The enzyme activity was compared to an equal mass of HRP which did not undergo the electrospinning process in order to compare the change in activity. The indicator TMB is a chromogen that yields a blue color when oxidized, typically as a result of oxygen radicals produced by the hydrolysis of hydrogen peroxide by HRP. The oxidized TMB has maximal absorbance at 652 nm [18]. For the activity assay, 150 μ L of 1-step slow TMB kit was added to 100 μ L water and added to the well containing the nanofibers. The plate was then inserted into a microtiter plate reader (Biotek, Winooski, VT) where the absorption at 652 nm was measured over time. Activity was quantified by an increase in adsorption at 652 nm.

A negative control representing equivalent concentrations of PVP and sucrose without HRP was also measured. The enzyme activity comparison was measured immediately after electrospinning to determine the initial activity. After storage in desiccator for 45 and 280 days, enzyme activity within the fibers was again characterized.

2.3.5 On-chip Microfluidic Devices with Nanofibers

In order to demonstrate the ability of enzyme containing nanofibers to deliver reactive enzymes on-chip, a microfluidic on-chip device was designed using auto CAD and fabricated by a 30W desktop laser (Epilog Laser, Golden, CO). The device consisted of a two bonded pieces of PMMA, the nanofiber mat and an absorbent pad. One of the pieces of PMMA was structured with microfluidic channels, an inlet port and a cavity for the absorbent pad and nanofiber, while the other piece remained unpatterned. These structures were all fabricated on the PMMA sheet using laser ablation. Following laser ablation, polymethyl methacrylate (PMMA) chips were sonicated in 15% isopropanol for five minutes (Branson Ultrasonic Corp, Danbury, CT) and UV treatment for 5 min. For bonding of the two PMMA pieces, 20 L 2,4-pentanedione was deposited onto the unpatterned piece of PMMA and allowed to sit for 25 s before the PMMA was spun at 1,250 rpm on spin coater for five seconds (Laurell, North Wales, PA) [19]. The nanofiber mats and an absorbent pad (CF5, Whatman, UK) were placed into their respective laser ablated chambers of the patterned PMMA and the two PMMA pieces were then pressed together at 4,500 MPa at 37 °C for five minutes using a hydraulic press with heated platens (Carver Inc., Wabash, IN).

In order to qualitatively demonstrate the activity of the enzymes in the microfluidic chamber, 100 L of the TMB solution was placed into the inlet of the microfluidic chip. The solution was transported through the channels and into the nanofiber chamber using capillary flow. Once in the chamber, the solution dissolved the nanofibers and continued to the absorbent pad. The change in color was observed visually and captured with a camera.

2.4. Results and Discussions

2.4.1 Morphology of Nanofibers

Following eletrospinning for one hour, nanofiber mats of approximately 2 cm diameters were removed from the copper collection plate. The individual PVP fibers containing sucrose and HRP had an average diameter of 155 ± 34 nm (Figure 1). The addition of up to 10% (wt/v) sucrose and 1% (wt/v) protein did not have an effect on the morphology of the nanofibers.

Figure 1. The SEM imagine of polyvinylpyrrolidone (PVP) nanofibers electrospun from 15wt% PVP, 5wt% wt sucrose in 0.1 mg/mL HRP water solution at a gap distance of 12 cm with the applied voltage of 20 kV.

2.4.2 HRP Enzyme Activity

HRP activity was determined by reacting with TMB. As this reaction starts, the oxidized TMB produces a blue color with an absorbance peak at 652 nm. A continuation of the reaction yields a yellow shift with an absorbance peak at 450 nm and a subsequent drop at 652 nm.

The average weight of each 1 cm fiber mat was 0.8 mg and was therefore calculated to contain approximately 0.04 g HRP. Therefore, during activity measurements, the control contained 0.04 g HRP with similar rations of PVP and sucrose. Following the addition of TMB-containing reaction solution to the nanofibers, the absorbance at 652 nm was monitored over time Figure 2A. The results indicate that the HRP control solution without having been electrospun peaked in 30 s and sharply declined. The average maximum absorption for the control was 1.21. The absorption peak of the electrospun nanofibers was 0.99 and occurred only after 1,300 seconds. This is most likely due to a slower hydration resulting from the PVP matrix. Part of the slow hydration may have been due to bunching of the relatively large area matt being placed into a relatively small well.

Following desiccated storage at room temperature for 45 days, the activity of the electrospun HRP decreased to 60% and stabilized at approximately 40% (Figure 2B).

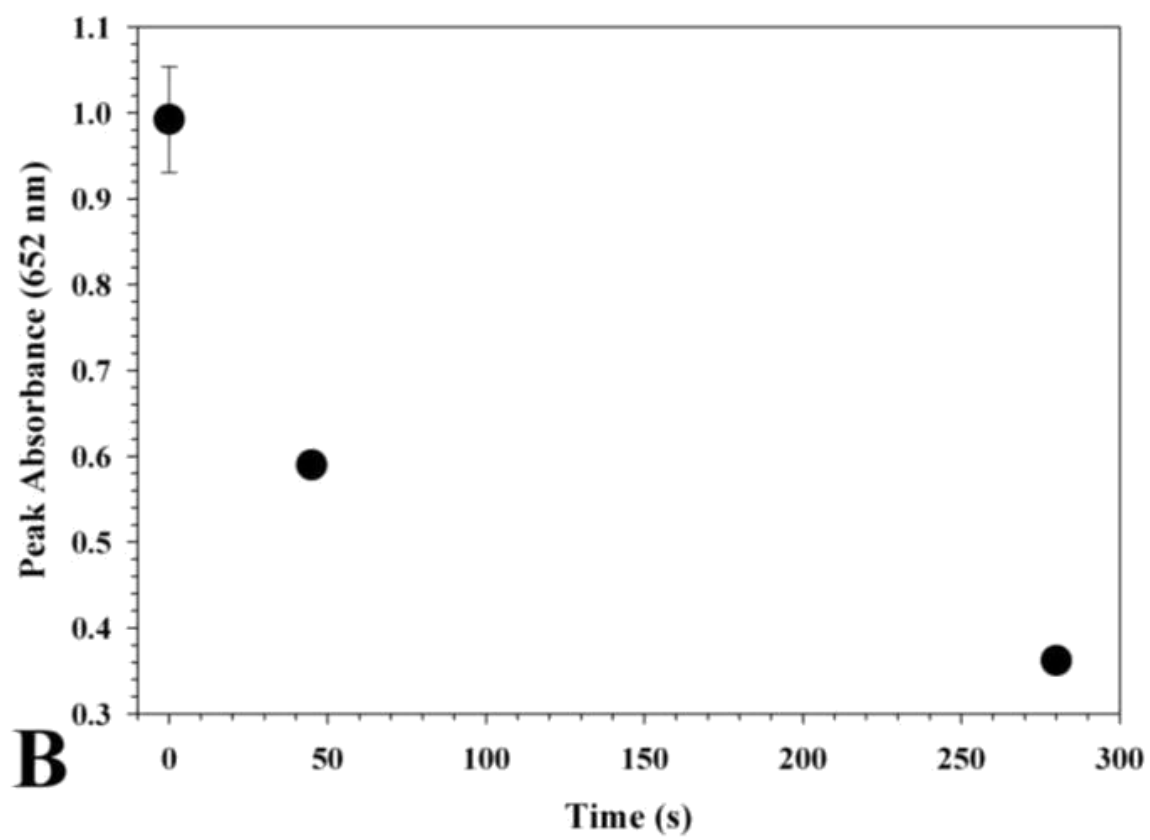
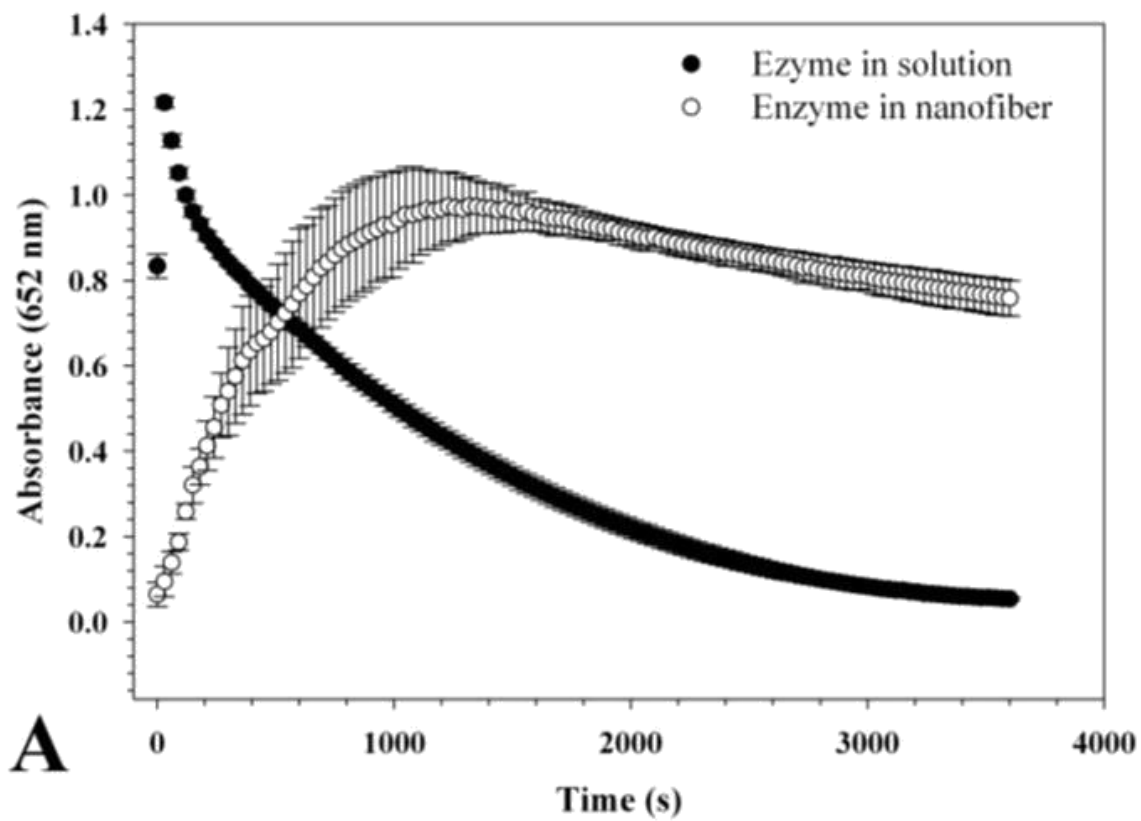


Fig 2.2 (A) Horseradish peroxidase (HRP) activities before and after electrospinning was detected by 1-step slow TMB kit. 150 μ l 1-step slow TMB kit mixed with 100 μ l water was used by measuring change in absorption at 652 nm every 15 s for 1 h. The equivalent quantity of HRP was 0.04g. The reaction initially oxidized the TMB substrate yielding a blue color and 652 nm peak in absorbance. As the reaction progresses, the color shifts to yellow and has a 450 nm maximal absorbance. (B) The activity of the enzyme initially dropped and stabilized over time.

2.4.3 On-Chip Microfluidic System

Electrospun nanofiber mats in microfluidic chip appeared white prior to the addition of the TMB solution Figure 3(A). After the addition of the TMB solution, the fiber dissolved and became transparent soon after the solution reached the white mat. After approximately 60 s, the mat turned blue and the solution passed through microfluidic channel to the absorbent pad Figure 3(B). This reaction time was significantly shorter than the results observed using the plate reader. After the solution passed through the nanofiber channel and into the absorbent pad, there were no visible signs of the nanofiber left suggesting it was fully dissolved. Microfluidic chips were tested both immediately following fabrication and after storage in a room temperature desiccator at for 45 days. Given the nature of the assay, it was not possible to visually quantify the enzyme activity of the nanofibers within the microfluidic chip.

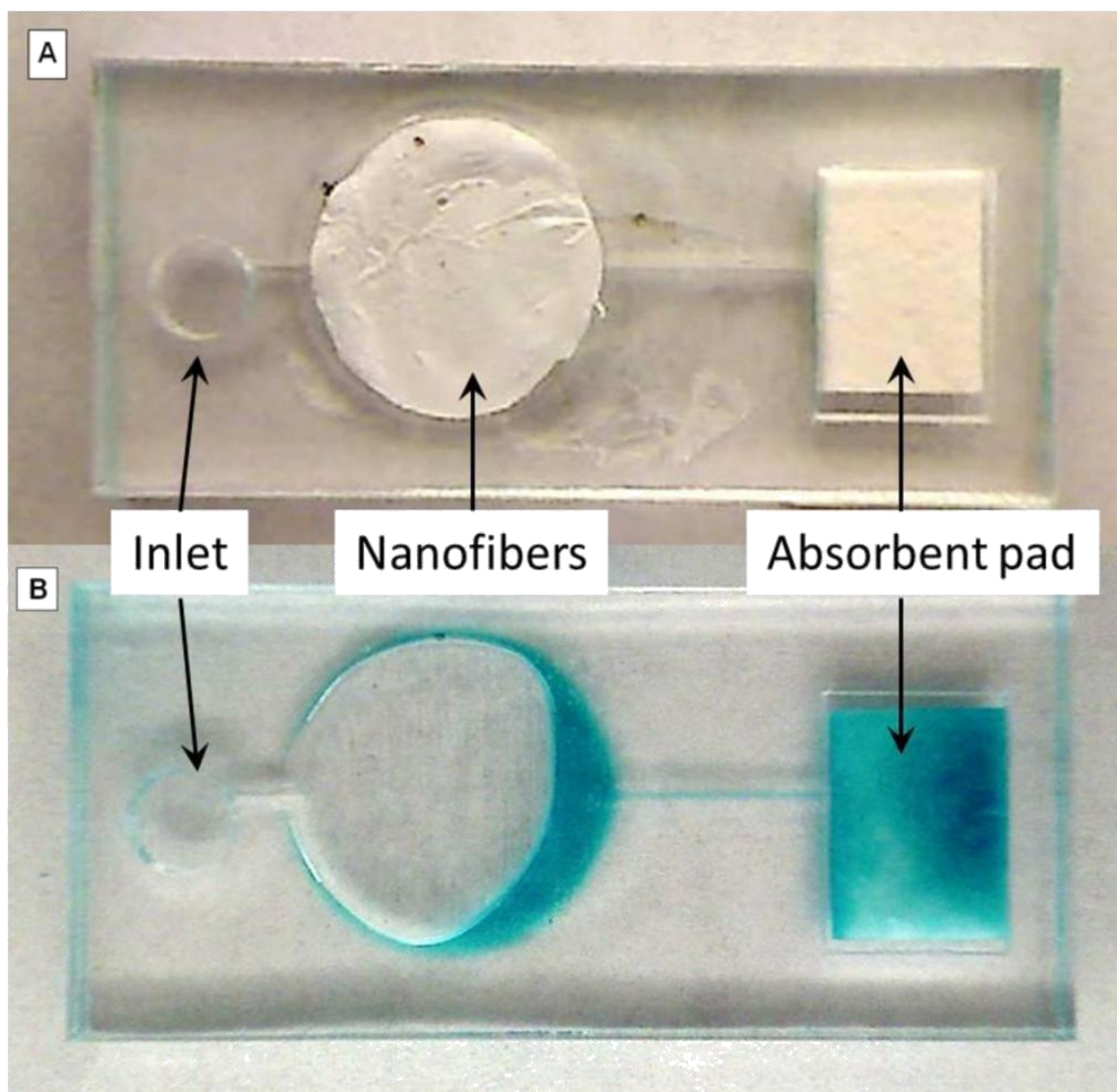


Fig 2.3 Images of electrospun nanofiber in microfluidic chip. The image demonstrates how a nanofiber mat can be incorporated into a microfluidic chip. The images are before (A) and after (B) 100 L 1-step TMB reaction solution was added. The color change was observed after approximately 60 s.

2.5 Conclusions

In these experiments, we have demonstrated the use of water-soluble nanofibers for the storage of enzymes within a microfluidic chip. Horseradish peroxidase was selected due to its ubiquity in diagnostic assays. The results demonstrated an initial drop in activity following electrospinning. After 45 days the activity dropped to 60% and began to stabilize at approximately 40%. The storage was demonstrated in a microfluidic chip where the nanofibers were able to be rapidly dissolved and the released enzymes then catalyzed a reaction with TMB and hydrogen peroxide.

Water-soluble nanofibers can provide an ideal reagent format for microfluidics. Dehydration during the electrospinning process occurs in very short periods of time resulting in an almost instantaneous transformation from an enzyme in solution to a dried enzyme trapped in a polymer and sucrose matrix. The ability to store sensitive reagents inside a microfluidic sensor will enable increased portability and user friendliness. By containing reagents within the chip, the operator will be required to perform fewer steps thus increasing the ease-of-use. A self-contained device would be ideal for resource-limited areas where these characteristics are necessary.

CHAPTER 3

BACTERIOPHAGE *T7* DEHYDRATION AND STORAGE IN ELECTROSPUN POLYVINYLPIRROLIDONE NANOFIBERS

3.1 Abstract

To determine the effectiveness of water-soluble electrospun nanofibers as a means of dehydration and storage of bacteriophage *T7*. The bacteriophage *T7* was added to mixtures of polyvinylpyrrolidone and water and electrospun onto a grounded plate. Trehalose and magnesium salts were added to the mixtures to determine their effect on the infectivity of the bacteriophage following electrospinning and during storage. The fibers were stored at 20 °C in dry conditions for predetermined amounts of time. The loss of *T7* infectivity was determined immediately following electrospinning and during storage using agar overlay plating and plaque counting. It was found that the addition of the magnesium salts resulted in less than a 1 log drop of infective *T7* as compared to a drop of approximately 4 logs without the salts. The trehalose did not protect the *T7* during the electrospinning process, but had a more significant storage effect. None of the electrospinning methods were as effective as lyophilization. The results indicate that the addition of magnesium salts protects the bacteriophage during the relatively violent and high voltage electrospinning process, but is not as effective as a protectant during storage of the dried *T7*. Conversely, the addition of trehalose into the electrospinning mix has little effect on the electrospinning, but a more significant role as a protectant during storage. Previous studies have attempted to encapsulate bacteriophage in water-soluble nanofibers for delivery and storage, but the treatment has typically resulted almost complete deactivation of the phage. Here we investigated the effect reagents on the activity of *T7* during the electrospinning process as well as

storage following the electrospinning. Electrospinning can therefore be seen as a low-cost method for rapid dehydration of viruses.

Key words: electrospinning, *T7 phage*, phage therapy, trehalose, SM buffer, storage, nanofiber.

3.2 Introduction

3.2.1 Introduction of bacteriophages

Bacteriophages have played a significant role in health and medicine. These viruses are able to selectively or broadly infect bacteria and can be used to either introduce genes without lysing the organism (lysogenic cycle), or replicate within the organism until lysis thereby disinfecting the sample (lytic cycle) ^[69]. Phage therapy is a method of combating a bacterial infection by the introduction of bacteriophage specific to the pathogen. The phage then target and deactivate the pathogens present in the host organism. This treatment has seen applications in human health as well as veterinary medicine.

3.2.2 Bacteriophage application in food safety

Bacteriophages have also been used as a method to decontaminate produce post-harvest. Microbiological food safety related to fruits and vegetables continues to be of great concern. As part of the newly established Food Safety Modernization Act, the FDA has given special attention to the need for sanitary agricultural water ^[70]. This water includes produce rinse water as well as irrigation water. The reason for this attention is that agricultural water sources may play a role in the initial contamination of fresh produce. Foodborne outbreaks associated with produce have increased significantly from 0.7% in the 1970's to 13% between 1990 and 2005 ^[71]. Recently, a study by the Centers for Disease Control has concluded that largest source of outbreaks in the United States can be attributed to leafy greens ^[72]. From 1990 to 2005, there has been 713 recorded produce related outbreaks and approximately 34,000 cases of illness associated with produce contamination ^[71].

The lytic activity and propagation of bacteriophages has made them an attractive method for the decontamination of sensitive raw products such as meat and fresh produce. A cocktail of lytic bacteriophages was found to reduce the *E. coli* levels in beef by $\geq 94\%$ and in lettuce by 87% ^[73]. Phages have also been applied to control the growth of pathogens such as

of *Listeria monocytogenes*, *Salmonella*, and *Campylobacter jejuni* in a variety of fresh foods. [74-76]

3.2.3 Dehydration and storage methods of bacteriophages

As the roll of bacteriophages in human health continues to grow, there is a need to study improved storage and delivery methods for their use. Storing phages in a liquid form can be expensive and technically troublesome. Comparatively, encapsulating the phages in dry form is far more attractive. Freeze-drying is the most common and efficient method for long-term preservation of phage. It was reported that the freeze dried phages can be stored at 5 °C under vacuum for 10 years [77]. Nevertheless, freeze-drying method is time consuming and expensive. As an alternative, a novel bioprocess which dries the phages by using a water miscible organic solvent onto glutamine or glycine microcrystals has been developed. The phages were dried and stored for one month with a significant loss of phage activity (10^3 PFU/mL) [78].

3.2.4 Review of electrospinning of bacteriophages

Electrospinning of polymers has been is an attractive and inexpensive method for creating nanostructured fibers with high surface areas [79]. The fibers are made by drawing a charged polymer/solvent liquid onto a grounded collector while evaporating the solvent. Electrospun bio-composite fibers are considered a promising delivery system for many bioactive agents such asenzymes. In our previous work, horseradish peroxidase was spun withpolyvinylpyrrolidone (PVP) for microfluidic devices on-chip storage for further microchip detection. [80]In other experiments, PVP fibers encapsulating M13 bacteriophages exhibited some infection activity following electrospinning. However, the percent viability following electrospinning and storage was not reported. [81]Additionally, *T4*, *T7* and λ bacteriophages were electrospun with Polyvinyl alcohol(PVA) and showed a very low viability following the process. Following storage at 24 °C for 4 weeks, all phages lost viability [82].The loss of viability during electrospinning was reported to be caused by rapid evaporation of water and a drastic change in the osmotic environment around the phage. In order to solve this problem, emulsion and co-axial electrospinning of *T4* phage

were studied^[84]. The phage was spun in the core layer and found to be better protected against the harsh conditions during electrospinning. Even though the viability after electrospinning increased, phage activity was still not detectable after 30 days of storage at 20 °C.

In order to effectively store bacteriophages in nanofibers, the investigation into protective reagents must be conducted. In this work we demonstrate the feasibility of electrospinning *T7* phage from a storage media buffer with trehalose as protector. Additionally, the activity of phage during storage in ambient condition was also tested. In order to alleviate various issues in current available methods, our goal is to develop a rapid, inexpensive and highly efficient desiccation method of bacteriophage. This will benefit long term storage and delivery in ambient conditions.

3.3 Materials and Methods

3.3.1 Materials

Polyvinylpyrrolidone (PVP, MW 130,000) was purchased from Sigma-Aldrich (St. Louis, MO), and trehalose, gelatin, magnesium sulfide heptahydrate, sodium chloride, agar, yeast extract and tryptone were purchased from ThermoFisher (Waltham, MA), bacteriophage T-7 was obtained from ATCC (Manassas, VA) and *E. coli* BL21 from EMD Millipore (Billerica, MA).

3.3.2 Bacteriophage harvest

E. coli BL21 was grown in LB broth (1% tryptone, 0.5% yeast extract, 1% NaCl, pH 7.5) at 37 °C with agitation overnight. A 0.3 mL aliquot of the bacterial culture was mixed with 3.0 mL of warm top agar (LB broth with 0.75% agar) and spread onto an LB agar plate (LB broth with 1.5% agar) for incubation at 37 °C. After 4 hours, 0.5 mL of a bacteriophage T7 stock solution (10^6 PFU/mL) was added on top of the plate and incubated for another 4 hours. During this incubation step, the plaques were allowed to grow until the plate was cleared. To extract the bacteriophage, 5 mL of a storage medium buffer (SM buffer, 1M Tris-HCl, 0.1M NaCl, 8mM MgSO₄, 0.1g/L gelatin, pH 7.5) was then added to the plate and the plate was gently swirled every 30 minutes over 2 hours at 4 °C. The suspension stock was collected and then passed through a 0.22 µm sterile filter. The lysate activity of the suspension was determined by plaque assay test.

This resulted in a highly concentrated bacteriophage stock solution (10^{10} - 10^{11} PFU/mL).

3.3.3 Electrospraying and freeze -drying

PVP solutions were prepared by dissolving 1.5g PVP polymer in either 8.9mL SM buffer or DI water with or without 0.5g trehalose. The formulations are shown in **Table 1**. The bacteriophage stock solution (1mL) and 0.1mL red food dye were mixed into the PVP containing solution for 30 minutes with gentle agitation. The solution was then drawn into a 5mL plastic syringe with a blunt 25gauge stainless steel needle. The needle was placed into a syringe pump (Fisher Model 78-01001,

Holliston, MA) and the positive terminal of the high voltage source was attached to the needle. The syringe pump was set for 0.5mL/hour for 10minutes with a spinning voltage of 25kV applied using a high voltage source (ES30P-5W, Gamma High Voltage Research, Ormond Beach, FL). The distance between the needle tip and grounded aluminum foil sheet was 12 cm. During all electrospinning runs the relative humidity was monitored. Electrospinning was only performed if the relative humidity was below 40%. Following the 10 minutes of electrospinning, the fibers on the foil were packed directly into vacuum bags and sealed. Freeze - drying was performed using 10 times diluted polymer solutions in tubes and liquid nitrogen. All tubes were dehydrated in freeze-dryer for 3 days and packed in vacuum bags. Fibers and freeze-dried samples were all stored in room temperature below 40% humidity.

Table 1 Polymer mixture formulation and bacteriophage initial titer

Formulation (w/v)	Solvent	Titer of the initial phage (PFU/mL)
PVP 15%	DI-water	1.55×10^8
PVP 15%, Trehalose 5%	DI-water	2.55×10^8
PVP 15%	SM buffer	2.90×10^8
PVP 15%, Trehalose 5%	SM buffer	3.35×10^8

3.3.4 Quantification of infectious bacteriophage

Due to the difficulty of determining the mass of the recovered nanofibers, the food dye was incorporated into the fiber mat. The mass of the nanofibers mat was then determined by determining the absorbance of the rehydrated mat. A standard curve was obtained by plotting the absorbance (A) at 523nm of 100, 50, and 20 times diluted polymer solutions. Each fiber mat and freeze-dried sample

was dissolved in 0.5mL SM buffer prior to absorbance measurements. The initial bacteriophage concentrations of those samples were calculated according to the standard curve, while the current infectious bacteriophage counts were determined using a plaque assay test.

In the plaque assay test, serial dilutions (10 times dilution) of the bacteriophage stock were prepared. Aliquots (100 μ L) of each dilution were added to 300 μ L *E. coli* BL21 broth, respectively. The mixture was then added 3mL of warm LB top agar and poured onto LB plates. After 3 hours of incubation at 37 °C, the number of plaques was counted for each dilution and reported as Plaque Forming Units/ mL (PFU/mL).

3.3.5 Electronic-microscopy analysis

Morphology of the electrospun fibers was examined by scanning electron microscopy (SEM) and transmission electron microscopy (TEM). For the former, fibers were gold sputter coated for 180 seconds and imaged using JEOL 6320 (Peabody, MA) at 5kV at varying magnifications. The TEM samples were prepared by directly spinning fibers onto the carbon film coated copper grid and then imaged with JEOL 2000FX (Peabody, MA) at 200kV. Diameters of fibers were analyzed using Image-J software and reported as average \pm standard deviation.

3.4 Results and discussions

3.4.1 Morphology from electron microscopy

The diameters of all the electrospun fibers ranged between 100 and 200nm with no visible beading. The SEM images of the bacteriophage encapsulating PVP fibers immediately after electrospinning and following two months of storage are shown in **Fig3.1**. Fibers made with PVP and water had an average diameter of 150 ± 37 nm immediately following electrospinning. Following two months of storage, the average diameter of the fibers was 165 ± 43 nm without obvious morphology change. This represents a 10% change in the diameter during storage. When trehalose was added to the nanofibers solution, the initial diameter was 135 ± 34 nm immediately following electrospinning and 169 ± 64 nm after storage demonstrating a 25% increase in diameter during storage. The fibers also appeared to fuse at the intersecting junctions during storage.

Fibers containing SM buffer had numerous cubic crystals in the surrounding area **Fig3.1(c1)**. The average fiber diameter was 138 ± 65 nm and the average cubic diagonal length of the crystals was 127 ± 33 nm. The diameters of the fibers varied significantly with the smallest being less than 50nm. After two months storage, the average diameter of these fibers increased to 154 ± 29 nm representing a 21% increase. The crystals also increased in size with most of them converting from cubes to spheres during the two month storage time **Fig3.1(c2)**. TEM analysis of the fibers revealed that the cubic crystal were distributed unevenly as shown in **Fig3.2(a)**. During the TEM observations, it was observed that the 200 kV electronic beam emission had a damaging effect on the crystals which was shown in **Fig3.2(b)**.

The average diameter of fibers spun from SM buffer with 5% trehalose was 161 ± 23 nm. Although no protruding cubic crystals were observed, the surface of the fibers was rough with amorphous bright knots of inorganic composites. Compared to fibers spun from SM buffer only,

fibers with trehalose had smaller salt crystals and slightly larger fiber diameters. After 2 months storage, the diameter of the fibers (174 ± 30 nm) did not change significantly (8%). The difference between fibers spun from SM buffers and SM buffers with trehalose was shown in

Fig3.3. With no trehalose, numerous bright cubic crystals were observed with diameter around 100 nm. With 5% trehalose, amorphous and smaller bright knots were observed. When 10% trehalose was added, fibers became more hygroscopic and swelled to form smooth fibers without solid bright knots.

3.4.2 Bacteriophage infectivity change after desiccation(electrospinningvs freeze-drying)

Bacteriophage *T-7* has a fragile tail structure which is vulnerable to physical damage during desiccation. In order to determine the effect of electrospinning on bacteriophage infectivity, plaque assays were conducted immediately before and after electrospinning. We found that the inclusion of SM buffer had a significant effect on the final infectivity of the electrospun bacteriophage (One-way ANOVA, $p < 0.050$). The effect of the trehalose on the deactivation of bacteriophage in SM buffer during electrospinning was negligible, no significant difference based on one-way ANOVA test. (**Fig3.4**). The bacteriophage infectivity decreased less than one order of magnitude following electrospinning. On the other hand, infectivity of bacteriophage in nanofibers spun from DI-water dropped from 10^8 to 10^4 PFU/mL during the electrospinning process. These results indicated that the SM buffer played a critical role in protecting bacteriophage from the rapid drying, confinement and high voltage of the process. Meanwhile, the bacteriophage activity in fibers spun from DI-water with trehalose as the protector only dropped to 10^6 PFU/mL, which showed significant difference from pure DI-water (One-way ANOVA, $p < 0.050$). It indicated that trehalose had a positive effect in stabilizing bacteriophage during electrospinning. For samples treated by freeze-drying, the bacteriophage activity dropped less than one order of magnitude in all four formulas, suggesting that compared

to electrospinning method, freeze-drying had less effect on the bacteriophage activity. Only nanofibers electrospun from a solution containing SM buffer and trehalose had similar activity.

3.4.3 Bacteriophage activity change during storage

Given the large surface area of nanofibers, ambient activity such as heat and moisture may have a more immediate effect on their contents. In order to measure the activity change during storage, each fiber was cut into similar size pieces individually packed and vacuum sealed. The activity of the bacteriophage was measured weekly using plaque assays. The data showed in **Fig3.5** suggests that samples without trehalose had a more significant drop in bacteriophage lytic activity compared to those with trehalose. The samples without trehalose both experienced a drop of approximately 3 orders of magnitude as compared to a loss of approximately 1 order of magnitude when trehalose was added. Interestingly, the long-term storage appears to be more affected by the addition of SM buffer rather than trehalose. Following eight weeks of storage the fibers without the SM buffer both had a drop in PFU/mL of approximately 7 logs while the fibers containing the SM buffer had a drop of approximately 3 logs. This suggests that short term stabilization is improved by the addition of trehalose while long term stabilization is improved with SM buffer salts. As the results, SM buffer salt plus trehalose could provide better stabilization.

The freeze dried samples gave significantly different results from those of the electrospun fibers based on one-way ANOVA, $p < 0.050$. The effect of the addition of trehalose seemed to be more consistent throughout the 8 weeks of storage of freeze dried samples. While the best results for both drying treatments were observed with the SM Buffer with trehalose, the activity of bacteriophage freeze-dried with trehalose and SM buffer had no significant difference following 8 weeks of storage while the nanofibers showed a decrease of 2-3 logs. On the other hand, activity in sample freeze-dried from pure DI-water lost 7.5 orders of magnitude after 8 weeks. The best method for the preservation

of the lytic activity of bacteriophage was the freeze dried sample with SM buffer and trehalose.

Bacteriophages are sensitive during dehydration and storage, Our research showed that T7 bacteriophage could survive the air-drying process associated with electrospinning when additives and buffer applied. Electron microscopy analysis results implied morphological variations between different formulas of electrospun fibers, and those variations lead to dehydration and storage difference.

Morphology of electrospun fibers with SM buffer shows difference from the one with DI-water. Unlike smooth fibers made of DI-water, fibers electrospun from SM buffer had small "hairs" on the outside. The difference can be attributed to the solvent. Theoretically, four key properties of solvent are particularly important in electrospinning: conductivity, surface tension, dielectric properties and volatility^[85]. Varying any of these properties with additives can cause changes of several other properties simultaneously. For instance, salt in buffer, such as sodium chloride, increased the solvent conductivity with more charge density, which then leads to higher electrical distortion of the droplet shape, resulting in a thinner jet. Under a certain feeding rate, the thinner jet restricts the flow and allows less of the solids to reach the collector. This forms smaller fibers^[86], like those fibers under 50 nm thick. On the other hand, the salt also increased the surface tension of the buffer^[87, 88]. Therefore, a larger potential is required during electrospinning as compared to those with pure water. As a result, the majority of the fibers would be in the 100 to 200nm range as shown in the SEM images. Lastly, Tris (tris(hydroxymethyl)aminomethane) decreases free water molecules via hydrogen bonding. During electrospinning, more water molecules were trapped around the Tris component resulting in thicker fibers. All those effects counteracted with each other and the average diameter of resulting fibers actually had no significant difference from the DI-water fibers. It has also been reported that salts in the electrospinning solution can stabilize the Taylor core^[89]. However, this

effect was not observed in the experiment. The author believed that this might have something to do with the hydrogen bonding formed by the Tris salts.

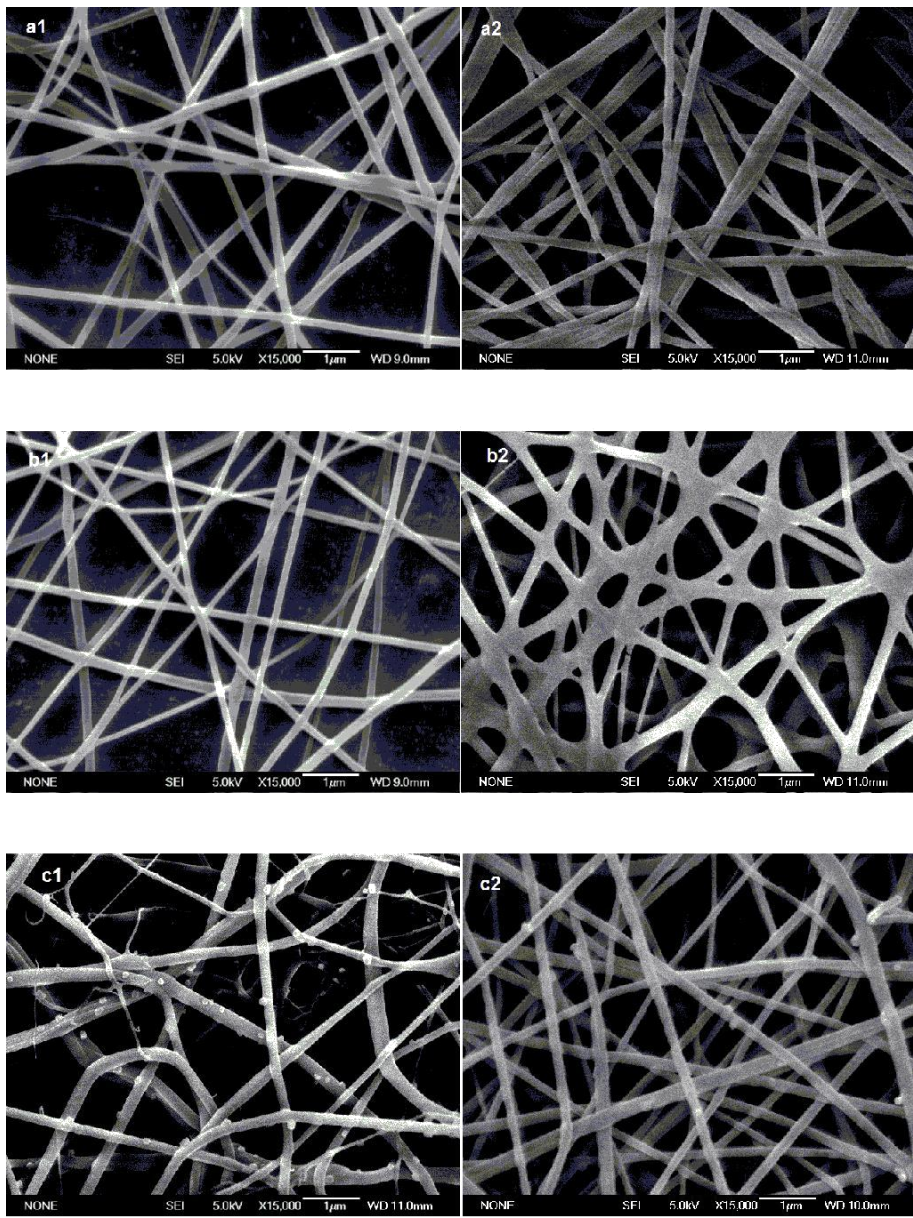
Besides those small "hairs", fibers containing SM buffer had numerous cubic crystals on the surrounding area. These crystals were inorganic salts solidified from SM buffer, such as sodium chloride and magnesium sulfate. During the TEM analysis, inorganic salts crystals were damaged by electron beam emission (**Fig3.2(b)**). An assumption might be drawn from these phenomena that during storage, ambient condition, such as heat, can also change the morphology of the crystals but with a milder rate. Because of small "hair" and cubic crystal structure, surface area was larger than those smooth fibers from DI-water and the randomly distributed bacteriophage had big chance to contact to salts in SM buffer. The buffer solution provides a relevant thermodynamic favorable osmotic environment for protein structure of bacteriophages. Even though, water evaporated during the electrospinning, some water molecules trapped in the fibers might still provide an ideal micro-environment for the phage. Additionally, the Tris buffer salts hydrogen bonds could trap water molecules and form a protective coating with the proteins of the phage capsid and tail.

Trehalose as a additive in electrospun fibers provided protection of bacteriophage during dehydration and short period storage. This could be explained by its properties such as hydrogen bonding with biomolecules or the ability to modify the salvation of proteins ^[90], [HYPERLINK \l "page104" ^{\[91\]}](#). Trehalose and SM buffer were the best combination for bacteriophage long term storage due to morphology of SM buffer fibers also changed with trehalose. The difference between fibers spun from SM buffers and SM buffers with trehalose was attributed to the fact that trehalose replaced water molecules to form bonds with inorganic salts. This mechanism could prevent inorganic salt from forming pure crystals. This hypothesis was supported by SEM image of PVP fibers spun from SM buffer with different concentrations of trehalose **Fig3.3**. As trehalose partial increased, crystal size decreased. As the result, the embedded bacteriophages had large possibility surface contact with salts in buffer. In our study SM buffer with 5% trehalose is the

ideal formulation which had enough hydrogen bonding for preservation but less hygroscopic than fibers spun with 10% trehalose.

3.5 Conclusions

As a conclusion the use of nanofibers for delivery and storage can offer significant advantages over traditional methods. Although several studies have investigated the entrapping bacteriophages in nanofibers, there has been little work on investigating methods to improve stability of the phages. The current work shows that the bacteriophage *T7* can be encapsulated in fibers and that the stability of the phage can be enhanced with additives. The results suggest that the addition of SM buffer in the electrospinning solution had a significant stabilization effect on the phages while trehalose had a lesser effect during the process. While other studies found a 2% recovery of *T7* phages immediately following electrospinning, the current study was able to find a loss of less than one log. The storage study revealed that the trehalose provided a protection during the first week, but that longer-term storage was more significantly affected by the SM buffer. Although none of the electrospinning treatments achieved the stability of the freeze dried sample with SM buffer and trehalose, it is clear that significant improvements can still be made. It is possible that a combination of electrospinning for initial desiccation followed by freeze drying would result in a stabilized sample which is easier to manipulate and transport.



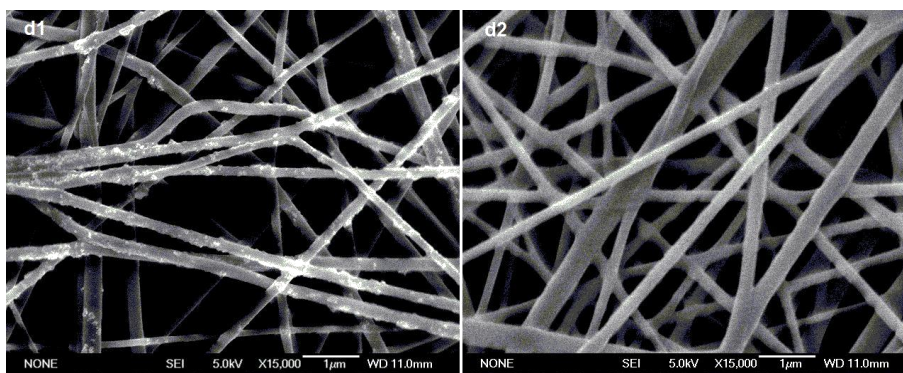


Fig 3.1 SEM images of electrospun PVP (15% w/v) fibers with *T-7* phages:(a1) DI-water,(a2) DI-water after 2 months storage,(b1)5% trehalose in DI-water,(b2)5% trehalose in DI-water after 2 months storage, (c1)SM buffer,(c2)SM buffer after 2 months storage,(d1)5% trehalose in SM buffer, (d2)5% trehalose in SM buffer after 2 months storage.

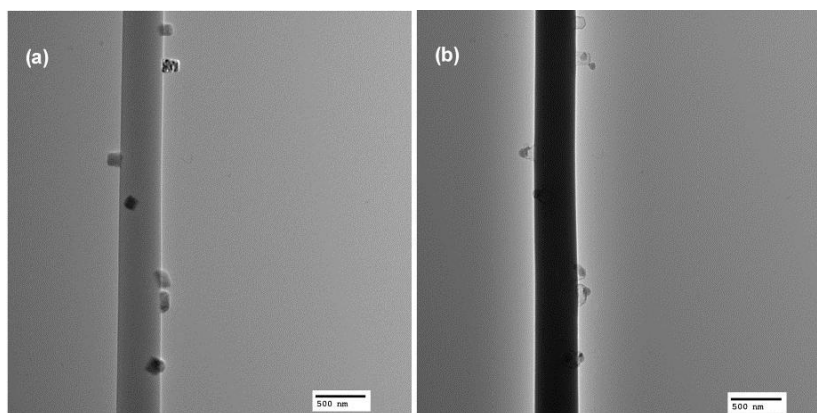


Fig 3.2 TEM images of electrospun PVP nanofibers from SM buffer solution before 200kV electron beam damaging (a) and after (b).

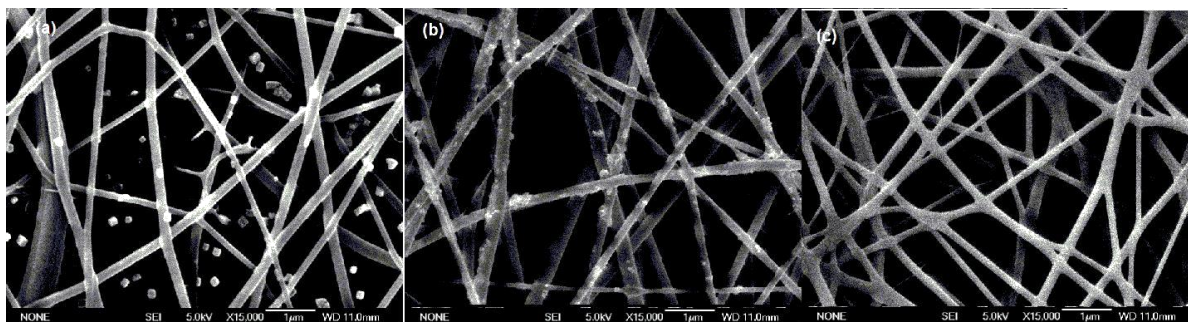


Fig 3.3 SEM images of PVP nanofibers electrospun from SM buffer with trehalose 0% (a), 5% (b), 10% (c).

Lytic Activity after Desiccation (Electrospinning and freeze-drying)

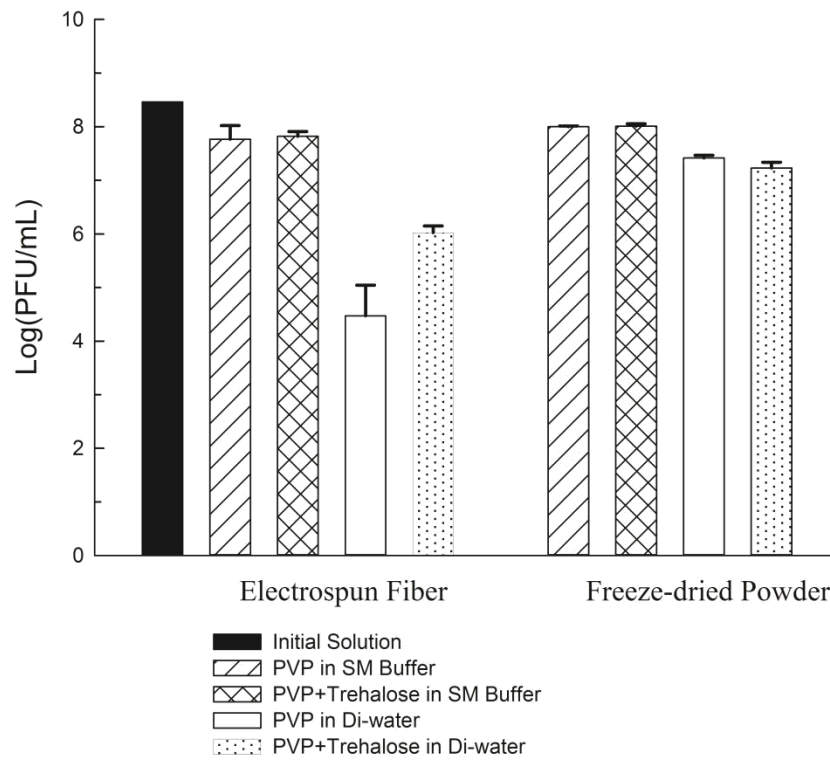


Fig 3.4 The bacteriophage activity after electrospinning and freeze-drying four PVP mixture solutions. The data represent the averages of a minimum of three replicates and error bars represent the standard deviations of the replicates.

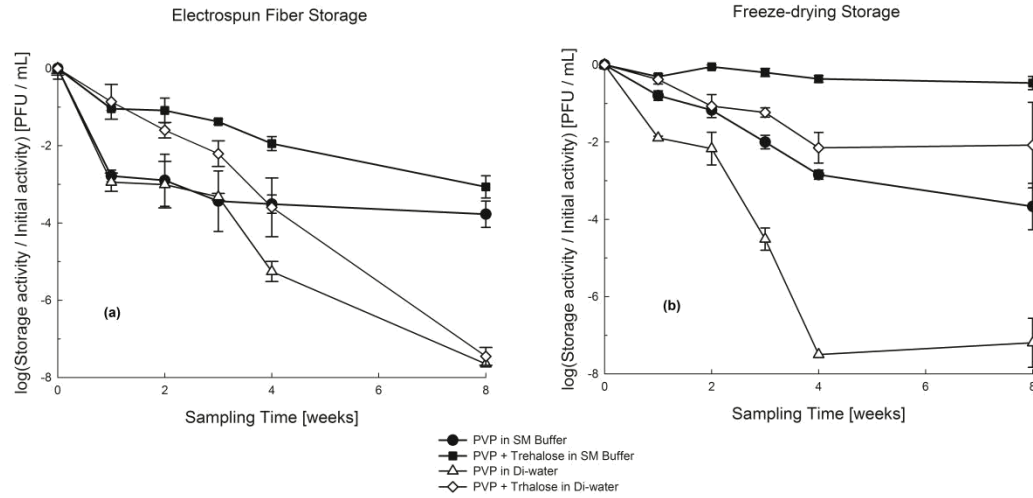


Fig 3.5 Bacteriophage activity changing during storage at 20 °C. Phage activity changing in electrospun fiber format(a), freeze-dried powder format(b). The data represent the averages of a minimum of three replicates and error bars represent the standard deviations of the replicates.

CHAPTER 4

VAPOR-PHASE POLYMERIZATION WITH GOLD PARTICLE SYNTHESIS FOR ELECTROCHEMICAL ELECTRODES

4.1 Abstract

Nanofiber structures of PEDOT, a conductive polymer with gold particle composite on, enhance the electrochemical reaction area and bio-component bonding. However, using traditional electrospinning method could only produce high ration nanofibers under extremely low humidity condition and two steps manufactures. A new method introduced by Julio M, was using one-step vapor-phase polymerization method to produce large quantity of fibers using one step vapor polymerization(OSVP). Our research was using two methods eletrospinnig with vapor polymerization(EVP) and one step vapor polymerization (OSVP) to produce PEDOT fibers and synthesized gold particles on the surface of fiber structures. Gold particles were formed by residue vapor of monomer EDOT being oxidized by chloroauric acid in THF solvent. An alkanethiol monolayer of the self-assembly membrane (SAM) was added on bare gold particles, as the results, gold particles were positive charged, which could electrostatic absorb streptavidin(SA) on the gold surface. Streptavidin gave the position for biotinated target to non-specific bond on the surface.

4.2 Introduction

PEDOT among all different conducting conjugated polymers, is an important working electrode material. Although the monomer EDOT was known for decades, PEDOT polymer is a kind of new synthesis materials and gains more and more popularities for electro-analysis because of its low redox potential, high conductivity and high thermal, electrochemical stability. The oxidant polymerization was not found nor well studied until 1988. There are several common methods of PEDOT polymerization because EDOT is not stable against oxidation. In the other words, monomers could be completely oxidized by very strong oxidants such as Ferric salts(Fe^{3+}) and perchloric acid(HClO_4). The first systematic experiments for oxidizing EDOT was solvent oxidations by using FeCl_3 . Polymerization requires two steps, first is oxidation of monomer to form polymers, second step is to dope the new formed polymers to make them conductive. PEDOT was synthesized in boiling acetonitrile and exhibited conductivity of 15S/cm. Not only Ferric salt could able to oxidize EDOT, other oxidant metal salts such as Ce^{4+} and Cu^{2+} can oxidize monomer to form conductive polymers. However, this method remains a drawback that solubility of reactant monomer EDOT and metal salts are different in polarized solvent. For example, FeCl_3 has high solubility in water while EDOT could not dissolve in water. To solve this problem, the salts of toluene sulfonic acid was used by Bayer who lately made first commercially available PEDOT. This PEDOT aqueous solution was a suspension of PEDOT:PSS which was printable or spinnable on different substrates.

Another common polymerization methods is electrochemical polymerization. This method was first invented by G. Heywang in 1992[92]. There are many studies using electropolymerization in different solutions such as THF with NiCl_2 as catalyst [93], acetonitrile with lithium perchlorate[94] and also in water based buffer solutions [95]. Usually PEDOT was synthesized by being applied to cyclic voltage or constant voltage. Besides polymerization applied potential and solvent, the electrode, catalysts and supporting electrolyte affect the properties of the PEDOT

polymerized films. Unlike the chemical oxidant polymerization doped polymers can be over-oxidized at higher potentials. Partially doping increases mobility of free valence electrons, on the contrary over-doping leads to the decrease of this mobility and even destruct polymer films[96]. The most benefits of using electrochemistry polymerization is that PEDOT is formed on the electrode with bio-composites at the same time. Sarah M polymerized PEDOT with living neural cells[97]. Live cells embedded within the PEDOT matrix remained viable for at least 120 hours. Another study was using M13 bacteriophage to polymerize PEDOT and form hybrids of conducting polymers and viruses for biosensor applications. The virus was incorporated into the polymeric backbone of PEDOT via electro-polymerization[55].

Vapor-phase polymerization (VPP) of PEDOT was a chemical polymerization methods including in chemical polymerizations. However, this method uses monomer vapor instead of mixture solvents. VPP could generate homogenous films which is attached better on substrates compared to solvent polymerizations. VPP gains popularity recently start from 2003. It was firstly described by Mohammadi in 1986[98]. He used FeCl_3 or H_2O_2 as oxidants and polymerized polypyrrole films by applying pyrrole vapor. The first reported study of VPP PEDOT was done by J Kim in 2003[99]. He used 1–5 wt.% solutions of FeCl_3 and made thin film of PEDOT directly on substrates. However, the conductivity of PEDOT from this study was only around 70 S/cm. Soon after Kim, B Winther-Jensen produced a VPP of PEDOT film with a conductivity exceeding 1000 S/cm. In this study, the salts of toluene sulfonic acid, ferric p-toluenesulfonate, was used as oxidant[100]. While during polymerization sulfonate acid generated and inhibit continuously polymerization reaction, a base, pyridine, as a acid inhibitor was added. This present chapter presents a route of VPP of PEDOT film using ferric p-toluenesulfonate as oxidant, a volatile base (pyridine) and being exposed to 3,4-ethylenedioxythiophene (EDOT) vapors reported which is the same as B Winther-Jensen

introduced. However, in order to get a homogenous and thick PEDOT film, in this work, we added a polymer polyvinylpyrrolidone (PVP) to avoid salt crystallization.

Nanostructured shapes were introduced to increase the surface area which would allow more target analytes loaded on the electrodes, which would result in increasing sensing sensitivity. Among all different techniques used to manufacture nanostructures, the electrospinning was an easy way to obtain nanostructures without using clean room or other large equipment. Electrospinning has been successfully applied to produce nanofibers with other conductive polymers such as polyaniline (PANI), (15, 16) and polypyrrole (PPy), (17, 18). While directly electrospinning had a great restriction, which because of the low solubility of conductive polymers. Non-homogeneous solution brought huge troubles during electrospinning. Recently, a two step method was invented by Jaewon Choi's group, they used a two-step in situ polymerization process, first using the oxidant salt to form fibers, and monomer vapors were oxidized on the fibers to form polymers. This method would achieve high number of conductive polymers fibers. Despite the electrospinning method, Julio M. D'Arcy group invented an one -step vapor polymerization method. Since vapor-phase polymerization method could lead to high conductivity and smooth and flat morphology, they demonstrated a simple and direct method to achieve high conductive and ratio of PEDOT.

EDOT is hard to co-valent bonding other molecules because it is lack of side chain after polymerization. In order to expand the application of EDOT, gold particles were introduced on the surface of PEDOT nanofibers. This paper describes an one-step procedure for synthesis gold particles on vapor phase polymerization PEDOT electrospun nanofibers(EVP) and one step nanofibers(OSVP). In order to load more proteins on bare gold surface, the gold particles is modified with thiolated carboxylic PEG.

4.3 Materials and Methods

4.3.1 Materials and equipment

The PVP of M.W. 130,000, 1-Butanol, pyridine, acetonitrile, *N,N*-Dimethylformamide (DMF), ethanol, methanol, tetrahydrofuran (THF) and ascorbic acid were all purchased from Fisher Scientific (USA) was purchased from Sigma-Aldrich (St. Louis, MO). Streptavidin and Biotin-HRP (biotinylated peroxidase) and 1-step slow 3,3',5,5'-tetramethylbenzidine (TMB) kit (1-StepTMSlow TMB-ELISA) was obtained from Thermo Fisher Scientific Inc. (Rockford, IL). 3,4-ethylenedioxythiophene (EDOT) from Sigma Aldrich(USA). Iron(III) p-toluenesulfonate hexahydrate(FeTos) was purchased from AKSci (USA). Toluidine blue O (TBO) was purchased from MP Biomedicals (USA). 5mm Kapton film was purchased from Cole-Parmer (USA).

Cyclic voltammetry (CV) and amperometric (AM) measurements were performed using an electrochemical station analyzer (CHI 760B, CH Instruments, Austin, TX). A Pt wire (Aldrich, 99.9% purity, 1 mm diameter) was used as a counter electrode and an Ag/AgCl as reference electrode. Fiber mats were sputter-coated with gold for 90 s and observed with a scanning electronic microscope, JEOL (Nikon Instruments, Inc. Melville, NY). The SEM operated at a voltage of 10 kV. The average fiber diameters, the standard deviations were calculated from the SEM images using the software Image J (National Institutes of Health) to measure 30 fibers.

4.3.2 Preparation of FeTos film

Gold coated kapton film was prepared by coating 15 nm chromium as adhesive layer and 100nm gold layer. 40 % (w/v) of FeTos and 2.5% (w/v) PVP were dissolved into 1-butanol solution together with a small amount of pyridine(0.5mol/mol FeTos). FeTos coated films with average thickness of 10 ± 2 μm was produced by spin coating with speed at 2000 rpm/s for 10 s. Films were dried on hot plate at 75 $^{\circ}\text{C}$ for 15 min.

4.3.3 Electrospinning of FeTos and PVP nano-fibers

40% of FeTos was first fully dissolved into 1-butanol solution by stirring for 2h. 2% PVP powder then was added in the mixture solution and stirred for overnight until PVP was fully dissolved. A small amount of pyridine (0.5 mol/mol FeTos) as a acid inhibitor was added into mixture solution and stirred for another 2h. The dark brown colored viscous solution was placed into a plastic disposable syringe on an automatic pump, which was fixed on a home -made electrospinning set-up. A flat end steel-needle set with the syringe on auto syringe pump. A copper connector was covered with a Al-foil to connect FeTos fibers. A box was to prevent air flow influences and avoid moisture transmit. The needle was connected with high power supply and connector was well grounded. As the result a high electrical field was produced between needle and connector. The distance between the needle and the connector was 10 cm and the voltage at 20 kV. Relative humidity (RH) in the electrospinning chamber was less than 4% because of little amount of polymer in the solution. The electrospinning time was 10 min for each piece of FeTos fibers. Yellow colored dried fibers was formed when power was on.

4.3.4 Vapor-phase polymerization with Fetos films and electrospun(EVP) nanofibers

100 μ l of 10%(v/v) EDOT, was added respectively in acetonitrile. FeTos coated Kapton films were placed with 100 μ l solutions with these three monomers respectively in three individual petri dishes. Petri dishes were sealed by 25mm wide Kapton tape. The petri dish was heat in oven at three varies temperatures 60 $^{\circ}$ C for 45 min. Following the polymerization, the dark blue polymer films were generated and washed with methanol 3 times to remove un-reacted oxidant and monomers vapors. The reaction temperature were different from each monomers.

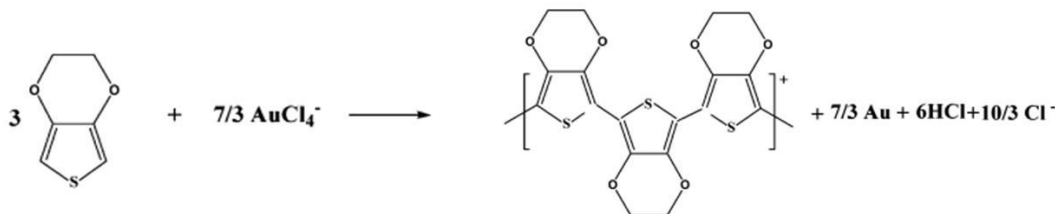
4.3.5 One step vapor-phase polymerization (OSVP) of PEDOT nanofibers

Gold coated kapton film was prepared by coating 15 nm chromium as adhesive layer and 100nm gold layer in clean room. A 150ul droplet of a 0.266M of FeCl_3 water solution was placed on kapton gold film. Quickly moved this film into a metal walled chamber(copper chamber),

where 4 corners were placed with four 5ml beakers filled with 200ul of 10% EDOT(V/V) in chlorobenzene solution. Then, the reaction metal chamber was closed with lid and placed into a preheated 130 °C oven for 27min. When the film was settled into the chamber and oven, the droplet should not be dehydrated. The nanofiber structures were formed between EDOT evaporation from chlorobenzene to polymerize and precipitate on the crystallized FeCl₃ surface. This method was introduced by D'Arcy.

4.3.6 Au-nanoparticle composite synthesis and SAM layer formed on Au-nanoparticle

After vapor phase polymerization, there would be un-reacted monomer EDOT vapor on the surface of porous fiber structures. This amount of residue monomer could react with AuCl₄⁻ to form PEDOT/Au nanocomposites.



All reaction glass containers were sonicated with water and rinsed with THF three time. 0.8ml of 50mM HAuCl₄ (in water solution) was added in 2.2ml 80 °C THF with over 200rpm/s stirring speed. And 50ul of 0.1 mM tricytamine(in THF solution) was mixed as a stabilizer. VPP PEDOT fibers was then added into this 80 °C homogenized THF solution for 60 s and then washed with methanol for three times. Au-composite films were dried in nitrogen flashed chamber for 4 h .

In order to apply carboxylic group and bonding space vacancy on the surface of gold particles, I used alkanethiol monolayer by the self-assembly on bare gold surface. 10mM of 3-mercaptopropionic acid (3-MPA) and 10mM of 11-mercaptoundecanoic acid(11-MUA) were

prepared separately in ethanol. As from a study from Lee's, the best mixture ratio of 3-MPA and 11-MUA was 10:1 for electrostatic binding with streptavidin (SA). SA has for bonding site for biotin, which was widely used as functional tag with bio-markers. The Au-composite nanofiber films were immersed in alkanethiol mixed solution for 24 h. Then films were rinsed with ethanol and water 3 times in turns. Films were dried and stored in nitrogen flashed chamber for future uses.

4.3.7 TBO assay

TBO dye assay was used to quantify how many carboxylic acids group or positive charged on certain area. PEDOT films, EVP PEDOT fibers, EVP/Au PEDOT fibers, OSVP PEDOT fibers and OSVP/Au PEDOT fibers PEDOT were shaken in 0.5 mM TBO solution (in pH 10 water) for 2 h in ambient temperature. The films then be rinsed with pH=10 water 3 times to remove non-absorbed dye and submerged into 50% (v/v) acetic acid to desorbed dye from film surfaces. The absorbance of the dye was detected at 633nm absorbance by Biotek.

4.3.8 Raman Spectroscopy

Raman characterization was carried by using a DXR Raman microscope (Thermo Scientific, Madison, WI, USA) with 50 \times objective lens, 780-nm excitation wavelength, 1-mW laser power. OMNICTM version 9.1 was used to control the Raman instrument. SERS spectra were collected 20 spots on the sample surface.

4.3.9 X-ray photoelectron spectroscopy (XPS)

Polymer structures and existence of gold were studied by X-ray photoelectron spectroscopy (XPS). XPS analysis was performed with a physical electronics quantum (Physical Electronics, Chanhassen, MN) at a spot size of 100 μ m at 25 W. Spectra were obtained at an angle of 45 $^{\circ}$ relative to the samples' plane. Survey scans of every sample were collected at a pass energy of

187.85 eV with a step size of 1.6 eV. High resolution spectra were collected at a pass energy of 46.95 eV and with a step size of 0.4 eV.

4.3.10 Electrostatic immobilization of streptavidin and quantification with Biotin-HRP

Streptavidin was immobilized through free-terminal carboxyl group on thiol monolayer SAM on gold particles. Streptavidin(SA) solution was produced 200ug/ml in 10nM sodium acetate buffer in pH 4.5. Samples were added in to SA solution and shake for 2 hours for fully electrostatic absorbance, then washed with PBS buffer at pH in 7.4 with 1% BSA in for blocking the un-bonding site for 30 min. Then films were washed with PBS for three times and stored in centrifuged tubes under -20 °C.

200ml of 5ng/ml Biotin-HRP solution with PBS was added in SA loaded samples centrifuged tubes and shake for bonding for 2 hours. Then samples were washed with PBS buffer until the washing solution was clear in TMB solution. Then the quantity of HRP was measured by the indicator TMB which yielded a blue color when oxidized by HRP. The blue color was measured at 652 nm in Biotek (Biotek, Winooski, VT). The quantity of HRP could in directly indicate the quantity of SA on samples.

4.3.11 Electrochemical Characterizations

Cyclic voltammograms (CVs) were carried in a one-compartment cell. Standard 2mm gold electrode, 100nm thin film gold with 4mm diameters and PEDOT films with 4mm diameters were used as the working electrodes. A platinum (Pt) wire as the counter electrode, and Ag/AgCl as the reference electrode. 0.1M H₂SO₄ solutions were measured by applying a repetitive potential scan from -0.2v to 0.8v (vs Ag/AgCl) at a scan rate of 50 mV s⁻¹. The resultant spectra were processed with SigmaPlot.

The varies concentration of ascorbic acid(AA) was used in amperometric measurement. This method was carried out at an applied potential of 0.4 V (vs AgCl) under continuous speed magnetic stirring flashing with nitrogen to prevent oxidation by air. The results was plot by Sigmaplot.

4.4 Results and discussions

4.4.1 Electrospinning with vapor phase polymerization(EVP) technique polymerization fiber morphology

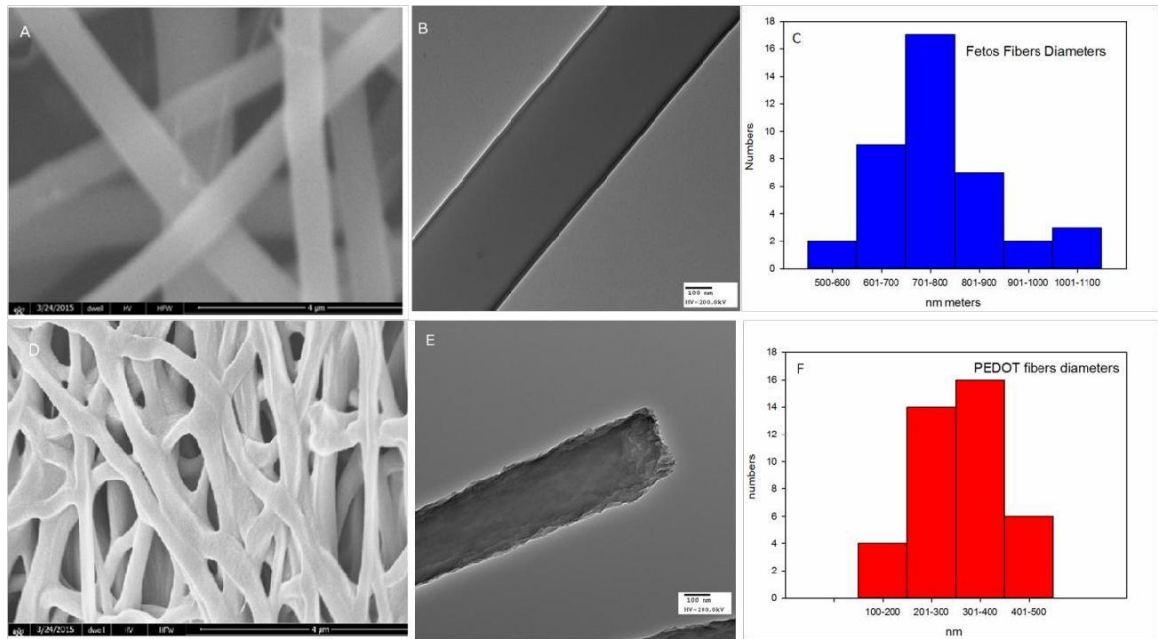


Fig 4.1 SEM TEM micrographs of Eletrospun FeTos and EVP PEDOT nanofibers and at 5000 \times magnification 5 kV accelerating voltage and 20000 \times magnification 200.0 kV. The diameter distribution was analyzed by Image J. Each distribution was composed of 50 counts fibers. A) SEM image of FeTos Fibers , B) TEM image of FeTos Fibers C) Fetos Nanofiber diameters range from 500 nm to 1100 nm, D) SEM ima ge of PEDOT Fibers , E) TEM image of PEDOT Fibers, F) PEDOT Nanofiber diameters range from 100 nm to 500 nm

Following eletrospinning for 30 mins, light yellow colored 40% FeTos with 2% PVP nanofiber mats on kapton films were removed from the copper collection plate. Fibers were made of FeTos salts and a little fibers forming water soluble polymers PVP. Therefore, FeTos fibers were really sensitive to humidity. The electrospinning condition should be kept within 5% humidity

or flashed with dried nitrogen all the time. **Fig4.1** showed the SEM and TEM images of FeTos fibers. The diameters of fibers were uniformly around 700-800nm which were studied by Image J software analysis (50 counts of fibers). And the surface of FeTos nanofibers were smooth. After vapor polymerization, monomer edot formed PEDOT on the surface of fibers, while polymers were not soluble in methanol, after being washed and dried, non-reacted FeTos salts were removed by washing, polymer fibers remained. **Fig 4.2** showed the PEDOT fibers' SEM and TEM images. The diameter of PEDOT fibers was 250-350nm, which was twice smaller than FeTos fibers. This was the result of removal of un-reacted FeTos and dehydration of fibers. As the Figure 4 d) showed the surface of PEDOTS fibers were rough and small crackers were on the fibers surface.

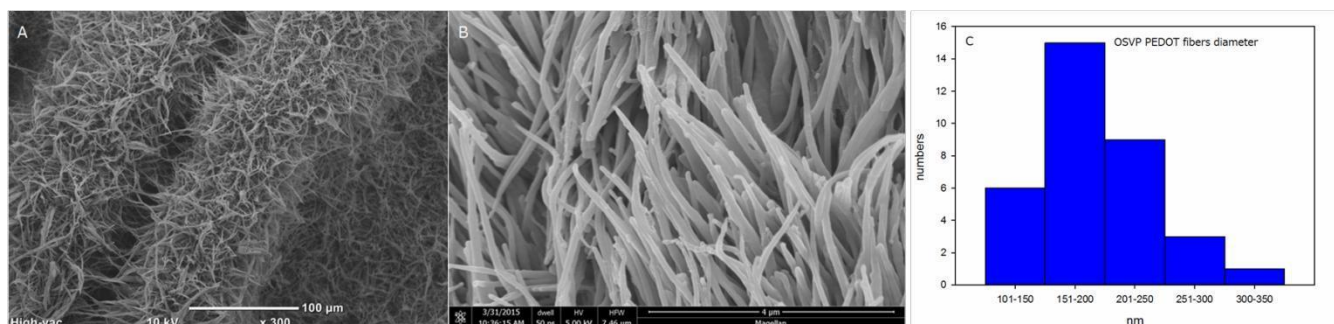


Fig 4.2 SEM of 27 min one step vapor phase polymerized PETOD(OSVP) nanofibers. The image was taken at 10KV in JEOL and 5 kV accelerating voltage by Magellan. The diameter distribution was analyzed by Image J. Each distribution was composed of 50 fibers count. A)300 \times magnification of OSVP fibers image was taken by JEOL, B) 5K magnification of OSVP fibers in Magellan, C) OSVP PEDOT Nanofiber diameters range from 100 nm to 350 nm

SEM of a vertical standing fibers film of OSVP PEDOT fibers shows that the numbers of fibers were more than EVP nanofiber. The direction of fibers were vertically directed and the length of fibers were more than 5um length. In a small magnitude lens, there were wrinkles between fibers, therefore the bulk fibers product was not as flat as EVP fibers. Diameters of SEM images shows

that the fibers were around 250nm which was smaller than EVP(400nm), that results in larger surface area.

As the SEM images showed OSVP PEDOT fibers not only turned out to be smaller diameters but also larger ration of fibers quantity. Furthermore compared with two steps of electrospun nanofibers processing, OSVP showed less complicated equipment set-up and less depend on manufacture conditions, such as humidity.

4.4.2 SEM results of gold nanoparticle synthesis composites

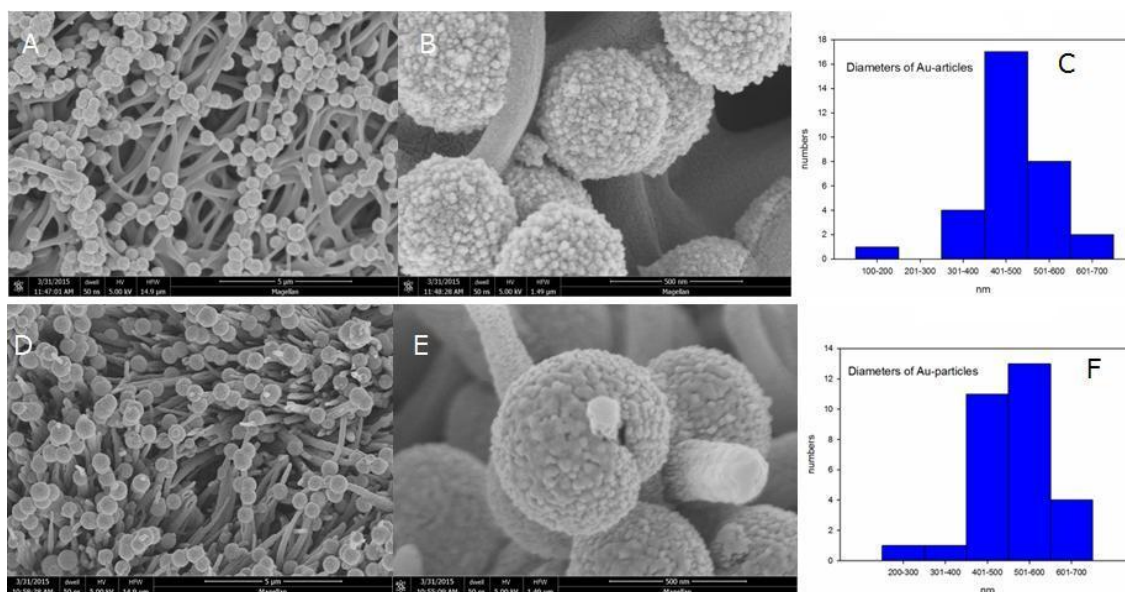


Fig 4.3 SEM of vapor phased polymerized PEDOT nanofibers with 60s gold synthesis. The image was taken at 5K and 20K magnification 5 kV accelerating voltage. The diameter distribution was analyzed by Image J. Each distribution was composed of 50 particles count. A) 5K magnification of EVP/Au particles, B) 20K magnification of EVP/Au particles, C) Gold diameters range from 100 nm to 700 nm, D) 5K magnification of OSVP/Au particles, E) 20K magnification of OSVP/Au particles, F) Gold diameters range from 200 nm to 700 nm on OSVP fibers.

Fig 4.3 shows the gold particles SEM images on two processing methods polymerized PEDOT nanofibers. In general, the morphology of the gold showed only slightly different on size. With analytical calculation results, gold particles generated on these two matrix showed no significant difference. Which means, gold particles synthesis on EVP and OSVP matrix were uniform in size and numbers. It was believed that EDOT vapor residue reacted with chloroauric acid and generated the same size of gold particles. Under 20K magnification of SEM microscopy, gold particles were formed by numerous nano sized gold particles and joined to form an aggregation. The carbon-oxygen-sulphur of PEDOT and Au nanoparticle ratio is given in **Table 2** and XPS results showed in **Fig4.4**.

4.4.3 X-ray photoelectron spectroscopy (XPS) results

Compared to four samples, spectroscopic analysis of EVP PEDOT fibers and OSVP polymerization PEDOT fibers with and without gold showed that showed that the chemical composition were identical within these two vapor phase polymerization, only OSVP had extra un-washed chloride element. With gold synthesis, three typical gold peaks determined by XPS. That means these two methods even with different ferric salts in different solvent produced similar structured PEDOT products. **Fig4.3** showed the XPS results of chemical composition and elemental analysis. XPS results of vapor polymerized PEDOT. The elemental analysis of PEDOT without gold shows that C/O ratio is 2.8 and 3.1 that is in close agreement with the theoretical value of 3. The peaks for O 1s and S 2p had relatively correct intensity. With the element surfing, gold quantity could be roughly determined, the results showed in **Table 2**. Gold element ratio in EVP and OSVP PEDOT fibers were 1.2% and 1.3% , which were really close. This results also met the agreement of SEM results. Gold particles were uniform in numbers with two different matrix .

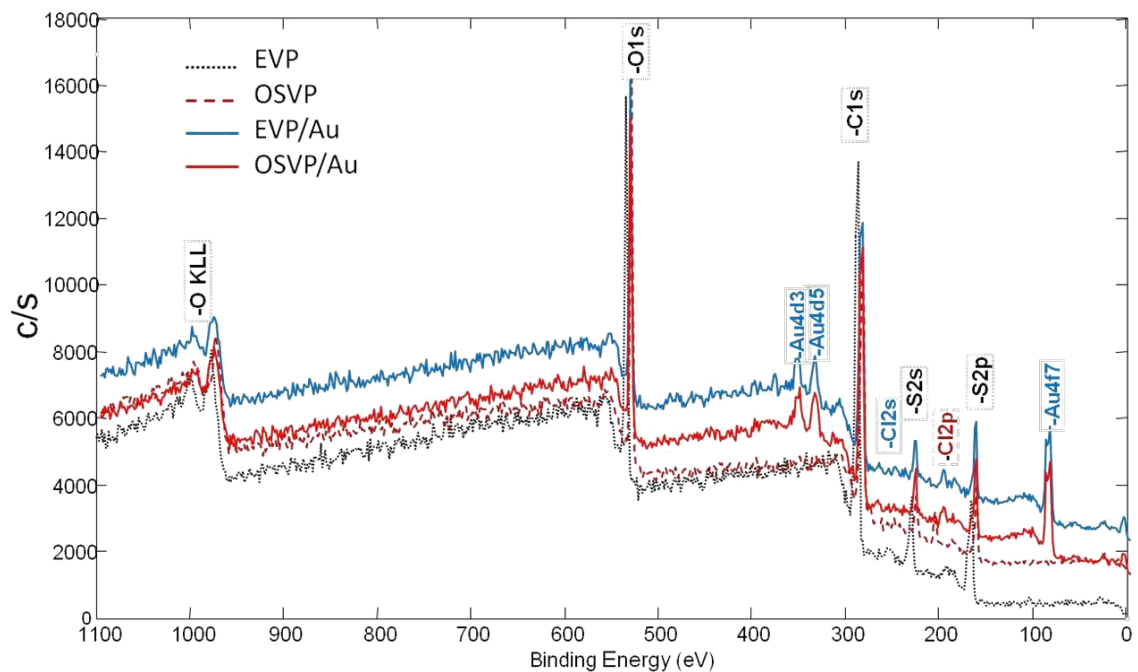


Fig 4.4 XPS results of electrospun with vapor phase polymerization (EVP) PEDOT fibers (dash black), one step vapor polymerization (OSVP) PEDOT fibers (dash maroon), EVP/Au (solid blue) and OSVP/Au (solid red).

Table 2 The elemental ration of electrospun vapor phase polymerized PEDOT (EVP) and one step vapor phase polymerized PEDOT(OSVP) fibers with/without Au synthesis

Atomic %						
Samples	C	O	S	Au	Cl	C/O
EVP	67.9	23.6	8.4	0	0	2.88
OSVP	70	22.2	5.4	0	2.4	3.15
EVP/Au	63.2	27.9	7.2	1.2	0.5	2.27
OSVP/Au	64.2	27	6.9	1.3	0.6	2.38

The table showed XPS results clearly that gold synthesis introduced chloride solvent in. And only a small amount of gold ration in the whole molecular structures. That was because that the residue EDOT was not enough to react with all chloroauric acid, only un reacted vapor on the fibers surface formed PEDOT and gold particle in this reaction.

4.4.4 Raman results

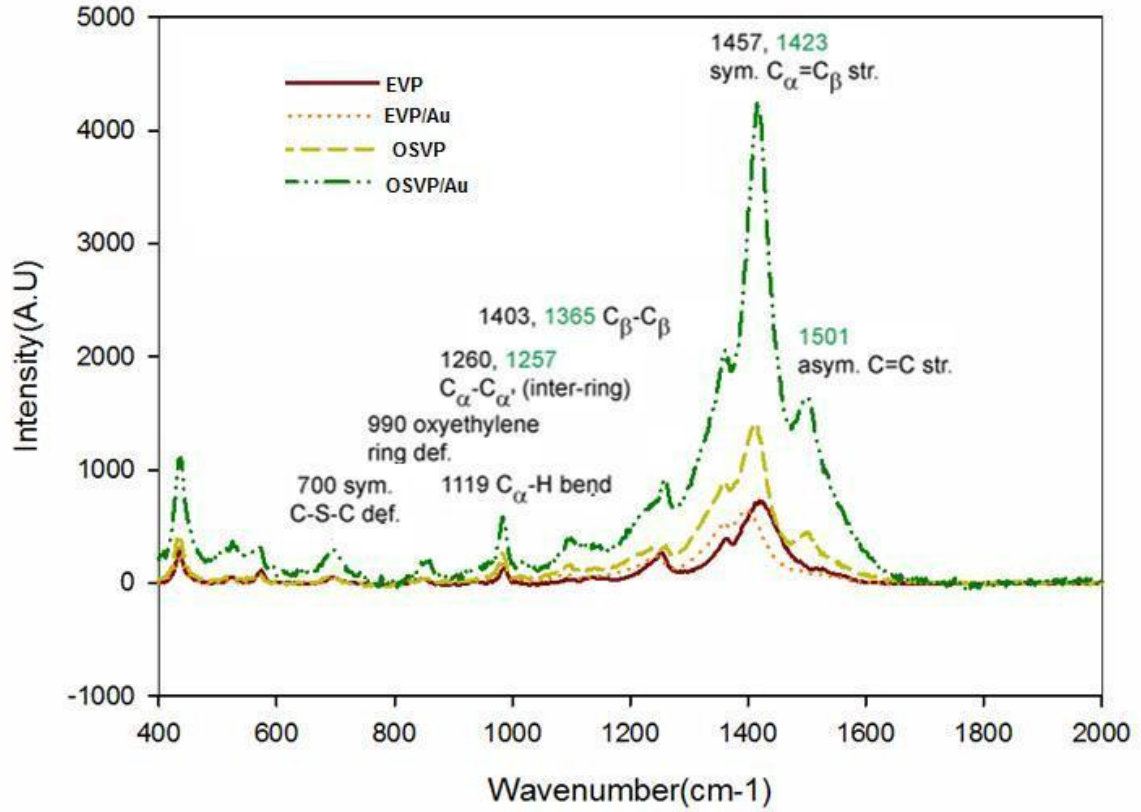


Fig 4.5 Overlapped Raman spectra results of electrospun vapor phase (EVP) (black) PEDOT and one step vapor phase polymerization (OSVP) (green) PEDOT fibers with or without gold.

Fig 4.5 shows the Raman results of two different fibers manufactures methods.

According to basic peaks, all of them had one strong peak at 1423 and 1457 cm^{-1} that was the main conjugated carbon symmetric $\text{C}_\alpha=\text{C}_\beta$ bonds region. The high level of symmetric carbon double bonds indicated the high level of oxidation. 1501 cm^{-1} was the asymmetric carbon double bonds, which was the region of stretching mode was characteristic of non PSS doping part. Also, $\text{C}_\beta-\text{C}_\beta$ stretch at 1365 cm^{-1} , inter-ring stretch at 1257 cm^{-1} 851 and 700 cm^{-1} ($\text{C}_\alpha-\text{S}-\text{C}_\alpha$ ring deformation). This overlapped spectra showed that no matter using electrospinning or one -step polymerization, the PEDOT conjugated bonds and C-S-C ring was formed. The only difference were slight stretching dislocation of symmetric peaks. That was because of OSVP PEDOT did

not has PSS symmetric doping oxidation chain. With gold being added in, similar peak patterns were observed, which indicates that Au oxidation only changed the oxidation level of backbone of carbon but the overall polymer structure was not affected.

4.4.4 TBO results

In this study TBO absorbance on the different surface of vapor phase polymerization and sample was studied. TBO was a negative dye which could be absorbed by carboxylic group under pH=10 condition. At pH=10, carboxylic group electrolysis and became positive charged, the amount of TBO absorbance indirectly indicated how many carboxylic group had on the surface of samples. The result showed that, in general OSVP PEDOT fibers had more absorptions of TBO dye. The results indicated that OSVP method could produce larger surface area compared to EVP(electrospun vapor phased) fibers. This assumption met the SEM morphology results, **Fig4.1** and **Fig4.2** showed that under low magnification, OSVP had larger ratio of fibers and diameters were smaller. Furthermore, with vertical directed shape, TBO dye had more chance to contact with entire fibers instead of only outside layer of flat electrospun nanofibers. With gold synthesized, TBO absorption on OSVP increased 40% while EVP had no significant difference compared with no gold PEDOT fibers. This result indicated that with gold particle introduced, EVP fibers surface area had no significant change while OSVP on the other hand, seemed introduced extra surface area. That was believed that, with gold modified, hydroxyl group on bare gold exposed which made the surface of PEDOT hydrophilic. OSVP had rough surface, this hydrophilicity brought efficient contact between solvent and immersed fibers. Large sized gold particles could not increase surface area, but hydrophilic gold particle brought more chance of vertical fibers to absorb TBO dye. Packed flat fibers blocked the solvent diffusion into the net fibers structures. With carboxylate terminal thiol added on gold particle, films had free carboxylic group and could absorb TBO dye. One-step polymerized fibers with gold functionalized with

SAM layer would absorb 4.22 mmol TBO dye which was twice as non functionalized films(1.84mmol) Compared to electrospun nanofibers.

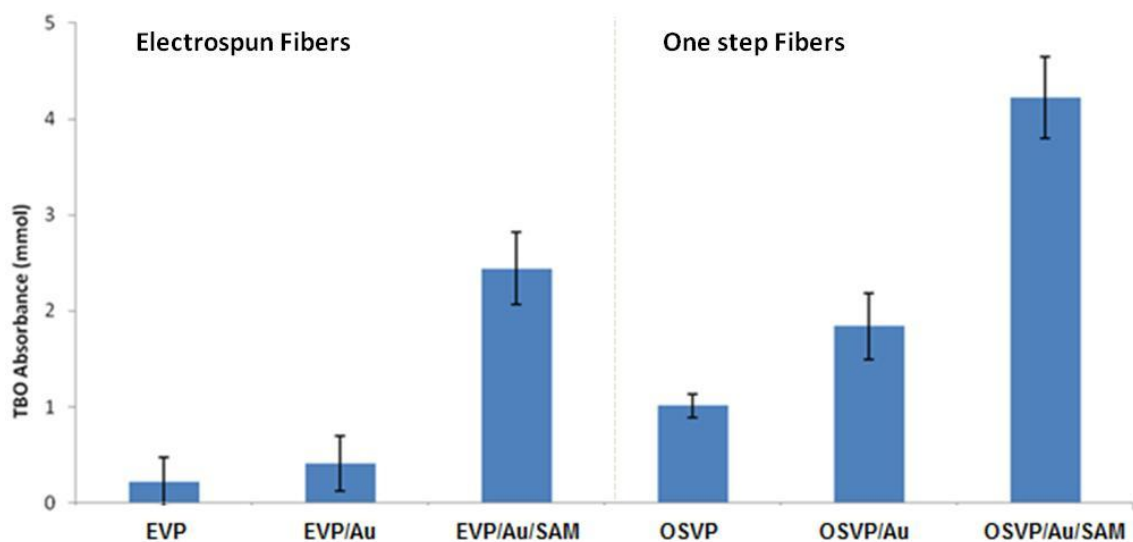


Fig 4.6 TBO absorbance on the surface of electrospun vapor phase polymerization and one step vapor phase polymerization PEDOT nanofibers with or without gold, or gold with or without self-assembly(SAM) alkanethiol monolayer (n=5).

4.4.5 Streptavidin (SA) immobilization and biotin-HRP measurement

In order to detect biological analyte, specific bio-markers should be introduced into the electrode. As previous research already added free carboxylic group by SAM layer on gold on the PEDOT fiber structures. Streptavidin had free amine group on the outside of the protein, it could be introduced through EDC/NHS reaction on the free carboxylic groups on the gold. While it was hard to directly determined how many SA we could add on to the surface. Each SA protein had four position for biotin to bond, therefore, how many biotin could be added on the surface that indirectly indicate how many SA was on the surface of gold. Free SA position offered the potential loading position for bio-markers to add such as DNA or antibodies. In this study, we only used biotin-HRP and used one-step TMB to show the quantity of SA bonding on the samples' surface.

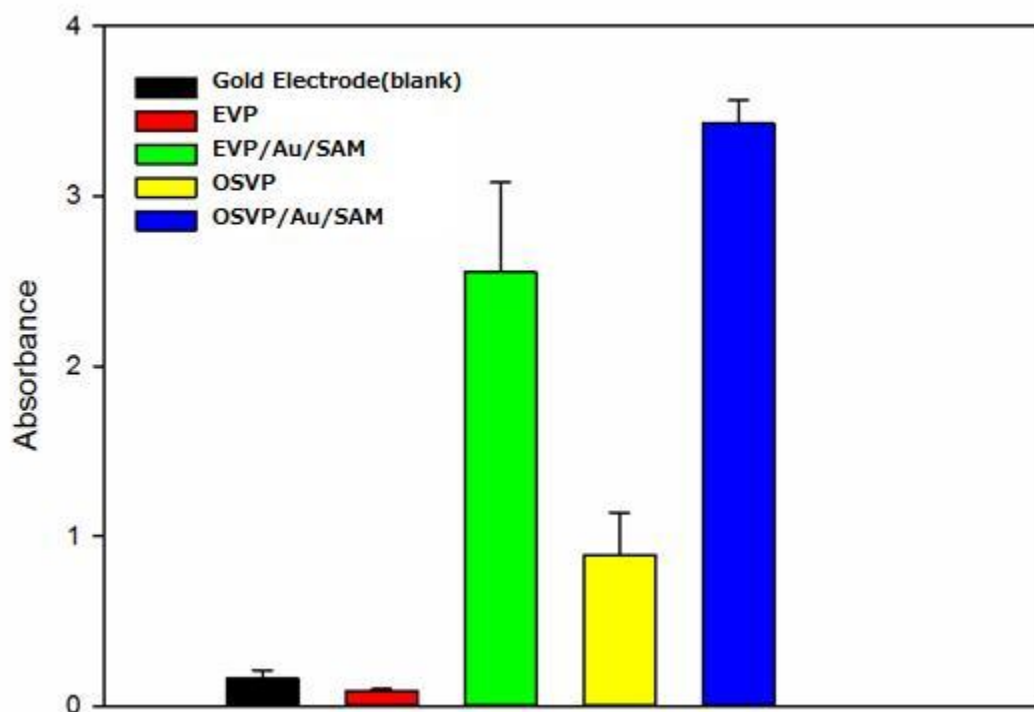


Fig 4.7 The absorbance of one-step TMB oxidation at 652nm of different samples, gold electrodes as blank and electrospun vapor phased PEDOT fibers and one-step vapor phase polymerization with or without gold.

From the results of measuring the quantity of TMB which directly indicated the amount of HRP. OSVP PEDOT fibers without gold particles still showed some non specific absorption of HRP. Because as mentioned previously, OSVP had large ratios of fiber structures, which brought larger surface area than EVP PEDOT fibers. With gold particle and with SAM layers on, PEDOT fibers showed over 20 times absorbance in EVP fibers while 5 times larger absorbance in OSVP fibers.

4.4.6 Amperometry detection of ascorbic acid(AA)

For the final goal of this project would be use the PEDOT polymer as a sensor electrode. I solved conductivity, poor bonding and manufacturing problems. The next step is to truly use this conductive polymer electrode for sensor application.

For my previous studies, I tried to use this electrode for basic ascorbic acid(AA) detection. AA is a widely used biosensor reactant on ascorbate oxidase. The enzyme could be worked as a bio-marker to oxidize AA. According to ascorbic acid concentration to present quantity of analyte. In order to test the electrode reaction with oxidized ascorbic acid. I used the electrode to test different concentration of AA. As the results shown, the one-step PEDOT fiber had higher reaction with AA changing. While gold nanoparticle showed no significant influence with current changing. Therefore gold particle only can benefit bonding site for this electrode. Only nano-structure could potentially increase sensitivity of polymer electrode.

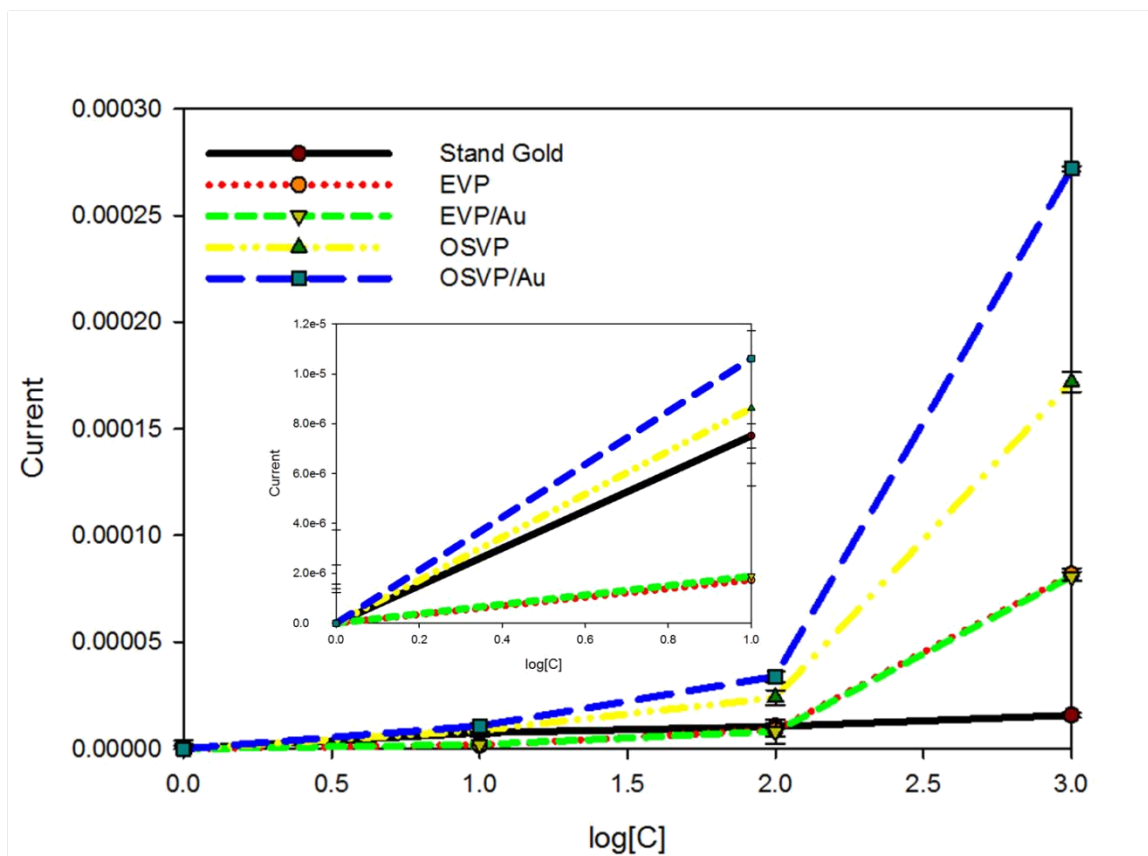


Fig 4.8 Amperometry test of different concentration of ascorbic by using standard gold electrode with our electrospun vapor phased electrode and one-step vapor polymerization electrode with or without gold on. The concentration of AA was 0, 0.01mmol/l, 0.1 mmol/l and 1 mmol/l. Log[C] indicated $\log[\text{AA concentration}/0.01\text{mmol/l}]$, $n=5$.

The result showed that with high concentration of AA, PEDOT electrodes showed higher response compared to stand gold electrodes. That was because, ascorbic acid is an oxidant, during the reaction ascorbic acid not only gave electrons to electrodes but also oxidized electrodes at the same time. The higher oxidation level on the carbon backbones, the more conductive PEDOT was. As the additive effects, more electrons transferred to detectors. While under low concentration of AA such as under 0.1mmol/l, only OSVP PEDOT showed the additive effects. The gold showed no significant effect with EVP PEDOT electrodes but showed positive effect on OSVP PEDOT fibers. As we proved previously, introducing gold, not only gave bio-bonding site on PEDOT but also changed the

hydrophilicity of PEDOT surface. Since OSVP was vertical directed structure, solvent could diffusion inside the fibers and increase the actual reaction area. On the other hand, electrospun fibers were full packed, solvent and gold particles were hard to get through the net, therefore, introducing gold showed have less effect compared with OSVP electrodes.

4.5 Conclusions

Vapor-phase polymerization(VPP) is a direct method to obtain highly conductive polymer layer on various conductive and nonconductive substrates. We used two method to obtain PEDOT nanofibers, one was electrospinning and the other was one-step vapor phase polymerization. Scanning electron microscopy (SEM) and transmission electron microscopy(TEM) were proved that these two methods could produce PEDOT nanofibers within 500nm (EVP) and 250nm(OSVP) . In order to load bio-markers on PEDOT we introduced gold particles on PEDOT nanofibers, SEM showed all gold particles were evenly distributed and uniform in size around(500nm) . XPS and raman spectra were used to analysis element information and polymers' chemical structures. XPS showed that gold was successfully introduced on the PEDOT, while raman spectra showed these two methods had no difference in polymerization of PEDOT structures and introducing gold did not affect PEDOT molecule structures either. We used alkanethiol monolayer by the self-assembly(SAM) on gold surface to introduce free carboxylic group on PEDOT electrode. TBO results showed under pH=10, OSVP with gold SAM layer absorb the most TBO dye. Furthermore we also used indirect method to prove that with gold and SAM layer, electrode could bond more streptavidin on its surface. And OSVP showed higher loading efficiency compared to EVP PEDOT fibers. With SA on its surface, all biotinylated bio-markers would be added on the electrodes by specific bonding between SA and biotin. We also used amperometry to detect ascorbic acid in the solution. At low AA concentration, OSVP showed higher response compared to other electrodes. Ascorbic acid oxidised PEDOT during the electron transportation which could boost the electronic response. Under high concentration of AA, electrode with PEDOT showed high response compared with standard gold electrodes. As a conclusion, we produced the nanofiber structured PEDOT by using two methods with gold, which not only increase the sensitivity of electrodes reaction but also gave electrodes ability to bind bio-components for biosensor applications.

REFERENCE

1. Anton, F. , *Production of artificial fibers from fiber forming liquids*, 1943, Google Patents.
2. Anton, F. , *Method and apparatus for spinning*, 1939, Google Patents.
3. Anton, F. , *Method and apparatus for spinning*, 1944, Google Patents.
4. Wilm, M.S. and M. Mann, *Electrospray and Taylor-Cone theory, Dole's beam of macromolecules at last?* International Journal of Mass Spectrometry and Ion Processes, 1994. **136**(2): p. 167-180.
5. Baumgarten, P.K., *Electrostatic spinning of acrylic microfibers*. Journal of colloid and interface science, 1971. **36**(1): p. 71-79.
6. Larrondo, L. and R. St John Manley, *Electrostatic fiber spinning from polymer melts. I. Experimental observations on fiber formation and properties*. Journal of Polymer Science: Polymer Physics Edition, 1981. **19**(6): p. 909-920.
7. Shin, Y., et al., *Experimental characterization of electrospinning: the electrically forced jet and instabilities*. Polymer, 2001. **42**(25): p. 09955-09967.
8. Doshi, J. and D.H. Reneker. *Electrospinning process and applications of electrospun fibers*. in *Industry Applications Society Annual Meeting, 1993., Conference Record of the 1993 IEEE*. 1993. IEEE.
9. Jaeger, R., et al. *Electrospinning of ultra-thin polymer fibers*. in *Macromolecular Symposia*. 1998. Wiley Online Library.
10. Gibson, P., H. Schreuder-Gibson, and D. Rivin, *Transport properties of porous membranes based on electrospun nanofibers*. Colloids and Surfaces A: Physicochemical and Engineering Aspects, 2001. **187**: p. 469-481.
11. Kim, J.s. and D.H. Reneker, *Mechanical properties of composites using ultrafine electrospun fibers*. Polymer composites, 1999. **20**(1): p. 124-131.

12. Deitzel, J., et al., *The effect of processing variables on the morphology of electrospun nanofibers and textiles*. Polymer, 2001. **42**(1): p. 261-272.
13. Demir, M.M., et al., *Electrospinning of polyurethane fibers*. Polymer, 2002. **43**(11): p. 3303-3309.
14. Wang, X., et al., *Electrospun nanofibrous membranes for highly sensitive optical sensors*. Nano Letters, 2002. **2**(11): p. 1273-1275.
15. Ramakrishna, S., et al., *An introduction to electrospinning and nanofibers*. Vol. 90. 2005: World Scientific.
16. Buchko, C.J., et al., *Processing and microstructural characterization of porous biocompatible protein polymer thin films*. Polymer, 1999. **40**(26): p. 7397-7407.
17. Fennessey, S.F. and R.J. Farris, *Fabrication of aligned and molecularly oriented electrospun polyacrylonitrile nanofibers and the mechanical behavior of their twisted yarns*. Polymer, 2004. **45**(12): p. 4217-4225.
18. Norris, I.D., et al., *Electrostatic fabrication of ultrafine conducting fibers: polyaniline/polyethylene oxide blends*. Synthetic metals, 2000. **114**(2): p. 109-114.
19. Lee, S. and S.K. Obendorf, *Use of electrospun nanofiber web for protective textile materials as barriers to liquid penetration*. Textile Research Journal, 2007. **77**(9): p. 696-702.
20. Sen, R., et al., *Preparation of single-walled carbon nanotube reinforced polystyrene and polyurethane nanofibers and membranes by electrospinning*. Nano letters, 2004. **4**(3): p. 459-464.
21. Ghasemi-Mobarakeh, L., et al., *Electrospun poly (ϵ -caprolactone)/gelatin nanofibrous scaffolds for nerve tissue engineering*. Biomaterials, 2008. **29**(34): p. 4532-4539.
22. Boland, E.D., et al., *Electrospinning polydioxanone for biomedical applications*. Acta Biomaterialia, 2005. **1**(1): p. 115-123.

23. You, Y., et al., *In vitro degradation behavior of electrospun polyglycolide, polylactide, and poly (lactide-co-glycolide)*. Journal of Applied Polymer Science, 2005. **95**(2): p. 193-200.
24. Yang, F., et al., *Electrospinning of nano/micro scale poly (L-lactic acid) aligned fibers and their potential in neural tissue engineering*. Biomaterials, 2005. **26**(15): p. 2603-2610.
25. Xie, J. and Y.-L. Hsieh, *Ultra-high surface fibrous membranes from electrospinning of natural proteins: casein and lipase enzyme*. Journal of Materials Science, 2003. **38**(10): p. 2125-2133.
26. Liu, H. and Y.L. Hsieh, *Ultrafine fibrous cellulose membranes from electrospinning of cellulose acetate*. Journal of Polymer Science Part B: Polymer Physics, 2002. **40**(18): p. 2119-2129.
27. Bhattarai, N., et al., *Electrospun chitosan-based nanofibers and their cellular compatibility*. Biomaterials, 2005. **26**(31): p. 6176-6184.
28. Matthews, J.A., et al., *Electrospinning of collagen nanofibers*. Biomacromolecules, 2002. **3**(2): p. 232-238.
29. Vega-Lugo, A.-C. and L.-T. Lim, *Controlled release of allyl isothiocyanate using soy protein and poly (lactic acid) electrospun fibers*. Food Research International, 2009. **42**(8): p. 933-940.
30. Torres-Giner, S., M.J. Ocio, and J.M. Lagaron, *Novel antimicrobial ultrathin structures of zein/chitosan blends obtained by electrospinning*. Carbohydrate Polymers, 2009. **77**(2): p. 261-266.
31. Nakagawa, T., et al., *Protective activity of green tea against free radical-and glucose-mediated protein damage*. Journal of Agricultural and Food Chemistry, 2002. **50**(8): p. 2418-2422.

32. Wang, S., et al., *Electrospun soy protein isolate-based fiber fortified with anthocyanin-rich red raspberry (Rubus strigosus) extracts*. Food Research International, 2013. **52**(2): p. 467-472.
33. Van der Schueren, L., et al., *The development of polyamide 6.6 nanofibres with a pH-sensitive function by electrospinning*. European Polymer Journal, 2010. **46**(12): p. 2229-2239.
34. Teng, M., et al., *Electrospun mesoporous carbon nanofibers produced from phenolic resin and their use in the adsorption of large dye molecules*. Carbon, 2012. **50**(8): p. 2877-2886.
35. Abe, H., M. Yoneda, and N. Fujiwara, *Developments of plasma etching technology for fabricating semiconductor devices*. Japanese Journal of Applied Physics, 2008. **47**: p. 1435.
36. Feng, C., et al., *Production of drinking water from saline water by air-gap membrane distillation using polyvinylidene fluoride nanofiber membrane*. Journal of Membrane Science, 2008. **311**(1): p. 1-6.
37. Arthanareeswaran, G., et al., *Removal of chromium from aqueous solution using cellulose acetate and sulfonated poly (ether ether ketone) blend ultrafiltration membranes*. Journal of hazardous materials, 2007. **139**(1): p. 44-49.
38. Veleirinho, B. and J. Lopes-da-Silva, *Application of electrospun poly (ethylene terephthalate) nanofiber mat to apple juice clarification*. Process Biochemistry, 2009. **44**(3): p. 353-356.
39. Wu, L., X. Yuan, and J. Sheng, *Immobilization of cellulase in nanofibrous PVA membranes by electrospinning*. Journal of Membrane Science, 2005. **250**(1): p. 167-173.
40. Song, J., et al., *Enhanced catalytic activity of lipase encapsulated in PCL nanofibers*. Langmuir, 2012. **28**(14): p. 6157-6162.

41. Sakai, S., et al., *An electrospun ultrafine fibrous silica catalyst incorporating an alkyl-silica coating containing lipase for reactions in organic solvents*. Journal of Molecular Catalysis B: Enzymatic, 2012. **83**: p. 120-124.
42. Ren, G., et al., *Electrospun poly (vinyl alcohol)/glucose oxidase biocomposite membranes for biosensor applications*. Reactive and Functional Polymers, 2006. **66**(12): p. 1559-1564.
43. Ge, L., et al., *Immobilization of glucose oxidase in electrospun nanofibrous membranes for food preservation*. Food Control, 2012. **26**(1): p. 188-193.
44. Anton, F. , *Production of artificial fibers from fiber forming liquids*, 1943, Google Patents.
45. Anton, F. , *Method and apparatus for spinning*, 1939, Google Patents.
46. Anton, F. , *Method and apparatus for spinning*, 1944, Google Patents.
47. Wilm, M.S. and M. Mann, *Electrospray and Taylor-Cone theory, Dole's beam of macromolecules at last?* International Journal of Mass Spectrometry and Ion Processes, 1994. **136**(2): p. 167-180.
48. Baumgarten, P.K., *Electrostatic spinning of acrylic microfibers*. Journal of colloid and interface science, 1971. **36**(1): p. 71-79.
49. Larrondo, L. and R. St John Manley, *Electrostatic fiber spinning from polymer melts. I. Experimental observations on fiber formation and properties*. Journal of Polymer Science: Polymer Physics Edition, 1981. **19**(6): p. 909-920.
50. Shin, Y., et al., *Experimental characterization of electrospinning: the electrically forced jet and instabilities*. Polymer, 2001. **42**(25): p. 09955-09967.
51. Doshi, J. and D.H. Reneker. *Electrospinning process and applications of electrospun fibers*. in *Industry Applications Society Annual Meeting, 1993., Conference Record of the 1993 IEEE*. 1993. IEEE.

- 52 Jaeger, R., et al. *Electrospinning of ultra-thin polymer fibers*. in *Macromolecular Symposia*. 1998. Wiley Online Library.
- 53 Gibson, P., H. Schreuder-Gibson, and D. Rivin, *Transport properties of porous membranes based on electrospun nanofibers*. *Colloids and Surfaces A: Physicochemical and Engineering Aspects*, 2001. **187**: p. 469-481.
- 54 Kim, J.s. and D.H. Reneker, *Mechanical properties of composites using ultrafine electrospun fibers*. *Polymer composites*, 1999. **20**(1): p. 124-131.
- 55 Deitzel, J., et al., *The effect of processing variables on the morphology of electrospun nanofibers and textiles*. *Polymer*, 2001. **42**(1): p. 261-272.
- 56 Demir, M.M., et al., *Electrospinning of polyurethane fibers*. *Polymer*, 2002. **43**(11): p. 3303-3309.
- 57 Wang, X., et al., *Electrospun nanofibrous membranes for highly sensitive optical sensors*.
Ramakrishna, S., et al., *An introduction to electrospinning and nanofibers*. Vol. 90. 2005: World Scientific.
- 58 Buchko, C.J., et al., *Processing and microstructural characterization of porous biocompatible protein polymer thin films*. *Polymer*, 1999. **40**(26): p. 7397-7407.
- 59 Fennessey, S.F. and R.J. Farris, *Fabrication of aligned and molecularly oriented electrospun polyacrylonitrile nanofibers and the mechanical behavior of their twisted yarns*. *Polymer*, 2004. **45**(12): p. 4217-4225.
- 60 Norris, I.D., et al., *Electrostatic fabrication of ultrafine conducting fibers: polyaniline/polyethylene oxide blends*. *Synthetic metals*, 2000. **114**(2): p. 109-114.
- 61 Lee, S. and S.K. Obendorf, *Use of electrospun nanofiber web for protective textile materials as barriers to liquid penetration*. *Textile Research Journal*, 2007. **77**(9): p. 696-702.

- 62 Sen, R., et al., *Preparation of single-walled carbon nanotube reinforced polystyrene and polyurethane nanofibers and membranes by electrospinning*. Nano letters, 2004. **4**(3): p. 459-464.
- 63 Ghasemi-Mobarakeh, L., et al., *Electrospun poly (ϵ -caprolactone)/gelatin nanofibrous scaffolds for nerve tissue engineering*. Biomaterials, 2008. **29**(34): p. 4532-4539.
- 64 Boland, E.D., et al., *Electrospinning polydioxanone for biomedical applications*. Acta Biomaterialia, 2005. **1**(1): p. 115-123.
- 65 You, Y., et al., *In vitro degradation behavior of electrospun polyglycolide, polylactide, and poly (lactide-co-glycolide)*. Journal of Applied Polymer Science, 2005. **95**(2): p. 193-200.
- 66 Yang, F., et al., *Electrospinning of nano/micro scale poly (L-lactic acid) aligned fibers and their potential in neural tissue engineering*. Biomaterials, 2005. **26**(15): p. 2603-2610.
- 67 Xie, J. and Y.-L. Hsieh, *Ultra-high surface fibrous membranes from electrospinning of natural proteins: casein and lipase enzyme*. Journal of Materials Science, 2003. **38**(10): p. 2125-2133.
- 68 Liu, H. and Y.L. Hsieh, *Ultrafine fibrous cellulose membranes from electrospinning of cellulose acetate*. Journal of Polymer Science Part B: Polymer Physics, 2002. **40**(18): p. 2119-2129.
- 69 Bhattarai, N., et al., *Electrospun chitosan-based nanofibers and their cellular compatibility*. Biomaterials, 2005. **26**(31): p. 6176-6184.
- 70 Matthews, J.A., et al., *Electrospinning of collagen nanofibers*. Biomacromolecules, 2002. **3**(2): p. 232-238.
- 71 Vega-Lugo, A.-C. and L.-T. Lim, *Controlled release of allyl isothiocyanate using soy protein and poly (lactic acid) electrospun fibers*. Food Research International, 2009. **42**(8): p. 933-940.

- 72 Torres-Giner, S., M.J. Ocio, and J.M. Lagaron, *Novel antimicrobial ultrathin structures of zein/chitosan blends obtained by electrospinning*. Carbohydrate Polymers, 2009. **77**(2): p. 261-266.
- 73 Nakagawa, T., et al., *Protective activity of green tea against free radical- and glucose-mediated protein damage*. Journal of Agricultural and Food Chemistry, 2002. **50**(8): p. 74
Wang, S., et al., *Electrospun soy protein isolate-based fiber fortified with anthocyanin-rich red raspberry (Rubus strigosus) extracts*. Food Research International, 2013. **52**(2): p. 467-472.
- 74 Van der Schueren, L., et al., *The development of polyamide 6.6 nanofibres with a pH-sensitive function by electrospinning*. European Polymer Journal, 2010. **46**(12): p. 2229-2239.
- 75 Teng, M., et al., *Electrospun mesoporous carbon nanofibers produced from phenolic resin and their use in the adsorption of large dye molecules*. Carbon, 2012. **50**(8): p. 2877-2886.
- 76 Abe, H., M. Yoneda, and N. Fujiwara, *Developments of plasma etching technology for fabricating semiconductor devices*. Japanese Journal of Applied Physics, 2008. **47**: p. 1435.
- 77 Feng, C., et al., *Production of drinking water from saline water by air-gap membrane distillation using polyvinylidene fluoride nanofiber membrane*. Journal of Membrane Science, 2008. **311**(1): p. 1-6.
- 78 Arthanareeswaran, G., et al., *Removal of chromium from aqueous solution using cellulose acetate and sulfonated poly (ether ether ketone) blend ultrafiltration membranes*. Journal of hazardous materials, 2007. **139**(1): p. 44-49.
79. Veleirinho, B. and J. Lopes-da-Silva, *Application of electrospun poly (ethylene terephthalate) nanofiber mat to apple juice clarification*. Process Biochemistry, 2009. **44**(3): p. 353-356.

- 80 Wu, L., X. Yuan, and J. Sheng, *Immobilization of cellulase in nanofibrous PVA membranes by electrospinning*. Journal of Membrane Science, 2005. **250**(1): p. 167-173.
- 81 Song, J., et al., *Enhanced catalytic activity of lipase encapsulated in PCL nanofibers*. Langmuir, 2012. **28**(14): p. 6157-6162.
- 82 Sakai, S., et al., *An electrospun ultrafine fibrous silica catalyst incorporating an alkyl-silica coating containing lipase for reactions in organic solvents*. Journal of Molecular Catalysis B: Enzymatic, 2012. **83**: p. 120-124.
- 83 Ren, G., et al., *Electrospun poly (vinyl alcohol)/glucose oxidase biocomposite membranes for biosensor applications*. Reactive and Functional Polymers, 2006. **66**(12): p. 1559-1564.
- 84 Ge, L., et al., *Immobilization of glucose oxidase in electrospun nanofibrous membranes for food preservation*. Food Control, 2012. **26**(1): p. 188-193.
- 85 McNeill, R., et al., *Electronic conduction in polymers. I. The chemical structure of polypyrrole*. Australian Journal of Chemistry, 1963. **16**(6): p. 1056-1075.
- 86 Bolto, B.A., R. McNeill, and D. Weiss, *Electronic conduction in polymers. III. Electronic properties of polypyrrole*. Australian Journal of Chemistry, 1963. **16**(6): p. 1090-1103.
- 87 Macdiarmid, A.G., et al., *"Polyaniline": interconversion of metallic and insulating forms*. Molecular Crystals and Liquid Crystals, 1985. **121**(1-4): p. 173-180.
- 88 Chiang, J.-C. and A.G. MacDiarmid, *'Polyaniline': protonic acid doping of the emeraldine form to the metallic regime*. Synthetic Metals, 1986. **13**(1): p. 193-205.
- 89 Shirakawa, H., et al., *Synthesis of electrically conducting organic polymers: halogen derivatives of polyacetylene, (CH)_x*. J. Chem. Soc., Chem. Commun., 1977(16): p. 578-580.
- 90 Naarmann, H. and N. Theophilou, *New process for the production of metal-like, stable polyacetylene*. Synthetic Metals, 1987. **22**(1): p. 1-8.

- 91 Armour, M., et al., *Colored electrically conducting polymers from furan, pyrrole, and thiophene*. Journal of Polymer Science Part A- 1: Polymer Chemistry, 1967. 5(7): p. 1527-1538.
- 92 Tourillon, G. and F. Garnier, *New electrochemically generated organic conducting polymers*. Journal of Electroanalytical Chemistry and Interfacial Electrochemistry, 1982. **135**(1): p. 173-178.
- 93 Ionescu, R.E., et al., *A polypyrrole cDNA electrode for the amperometric detection of the West Nile Virus*. Electrochemistry communications, 2006. **8**(11): p. 1741-1748.
- 94 Najari, A., H.A. Ho, and M. Leclerc, *Biosensors based on a cationic polythiophene: detection of DNA and proteins*. Polym Prepr, 2007. **48**(2): p. 3-4.
- 95 Shiddiky, M.J., M.A. Rahman, and Y.-B. Shim, *Hydrazine-catalyzed ultrasensitive detection of DNA and proteins*. Analytical chemistry, 2007. **79**(17): p. 6886-6890.
- 96 Donovan, K.C., et al., *Virus– Poly (3, 4-ethylenedioxythiophene) Composite Films for Impedance-Based Biosensing*. Analytical chemistry, 2011. **83**(7): p. 2420-2424.
- 97 Liu, G. and Y. Lin, *Biosensor based on self-assembling acetylcholinesterase on carbon nanotubes for flow injection/amperometric detection of organophosphate pesticides and nerve agents*. Analytical Chemistry, 2006. **78**(3): p. 835-843.
- 98 Zheng, Z., et al., *Validation of an ELISA test kit for the detection of total aflatoxins in grain and grain products by comparison with HPLC*. Mycopathologia, 2005. **159**(2): p. 255-263.
- 99 Sharma, S.K., et al., *Evaluation of lateral-flow Clostridium botulinum neurotoxin detection kits for food analysis*. Applied and environmental microbiology, 2005. **71**(7): p. 3935-3941.
- 100 Liu, Y., et al., *Immune-biosensor for aflatoxin B 1 based bio-electrocatalytic reaction on micro-comb electrode*. Biochemical Engineering Journal, 2006. **32**(3): p. 211-217.

- 101 Eissa, S., et al., *Electrochemical immunosensor for the milk allergen β -lactoglobulin based on electrografting of organic film on graphene modified screen-printed carbon electrodes*. Biosensors and Bioelectronics, 2012. **38**(1): p. 308-313.
- 102 DeMarco, D.R., et al., *Rapid detection of Escherichia coli O157: H7 in ground beef using a fiber-optic biosensor*. Journal of Food Protection®, 1999. **62**(7): p. 711-716.
- 103 Geng, T., M.T. Morgan, and A.K. Bhunia, *Detection of low levels of Listeria monocytogenes cells by using a fiber-optic immunosensor*. Applied and environmental microbiology, 2004. **70**(10): p. 6138-6146.
- 104 Ko, S. and S.A. Grant, *A novel FRET-based optical fiber biosensor for rapid detection of Salmonella typhimurium*. Biosensors and Bioelectronics, 2006. **21**(7): p. 1283-1290.
- 105 Taylor, A.D., et al., *Quantitative and simultaneous detection of four foodborne bacterial pathogens with a multi-channel SPR sensor*. Biosensors and Bioelectronics, 2006. **22**(5): p. 752-758.
- 106 Chen, S.-H., et al., *Using oligonucleotide-functionalized Au nanoparticles to rapidly detect foodborne pathogens on a piezoelectric biosensor*. Journal of Microbiological Methods, 2008. **73**(1): p. 7-17.
- 107 Gehring, A.G., et al., *Enzyme-linked immunomagnetic electrochemical detection of Salmonella typhimurium*. Journal of immunological methods, 1996. **195**(1): p. 15-25.
- 108 Rishpon, J. and D. Ivnitski, *An amperometric enzyme-channeling immunosensor*. Biosensors and Bioelectronics, 1997. **12**(3): p. 195-204.
- 109 Tully, E., S.P. Higson, and R. O’Kennedy, *The development of a ‘labelless’ immunosensor for the detection of Listeria monocytogenes cell surface protein, Internalin B*. Biosensors and Bioelectronics, 2008. **23**(6): p. 906-912.
- 110 Kutter, E. and A. Sulakvelidze, *Bacteriophages: biology and applications*. 2004: CRC Press.

- 111 Mullard, A., *2011 FDA drug approvals*. Nature Reviews Drug Discovery, 2012. **11**(2): p. 91-94.
- 112 DeWaal, C.S., *Food Protection and Defense: Preparing for a Crisis*. Minn. J. Sci. & Tech., 2007. **8**: p. 187.
- 113 Painter, J.A., et al., *Attribution of foodborne illnesses, hospitalizations, and deaths to food commodities by using outbreak data, United States, 1998 –2008*. Emerging infectious diseases, 2013. **19**(3): p. 407.
114. Carter, C.D., et al., *Bacteriophage cocktail significantly reduces Escherichia coli O157: H7 contamination of lettuce and beef, but does not protect against recontamination*. Bacteriophage, 2012. **2**(3): p. 178-185.
115. Greer, G.G., *Bacteriophage control of foodborne bacteria*. Journal of Food Protection®, 2005. **68**(5): p. 1102-1111.
- 116 Leverentz, B., et al., *Examination of bacteriophage as a biocontrol method for Salmonella on fresh-cut fruit: a model study*. Journal of Food Protection®, 2001. **64**(8): p. 1116-1121.
- 117 Leverentz, B., et al., *Optimizing concentration and timing of a phage spray application to reduce Listeria monocytogenes on honeydew melon tissue*. Journal of Food Protection®, 2004. **67**(8): p. 1682-1686.
118. Miyamoto-Shinohara, Y., et al., *Survival rate of microbes after freeze-drying and long-term storage*. Cryobiology, 2000. **41**(3): p. 251-255.
- 119 Alvarez- Gonzalez, E., et al., *Bioprocessing of bacteriophages via rapid drying onto microcrystals*. Biotechnology progress, 2012. **28**(2): p. 540-548.
- 120 Doshi, J. and D.H. Reneker, *Electrospinning process and applications of electrospun fibers*. Journal of electrostatics, 1995. **35**(2): p. 151-160.
- 121 Dai, M., S. Jin, and S.R. Nugen, *Water-Soluble Electrospun Nanofibers as a Method for On-Chip Reagent Storage*. Biosensors, 2012. **2**(4): p. 388-395.

- 122 Lee, S.-W. and A.M. Belcher, *Virus-based fabrication of micro-and nanofibers using electrospinning*. Nano letters, 2004. **4**(3): p. 387-390.
- 123 Salalha, W., et al., *Encapsulation of bacteria and viruses in electrospun nanofibres*. Nanotechnology, 2006. **17**(18): p. 4675.
- 124 Korehei, R. and J. Kadla, *Encapsulation of T4< i> Bacteriophage</i> in Electrospun Poly (Ethylene Oxide)/Cellulose Diacetate Fibers*. Carbohydrate Polymers, 2013.
- 124 Korehei, R. and J. Kadla, *Incorporation of T4 bacteriophage in electrospun fibres*. Journal of applied microbiology, 2013.
- 126 Lu, C., et al., *Computer simulation of electrospinning. Part I. Effect of solvent in electrospinning*. Polymer, 2006. **47**(3): p. 915-921.
- 127 Kim, S.J., C.K. Lee, and S.I. Kim, *Effect of ionic salts on the processing of poly (2-acrylamido-2-methyl-1-propane sulfonic acid) nanofibers*. Journal of applied polymer science, 2005. **96**(4): p. 1388-1393.
- 128 Patel, A.C., et al., *Electrospinning of porous silica nanofibers containing silver nanoparticles for catalytic applications*. Chemistry of materials, 2007. **19**(6): p. 1231-1238.
129. Qin, X.H., et al., *Effect of different salts on electrospinning of polyacrylonitrile (PAN) polymer solution*. Journal of applied polymer science, 2007. **103**(6): p. 3865-3870.
- 130 Lukas, D., A. Sarkar, and P. Pokorny, *Self-organization of jets in electrospinning from free liquid surface: A generalized approach*. Journal of Applied Physics, 2008. **103**(8): p. 084309-084309-7.
- 131 Sola-Penna, M. and J.R. Meyer-Fernandes, *Stabilization against thermal inactivation promoted by sugars on enzyme structure and function: why is trehalose more effective than other sugars?* Archives of Biochemistry and Biophysics, 1998. **360**(1): p. 10-14.

- 132 Leslie, S.B., et al., *Trehalose and sucrose protect both membranes and proteins in intact bacteria during drying*. Applied and environmental microbiology, 1995. **61**(10): p. 3592-3597.
- 133 Heywang, G. and F. Jonas, *Poly (alkylenedioxythiophene) s—new, very stable conducting polymers*. Advanced Materials, 1992. **4**(2): p. 116-118.
- 134 Sotzing, G., et al., *Redox active electrochromic polymers from low oxidation monomers containing 3, 4-ethylenedioxythiophene (EDOT)*. Synthetic metals, 1997. **84**(1): p. 199-201.
- 135 Randriamahazaka, H., V. Noel, and C. Chevrot, *Nucleation and growth of poly (3, 4-ethylenedioxythiophene) in acetonitrile on platinum under potentiostatic conditions*. Journal of Electroanalytical Chemistry, 1999. **472**(2): p. 103-111.
- 136 Yamato, H., M. Ohwa, and W. Wernet, *Stability of polypyrrole and poly (3, 4-ethylenedioxythiophene) for biosensor application*. Journal of Electroanalytical Chemistry, 1995. **397**(1): p. 163-170.
- 137 Du, X. and Z. Wang, *Effects of polymerization potential on the properties of electrosynthesized PEDOT films*. Electrochimica Acta, 2003. **48**(12): p. 1713-1717.
- 138 Chen, S.-H., et al., *Using oligonucleotide-functionalized Au nanoparticles to rapidly detect foodborne pathogens on a piezoelectric biosensor*. Journal of Microbiological Methods, 2008. **73**(1): p. 7-17.
- 139 Mohammadi, A., et al., *Chemical vapour deposition (cvd) of conducting polymers: polypyrrole*. Synthetic metals, 1986. **14**(3): p. 189-197.
- 140 Kim, J., et al., *The preparation and characteristics of conductive poly (3, 4 - ethylenedioxythiophene) thin film by vapor-phase polymerization*. Synthetic metals, 2003. **139**(2): p. 485-489.
- 141 Winther-Jensen, B., et al., *Vapor phase polymerization of pyrrole and thiophene using iron (III) sulfonates as oxidizing agents*. Macromolecules, 2004. **37**(16): p. 5930-5935.

- 142 Anton, F. , *Process and apparatus for preparing artificial threads*, 1934, Google Patents.
- 143 Kutter, E. and A. Sulakvelidze, *Bacteriophages: biology and applications*. 2004: CRC Press.
- 144 Mullard, A., *2011 FDA drug approvals*. Nature Reviews Drug Discovery, 2012. **11**(2): p. 91-94.
- 145 DeWaal, C.S., *Food Protection and Defense: Preparing for a Crisis*. Minn. JL Sci. & Tech., 2007. **8**: p. 187.
- 146 Painter, J.A., et al., *Attribution of foodborne illnesses, hospitalizations, and deaths to food commodities by using outbreak data, United States, 1998 –2008*. Emerging infectious diseases, 2013. **19**(3): p. 407.
- 147 Carter, C.D., et al., *Bacteriophage cocktail significantly reduces Escherichia coli O157: H7 contamination of lettuce and beef, but does not protect against recontamination*. Bacteriophage, 2012. **2**(3): p. 178-185.
- 148 Greer, G.G., *Bacteriophage control of foodborne bacteria*. Journal of Food Protection®, 2005. **68**(5): p. 1102-1111.
- 149 Leverentz, B., et al., *Examination of bacteriophage as a biocontrol method for Salmonella on fresh-cut fruit: a model study*. Journal of Food Protection®, 2001. **64**(8): p. 1116-1121.
- 150 Leverentz, B., et al., *Optimizing concentration and timing of a phage spray application to reduce Listeria monocytogenes on honeydew melon tissue*. Journal of Food Protection®, 2004. **67**(8): p. 1682-1686.
- 151 Miyamoto-Shinohara, Y., et al., *Survival rate of microbes after freeze-drying and long-term storage*. Cryobiology, 2000. **41**(3): p. 251-255.

152. Alvarez- Gonzalez, E., et al., *Bioprocessing of bacteriophages via rapid drying onto microcrystals*. Biotechnology progress, 2012. **28**(2): p. 540-548.
153. Doshi, J. and D.H. Reneker, *Electrospinning process and applications of electrospun fibers*. Journal of electrostatics, 1995. **35**(2): p. 151-160.
154. Dai, M., S. Jin, and S.R. Nugen, *Water-Soluble Electrospun Nanofibers as a Method for On-Chip Reagent Storage*. Biosensors, 2012. **2**(4): p. 388-395.
155. Lee, S.-W. and A.M. Belcher, *Virus-based fabrication of micro-and nanofibers using electrospinning*. Nano letters, 2004. **4**(3): p. 387-390.
156. Salalha, W., et al., *Encapsulation of bacteria and viruses in electrospun nanofibres*. Nanotechnology, 2006. **17**(18): p. 4675.
157. Korehei, R. and J. Kadla, *Encapsulation of T4 Bacteriophage in Electrospun Poly (Ethylene Oxide)/Cellulose Diacetate Fibers*. Carbohydrate Polymers, 2013.
158. Korehei, R. and J. Kadla, *Incorporation of T4 bacteriophage in electrospun fibres*. Journal of applied microbiology, 2013.
159. Lu, C., et al., *Computer simulation of electrospinning. Part I. Effect of solvent in electrospinning*. Polymer, 2006. **47**(3): p. 915-921.
160. Kim, S.J., C.K. Lee, and S.I. Kim, *Effect of ionic salts on the processing of poly (2- acrylamido- 2- methyl- 1- propane sulfonic acid) nanofibers*. Journal of applied polymer science, 2005. **96**(4): p. 1388-1393.
161. Patel, A.C., et al., *Electrospinning of porous silica nanofibers containing silver nanoparticles for catalytic applications*. Chemistry of materials, 2007. **19**(6): p. 1231-1238.
162. Qin, X.H., et al., *Effect of different salts on electrospinning of polyacrylonitrile (PAN) polymer solution*. Journal of applied polymer science, 2007. **103**(6): p. 3865-3870.

163. Lukas, D., A. Sarkar, and P. Pokorny, *Self-organization of jets in electrospinning from free liquid surface: A generalized approach*. Journal of Applied Physics, 2008. **103**(8): p. 084309-084309-7.
164. Sola-Penna, M. and J.R. Meyer-Fernandes, *Stabilization against thermal inactivation promoted by sugars on enzyme structure and function: why is trehalose more effective than other sugars?* Archives of Biochemistry and Biophysics, 1998. **360**(1): p. 10-14.
165. Leslie, S.B., et al., *Trehalose and sucrose protect both membranes and proteins in intact bacteria during drying*. Applied and environmental microbiology, 1995. **61**(10): p. 3592-3597.